Three Dimensional Printing and Computational Visualization for Surgical Planning and Medical Education

by

Justin Robert Ryan

A Dissertation Presented in Partial Fulfillment
of the Requirements for the Degree
Doctor of Philosophy

Approved April 2015 by the
Graduate Supervisory Committee:

David Frakes, Chair
Vincent Pizziconi
Stephen Pophal
Jeffrey LaBelle
Daniel Collins

ARIZONA STATE UNIVERSITY

May 2015

ABSTRACT

The advent of medical imaging has enabled significant advances in pre-procedural planning, allowing cardiovascular anatomy to be visualized noninvasively before a procedure. However, absolute scale and tactile information are not conveyed in traditional pre-procedural planning based on images alone. This information deficit fails to completely prepare clinicians for complex heart repair, where surgeons must consider the varied presentations of cardiac morphology and malformations. Three-dimensional (3D) visualization and 3D printing provide a mechanism to construct patient-specific, scale models of cardiovascular anatomy that surgeons and interventionalists can examine prior to a procedure. In addition, the same patient-specific models provide a valuable resource for educating future medical professionals. Instead of looking at idealized images on a computer screen or pages from medical textbooks, medical students can review a life-like model of patient anatomy.

In cases where surgical repair is insufficient to return the heart to normal function, a patient may proceed to advanced heart failure, and a heart transplant may be required. Unfortunately, a finite number of available donor hearts are available. A mechanical circulatory support (MCS) device can be used to bridge the time between heart failure and reception of a donor heart. These MCS devices are typically constructed for the adult population. Accordingly, the size associated to the device is a limiting factor for small adults or pediatric patients who often have smaller thoracic measurements. While current eligibility criteria are based on correlative measurements, the aforementioned 3D visualization capabilities can be leveraged to accomplish patient-specific fit analysis.

The main objectives of the work presented in this dissertation were 1) to develop and evaluate an optimized process for 3D printing cardiovascular anatomy for surgical planning and medical education and 2) to develop and evaluate computational tools to assess MCS device fit in specific patients. The evaluations for objectives 1 and 2 were completed with a collection of qualitative and quantitative validations. These validations include case studies to illustrate meaningful, qualitative results as well as quantitative results from surgical outcomes. The latter results present the first quantitative supporting evidence, beyond anecdotal case studies, regarding the efficacy of 3D printing for pre-procedural planning; this data is suitable as pilot data for clinical trials. The products of this work were used to plan 200 cardiovascular procedures (including 79 cardiothoracic surgeries at Phoenix Children's Hospital), via 3D printed heart models and assess MCS device fit in 29 patients across 6 countries.

ACKNOWLEDGMENTS

First, I would like to thank my advisor Dr. David Frakes for his incredible support in this interdisciplinary and pedagogical experiment. He had the foresight (or madness) to bring an undergraduate artist into a biomedical engineering laboratory. The possibilities were equal parts unknown and unrestrained. His guidance and mentorship exposed me to knowledge and skills that I will continue to refine for many years. He guided me down many intriguing research avenues while also giving me freedom to find my own initiatives. Through his mentorship, I now have an opportunity to explore biomedical challenges on my own terms.

A profound thank you must be extended to Drs. Stephen Pophal, John Nigro, Daniel Velez, Randy Richardson, and the extraordinary staff at Phoenix Children's Hospital and St. Joseph's Hospital and Medical Center. Many of these individuals were unknowing participants in this interdisciplinary endeavor that became my research. I am confident that the research we have developed together will create waves in the greater medical community. Thank you to my engineering committee members Drs. Jeffrey LaBelle and Vincent Pizziconi who have challenged me not to just be an engineer, but be the best engineer possible. I would like to thank them for working with me to refine my research goals while also giving me the freedom to develop something novel. Thank you to my final committee member, Dr. Daniel Collins, who was with me on the ground floor in figuring out just how far the definition of "interdisciplinary" could be pushed. His ideas and willingness to find unusual pathways pushed me to be a better researcher and academic.

Regrettably, it would be impossible for me to name each and every lab colleague, past and present, who have helped me in my research. There are far too many, but I thank you all to fit in this document. I would like to highlight Drs. Haithem Babiker and Christine Zwart, who were my mentors guiding me early on through this academic maze, as well as Chelsea Gregg and Katie Poterala, who were with me at the beginning of this research effort. Thank you for helping me establish my research foundation.

To my close friends,: without you all, maintaining the tenuous grasp of sanity – inherent to any doctoral program – would have been an insurmountable challenge. And to my family: for supporting my dreams of becoming a biomedical engineer with as much enthusiasm as my dreams of becoming an artist, I simply cannot thank you enough.

Sources of funding for this work include the American Heart Association (Beginning Grant-in-Aid), National Science Foundation (CAREER Grant), Science Foundation of Arizona (a special thank you to my educational mentor Dr. Tirupalavanam Ganesh), Phoenix Children's Hospital's Leadership Circle, the Achievement Rewards for College Scientists Foundation (and my sponsors Dr. and Mrs. Volker and Lynne Sonntag), and the Lund Foundation. Without the support of these institutions, none of the following would have been possible.

TABLE OF CONTENTS

Page

CHAPTER Page

CHAPTER Page

LIST OF TABLES

Table Page

CHAPTER 1

INTRODUCTION: CONGENITAL HEART DISEASE AND HEART FAILURE

1.1 The Human Heart

The cardiovascular system transports blood, carrying nutrients, oxygen, and waste products to and from cells throughout the body. The cardiovascular system includes the heart and its interconnected network of blood vessels. In a normal individual, the heart is comprised of two pumps driving two continuous circuits: pulmonary circulation and systemic circulation. The right side of the heart accepts oxygen-poor blood from the body via the vena cava. The blood then passes through the right atrium, right ventricle, and pulmonary arteries before reaching the lungs. The blood is re-oxygenated and returns to the left heart via the pulmonary veins. The blood then passes through the left atrium, left ventricle, and the aorta before traveling through the rest of the body. In a normal, healthy individual the left and right side of the heart are not confluent [1], [2]. An illustration of a normal heart is shown in Figure 1. Aberrations of this morphology, either congenital or acquired in origin, can affect an individual's circulatory system's ability to transport of blood.

1.2 Congenital Heart Disease

Congenital heart disease (CHD) is defined as a morphological aberration of anatomy present at birth [2]. While the incidence rates of CHDs are contested [3], some sources put prevalence as high as 5.3% of the fetal population and 1.08% of the pediatric population

[2]. CHDs may cause significant functional anomalies, needing intervention to correct. There are two main categories of CHDs: cyanotic and acyanotic disease.

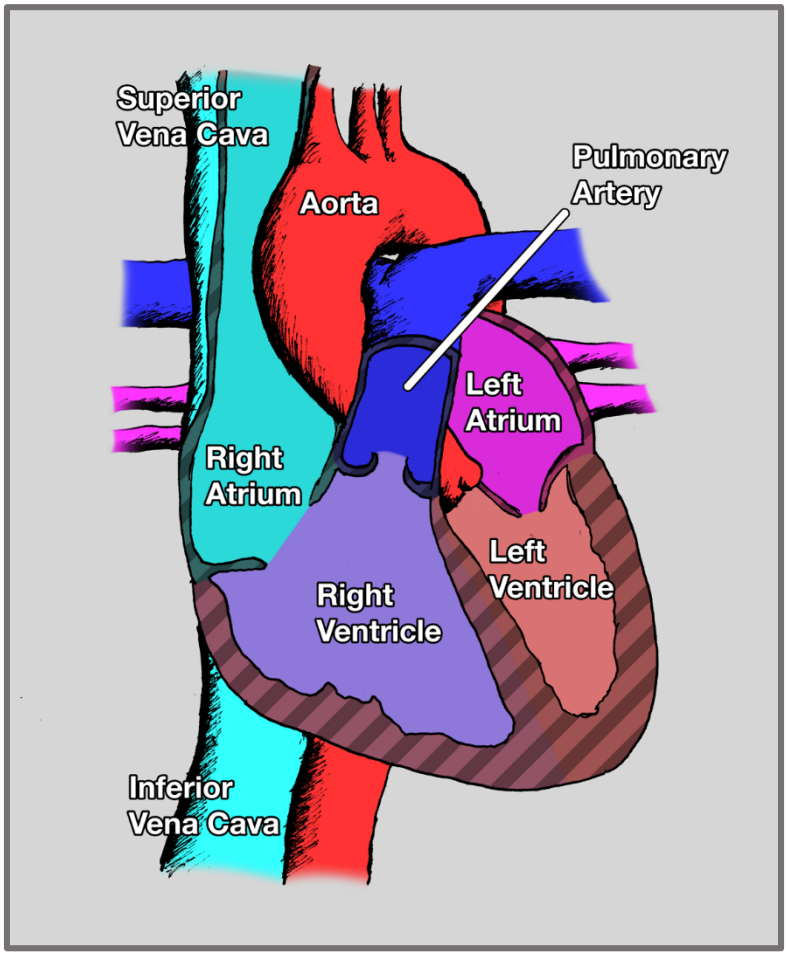

Figure 1: An anatomical illustration of normal cardiac anatomy. Blue colors represent components of the heart containing oxygen-deficient blood, while red colors present components containing oxygen-rich blood.

1.2.1 Cyanotic Congenital Heart Disease

Cyanotic congenital heart disease is a broad class of cardiac malformations causing oxygen-deficient blood to be returned to the systemic side of the circulation without first

being oxygenated in the lungs. This return of oxygen-deficient blood to the arterial circulation without oxygenation is also known as right-to-left shunting.

The shunting can have multiple morphological origins including aberrant systemic and pulmonary pathways, elevated pulmonary resistance, and single ventricle anatomy[1] [1]. Aberrant pathways in cyanosis include atrial and ventricular defects where oxygen-rich and oxygen-deficient blood mixes in addition to abnormal pathways where great vessels may be switched from normal presentation. The shunting presents with bluish coloration of the patients skin and mucous membrane [1]. An example of Tetralogy of Fallot, a cyanotic lesion, is shown in Figure 2. Surgical correction is likely necessary for the patient's ability to survive long term [1], [4].

[1] The following lesions are generally considered cyanotic CHD: transposition of the great arteries, Tetralogy of Fallot, heterotaxy, pulmonary atresia with intact ventricular septum, total anomalous pulmonary venous return, tricuspid atresia, double outlet right ventricle, truncus arteriosus, and Ebstein's anomaly. This list is not intended to be comprehensive as there are over 3000 lesion types including unique presentations and combinations.

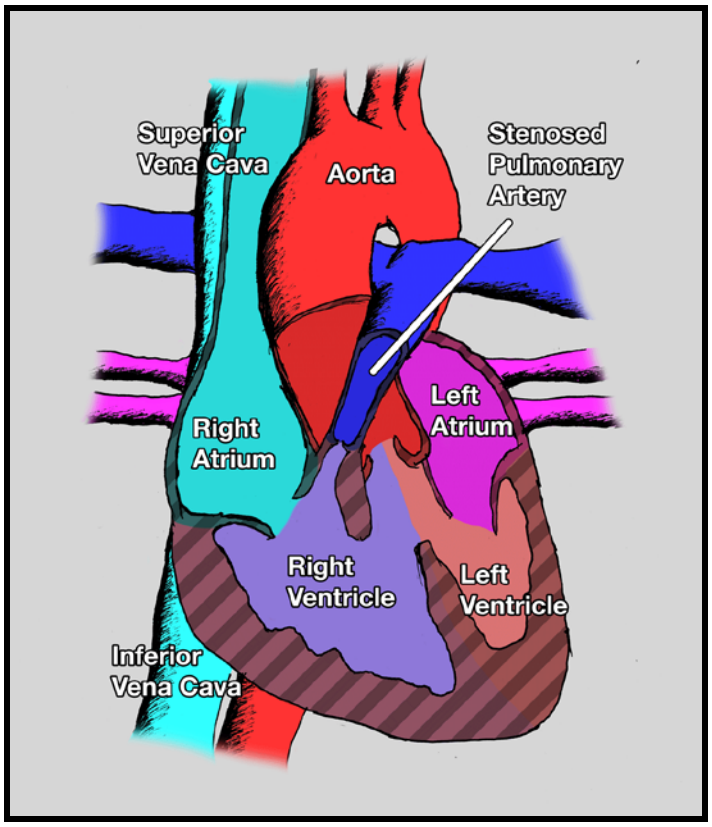

Figure 2: Illustration of Tetralogy of Fallot. This cyanotic lesion includes 4 defects: 1) ventricular septal defect, 2) overriding aorta, 3) pulmonary obstruction, and 4) hyperplastic right ventricle.

1.2.2 Acyanotic Congenital Heart Disease

Acyanotic congenital heart diseases are split into two categories: shunted and non-shunted acyanotic lesions[2]. In shunted lesions, oxygen-rich blood bypasses the systemic system and returns to the lungs. In non-shunted lesions, blood is obstructed by a morphological aberration of the cardiovascular anatomy. Non-shunted lesions often cause increases in

[2] The following classifications are generally considered ayanotic CHD lesions: atrial septal defect, ventricular septal defect, atrioventricular canal, patent ductus arteriosus, aortic stenosis, coarctation of the aorta, pulmonary stenosis, mitral stenosis, and mitral regurgitation. This list is not intended to be comprehensive.

pressure load on a ventricle, as the ventricle must overcome the increase vascular resistance from the obstruction [1]. An example of coarctation of the aorta, an acyanotic lesion, is seen in Figure 3.

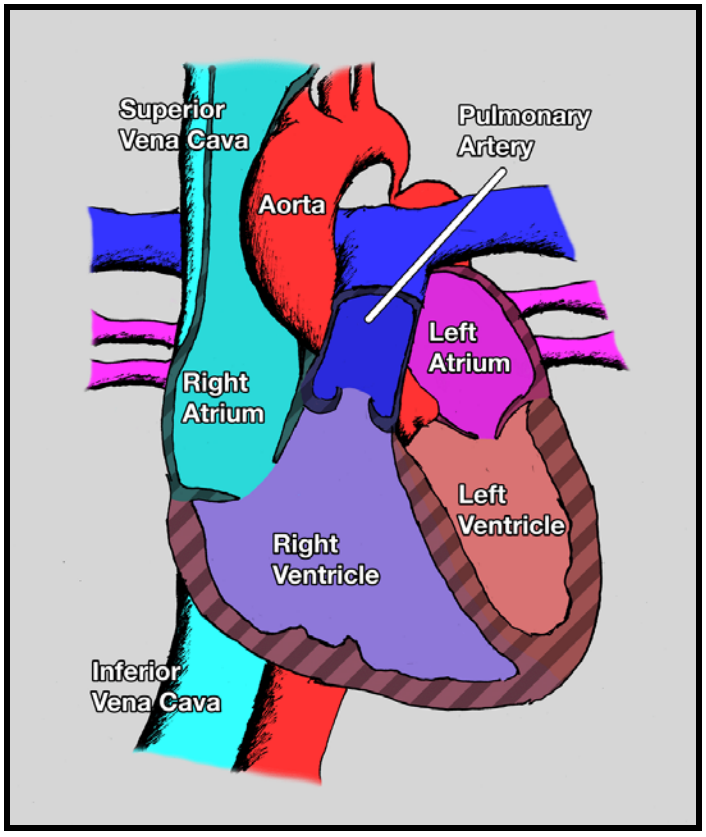

Figure 3: Illustration of coarctation of the aorta. This acyanotic lesion features an obstructed aortic arch.

1.2.3 CHD Repair & Planning

Some presentations of CHD lesions require surgical intervention early in life. In fact, most patients with cyanotic CHD undergo surgery (for repair or palliation) within the first week

of life [1]. Despite the latest development in medical technologies and techniques, neonates, infants, and children still have high rates of mortality from surgery.

According to the Fall 2014 data harvest by The Society of Thoracic Surgeons, participating hospitals report neonates, infants, and children have mortality rates of 7.7%, 2.5%, and 1.0%, respectively, following intervention; this figure does not include patient mortality indirectly related to surgeries [5]. While these mortality rates have decreased over the last 4 years, novel interventions or planning schemes may further reduce surgical complications and related deaths. One mechanism for reducing morbidity and mortality in the operating room is to reduce the time spent in surgery and the time spent in the operating room, as both are related to higher incidences of post-surgical infection [6]. An efficient surgical planning scheme may reduce the time-related factors in the operating room, minimizing morbidity and mortality associated with complications.

In order to better plan for CHD intervention, understanding the current mechanism for surgical planning is critical. Anatomical variation and physiological aberration can be imaged through multiple modalities including echocardiogram, computed tomography (CT), and magnetic resonance imaging (MRI) to name a few. While each modality collects data through different mechanisms, traditional visualization is through 2D images on a screen or printed media. This forced perspective leads the operator or clinician to convert the 2D images into 3D volumes in his or her head. The understanding of the spatial relationships of complex, diseased anatomy is determined by the visual system of the clinician; this process can lead to high errors in reading. Human errors in imaging reading and 2D-to-3D visual interpretation could be prevented by providing the user with native

3D visualization of the imaging data. Newer imaging systems enable 3D visualization of 2D medical images [7], [8].

Direct volume rendering (DVR) is one 3D visualization technique of 2D data. DVR recreates a 3D image similar to a point cloud representation of the 2D slices. Each pixel in a 2D image slice is recreated as a point (discrete voxel) and assigned a color value and opacity [9]. The effect is a ghost-like image where different tissues have discrete transparency and color values. This process heavily relies on the human visual system for real-time interpretation as shown in Figure 4; as such human error is present in the reading of DVR medical images.

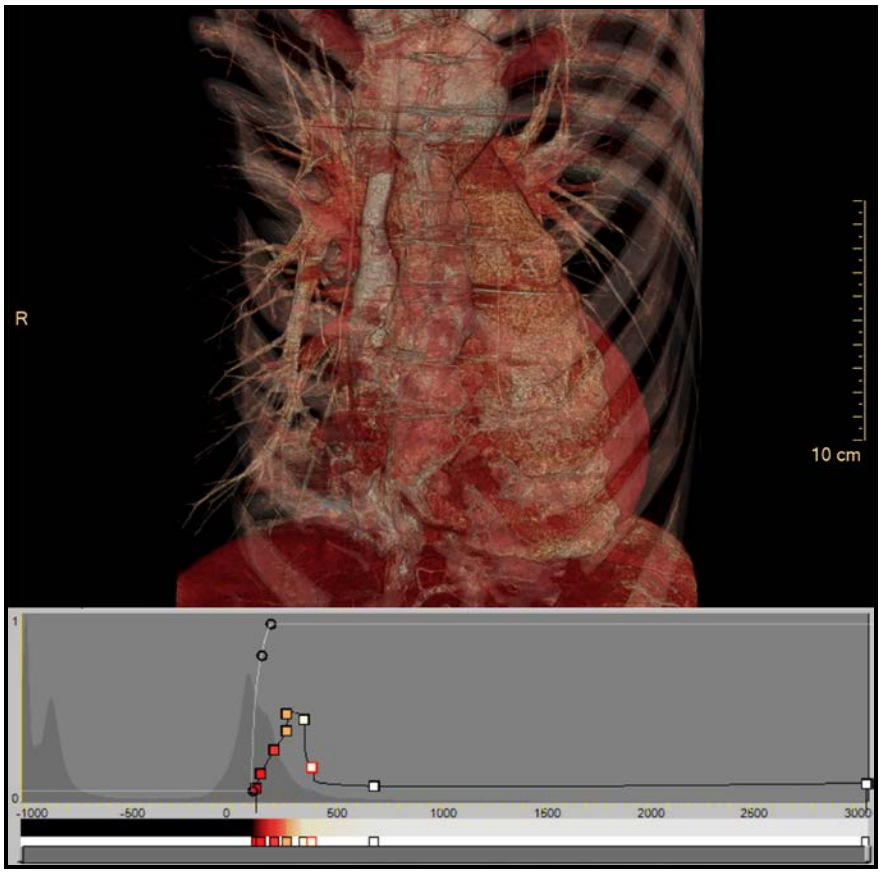

Figure 4: DVR of a CHD lesion. The histogram illustrates opacity and color for the tissues associated intensity value on a CT.

DVR has limitations to representing tissues of similar intensity value as well as limitations to segmenting a single tissue into constituent parts for further analysis or interventional planning. In complex CHD repair, accurate imaging and a controlled method of visualization are key in conceptualizing the complex anatomy prior to intervention. Novel image processing technologies such as image segmentation, surface mesh reconstruction, and 3D printing can reduce the amount of conceptualization by the human visual system, leading to stronger surgical planning schemes.

1.3 Advanced Heart Failure

In the event that CHD repair or acquired cardiac disease repair is insufficient to return compensated heart function, the patient may progress to decompensation, or advanced heart failure. The American Heart Association defines heart failure as a chronic, progressive condition in which the heart is unable to pump enough oxygenated blood to meet the body's requirements [10]. Advance heart failure is the final stage in which palliative treatments or symptom management is insufficient for patient survival [11].

In pediatrics, the largest source of advanced heart failure is dilated cardiomyopathy (DCM). This is an acquired disease that may or may not be present in patients with congenital malformations. DCM is the enlargement of the left or both ventricles in addition to lost contractility of the myocardium [12]. Approximately 1 in 100,000 pediatric patients are diagnosed each year with symptoms of DCM in the USA; although, this population may be underrepresented [12], [13]. In addition, DCM accounts for 10,000 deaths annually [12]. DCM is the primary indication for 65% of heart transplants in children 11-17 years of age [13]. Children diagnosed with DCM and decompensated heart failure represent a high-risk subgroup, often benefiting from optimal heart failure management and prompt evaluation for a heart transplant.

Each year in the United States, 250,000 people are diagnosed as having advanced heart failure; nearly 1% of that figure represents the pediatric population [14], [15]. Availability of donor hearts fall far short in meeting the demand needed to treat those with advanced heart failure. Only 2,200 donor hearts are available every year with 400 of those hearts used for pediatric transplants [14], [15]. In fact, children listed for a heart transplant

are subject to the highest waiting list mortality in solid-organ transplant medicine in the United States [16]. According to Almond *et al.*, 17% of pediatric patients died while awaiting heart transplantation (from 1999 – 2006) [16]. While acknowledging this deficit of available donor hearts and to improve patient outcomes and survival, it is critical that pediatric patients in advanced heart failure be promptly identified for emergent deployment of mechanical circulatory support (MCS) devices while waiting for heart transplantation.

1.3.1 Mechanical Circulatory Support

In the event that donor hearts are unavailable, devices may be used as a stop gap effort to extend the patient's time to receive a heart or return organ function necessary for the success of heart transplantation. This process of using a device to extend patient viability is known as bridge-to-transplantation or bridge-to-candidacy/decision [17]. MCS devices attempt to preserve end-organ function and quickly restore functional status of the circulatory system by augmenting or replacing cardiac function. Ventricular assist devices (VADs) and artificial hearts, subsets of MCS devices, have been used in the pediatric population, since the late 1980s, as a bridge-to-transplantation [18]. VADs augment ventricular function by supplementing the ventricular pumping action or completely taking on the pumping function. The Total Artificial Heart (SynCardia Systems, Tuscon, AZ)[3] is an MCS-variant in which the device fully replaces the patient's ventricles. While no unified

[3] While some media and publications exclude the TAH from VAD classification due to its physical replacement of the ventricles, this thesis will utilize International Society of Heart & Lung Transplantation's (ISHLT) classification of the TAH. ISHLT categorizes the TAH as a VAD.

database exists that tracks MCS deployment, the International Heart Lung Transplant Society provide evidence that MCS use is increasing, especially in pediatric medicine [13].

Expanded production of various types of VADs has allowed the technology to proliferate in the pediatric population, doubling in the last decade [19]. At present, nearly 20% of pediatric heart transplant recipients are bridged-to-transplantation with VADs [13]. The Total Artificial Heart (TAH) has been approved by the US Food and Drug Administration (FDA) as a bridge-to-transplant in patients with severe biventricular heart failure [20]. The device replaces the native ventricles and valves, resides in the pericardial space, and connects directly to the atria and the great vessels. The TAH provides biventricular pulsatile flow similar to normal body circulation. The device and its *in situ* implantation is show in Figure 5. Despite the need for MCS devices in pediatrics, development of pediatric-oriented VAD devices has been slow. Novel surgical interventions with of adult-oriented devices have been used to address the undersized patient's anatomical restrictions [21]. Until device manufacturers better address pediatric needs, visualization techniques can assist clinicians in determining whether a pediatric patient can accommodate an adult MCS device as well as plan for potential complications, thus expanding the potential population that can benefit from these life-saving devices.

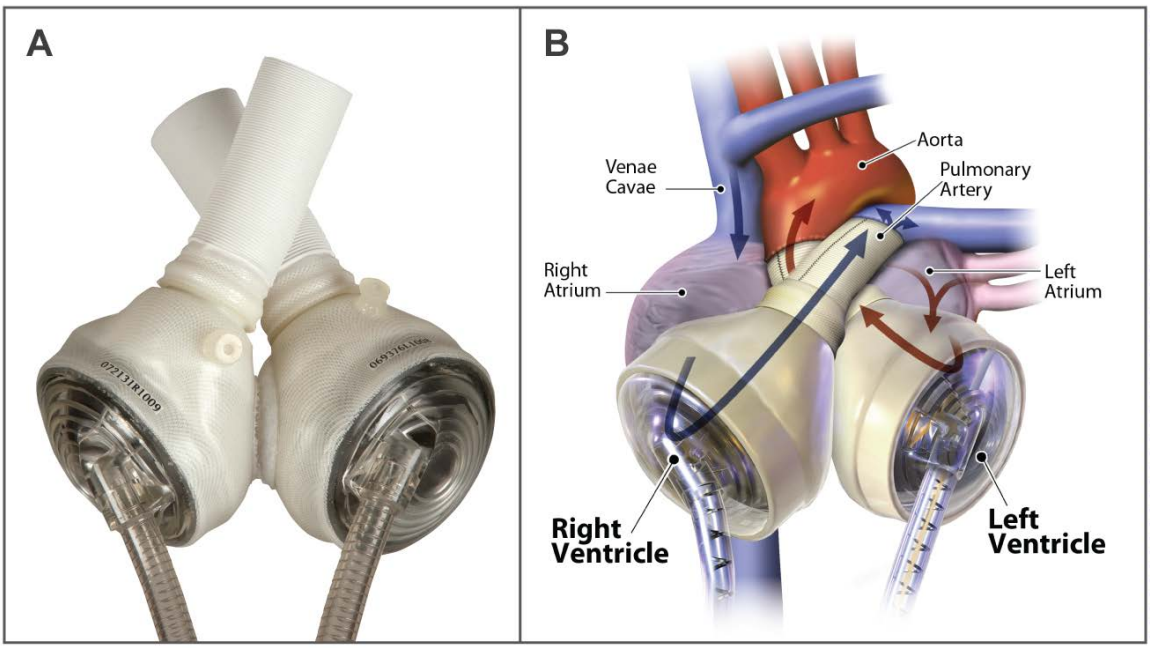

Figure 5A: A photo of the SynCardia 70cc Total Artificial Heart. The TAH is comprised of two mechanical ventricles. Figure 5B illustrates the *in situ* implantation. Inflow and outflow cuffs attach the mechanical ventricles to the right atrium and pulmonary artery for the right device and left atrium and aorta for the left device. Images Courtesy: SynCardia Systems, Inc.

CHAPTER 2

PHYSICAL MODELING OF CONGENITAL HEART DISEASE

2.1 Introduction: Current Challenges in CHD Surgical Planning

Pre-procedural planning has long been one of the most challenging aspects of cardiovascular surgery and intervention. The reason for this is simple: the cardiovascular anatomy is isolated, internal to the body and is not easily accessible prior to the start of a clinical procedure. The advent of medical imaging and image processing technologies have enabled significant advances in pre-procedural planning, allowing cardiovascular anatomy to be visualized noninvasively before an operation. However, pre-procedural planning based on images alone does not convey any tactile information and fails to completely prepare surgeons and interventionalists.

The surgical repair of complex congenital heart disease (CHD) or advanced heart failure is extremely challenging as the surgeon must consider the extraordinary number of variations and presentations of cardiac morphology including malformations. Traditionally, surgical and interventional planning was based on ultrasound or catheter-guided x-ray; the resulting images were two-dimensional (2D) slices or projections of patient anatomy. As interventions were unique to each morphological presentation of a lesion, clinicians would have to translate 2D images to three-dimensional (3D) structures in their head. The intervention would proceed with this conceptual 3D reconstruction from acquired 2D images.

The use of 3D visualization through DVR to plan for complex cardiovascular surgery has been well developed over the previous two decades [8]. An example of DVR

from a CT scan is seen in Figure 6. Volumetric rendering has its own limitations. Without a novel viewing system, the 3D reconstruction are viewed on a 2D dimensional screen. True 3D perspective is lost due to this viewing limitation. In addition, absolute size is lost in the viewing of a 3D model on a computer screen. However, 3D visualization coupled with 3D printing provide a mechanism to construct patient-specific, scale models of cardiovascular anatomy that surgeons and interventionalists can examine prior to a procedure. These 3D printed models, or physical heart defect models (PHDMs), are perceived to be a novel tool with the potential of enhancing surgical planning procedures.

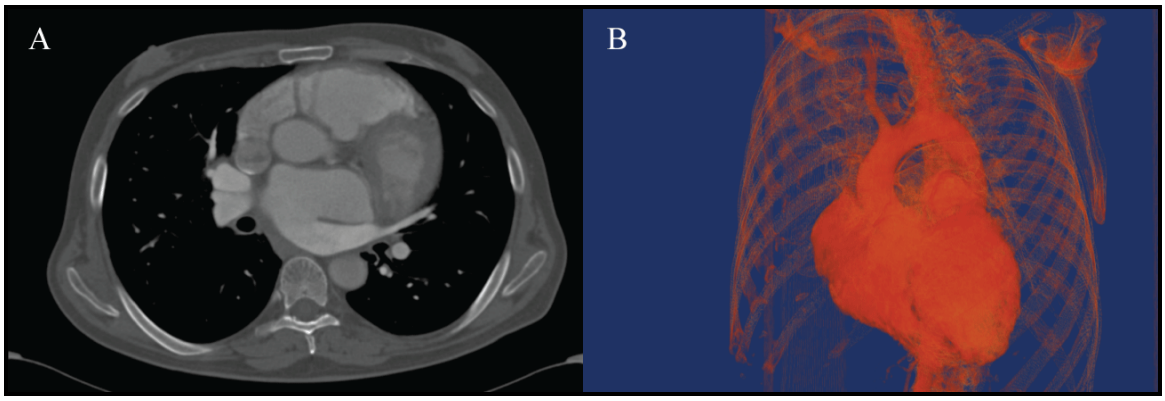

Figure 6A: Contrast-enhanced CT scan of a CHD patient. Figure 6B: A DVR reconstruction developed from the CT scan.

Prior works have developed mechanisms for improving automated means of reconstructing CT and MR images as 3D volumes. The result are 3D models that more accurately represent the actual patient's morphology. Prior works have also explored the use of 3D printing for various purposes including 1) surgical planning, 2) content-knowledge medical education, 3) procedural-knowledge medical education, and 4) family

consultation, to only name a few [22]–[24]. With regards to surgical planning models, patient geometry has been printed in multiple modalities and materials to help a clinician plan a complex intervention. However, few studies present a methodology of using 3D printing for surgical planning enhancement in a true clinical integration framework. In fact, this work presents the first strong evidence beyond anecdotal cases for the efficacy of 3D printing for cardiac surgical enhancement.

2.1.1 Technology Acceptance Model in Medicine

According to Davis *et al.*, the voluntary use of a technology is described as technology acceptance [25]. Accordingly, a technology acceptance model (TAM) is one of the established methods of examining the behavioral intention of or intent to adopt a new technology. The foundational TAM looks at perceived usefulness and perceived ease of use to describe behavioral intention associated to a specific technology [25]. Perceived usefulness is the perception that using the particular technology will be advantageous over the status quo. Perceived ease-of-use is the perception that the utilization of the new technology will be relatively non-obtrusive to implement. Both of these aspects are influenced by the attitude of an individual in relation to the technology. Attitude is the behavioral response to adopting the new technology. TAM is an attempt to quantify these behavioral responses either for understanding users' intent or to inform future design iterations. TAM has been expanded to include additional behavioral intention influences, known here as "adjustments" such as enjoyment, intention to use, and awareness; these adjustments are subsets of perceived ease-of-use [26], [27]. All of these subjective

behavioral metrics are affected by external variables. These variables can be related to an individual such as prior beliefs or general attitude (not related to attitude regarding the technology). The TAM construct can be seen in Figure 7.

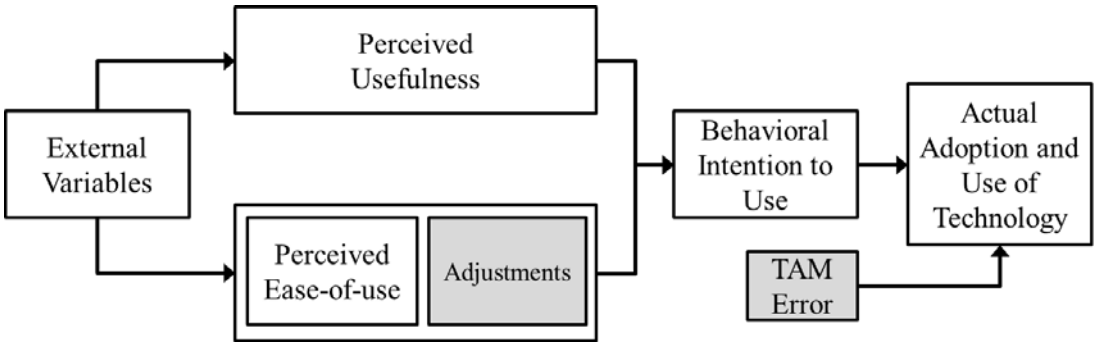

Figure 7: Technology acceptance model. The TAM investigates a user's behavioral intention to use a technology. This behavioral intention can be broken down to perceived usefulness and perceived ease of use. The user's attitude could be affected by external variables such as user's preconceptions. The TAM initially described by Davis *et al.* was later amended to include additional behavioral adjustments (shaded box).

TAM has been utilized in many fields including information technology, workforce management, and medicine [28]–[30]. An 88-study meta-analysis conclude that the TAM is a valid and robust predictive model of behavioral intention. The model was found to be considerably more effective in describing intention when the respondents were a professional cohort as opposed to a general population cohort [29]. Considering past studies and this meta-analysis, a professional cohort of cardiothoracic surgeons should be able to yield meaningful results on the behavioral intention to use PHDMs.

Without the perception of efficacy, defined by behavioral intention, the physical modeling of a patient's morphology would fail to be adopted into standard clinical practice.

To probe the cardiothoracic surgeons' technology acceptance of the PHDMs, a post-surgery assessment was implemented in the standard clinical care process at a collaborating institution. The post-assessment examined both perceived usefulness and perceived ease-of-use. To minimize workflow disruption in the clinical environment, TAM adjustments were not considered for this study. The techniques for developing the model, the educational study, and the associate advantages and disadvantages are discussed.

2.2 Methods: PHDM Construction

2.2.1 Patient Identification and Image Acquisition

Through the course of clinical care, cardiothoracic surgeons and cardiologist, at a collaborating pediatric hospital, identified 79 cases as candidates to receive a PHDM for surgical planning. The selection criteria was based on available image data in addition to perceived complexity of the anatomy (complex cases were more likely to produce a PHDM for surgical planning). For analysis purposes, the inclusion criteria was further defined as patients with a primary diagnosis of one of the following CHD lesions: 1) pulmonary atresia (ventricular septal defect variant), 2) Tetralogy of Fallot (pulmonary atresia and absent pulmonary valve variants), 3) double outlet right ventricle (transposition of the great arteries variant), 4) truncus arteriosus, 5) vascular rings, and 6) single ventricle. This restricted inclusion criteria truncated the cases for analysis to 33 cases.

Per standard-of-care, the 33 patients received a contrast-enhanced CT scan. The contrast agent illuminated blood volumes in CT image slices, enabling the differentiation

of cardiovascular anatomy from extra-cardiac anatomy as shown in Figure 8A. Spatial resolution of the CT datasets varied from patient-to-patient. Slice thickness (resolution in z-direction) commonly ranged from 0.325mm to 0.9mm; pixel spacing (resolution in x- and y-direction) ranged from 0.325mm to 0.625mm. Although less common to the PHDM process, MRI was used for 5 cases; although, only one such case was present in the restricted inclusion criteria. The MRI datasets lacked the spatial resolution found in the CT datasets. Voxel sizes for the MRI-based cases were as high as 2.5mm x 2.5mm x 2.5mm. The resulting images were packaged into Digital Imaging and Communication in Medicine (DICOM) files. The DICOM file format contains both the images that define the patient's anatomy as well as metadata. The metadata includes crucial information needed for the subsequent computational reconstruction such as voxel resolution.

2.2.2 Computational Reconstruction

The DICOM files were imported into Mimics Innovation Suite (Materialise, Lueven, Belgium), a medical image processing software suite. The software facilitated image segmentation, the process of separating regions of an image into discrete subsets. For common cardiac anatomy, the following blood volume subsets were segmented: left atrium (including pulmonary veins), right atrium (including vena cava), left ventricle, right ventricle, pulmonary arteries, aorta, and coronary arteries. Additional subsets were needed in instances where addition, anomalous structures were present (i.e., patent ductus arteriosus, aberrant vessels, etc.). The segmentation process produces binary masks of each

subset on each CT slice as shown in Figure 8B. These masks were reconstructed into three-dimensional (3D) surface mesh models.

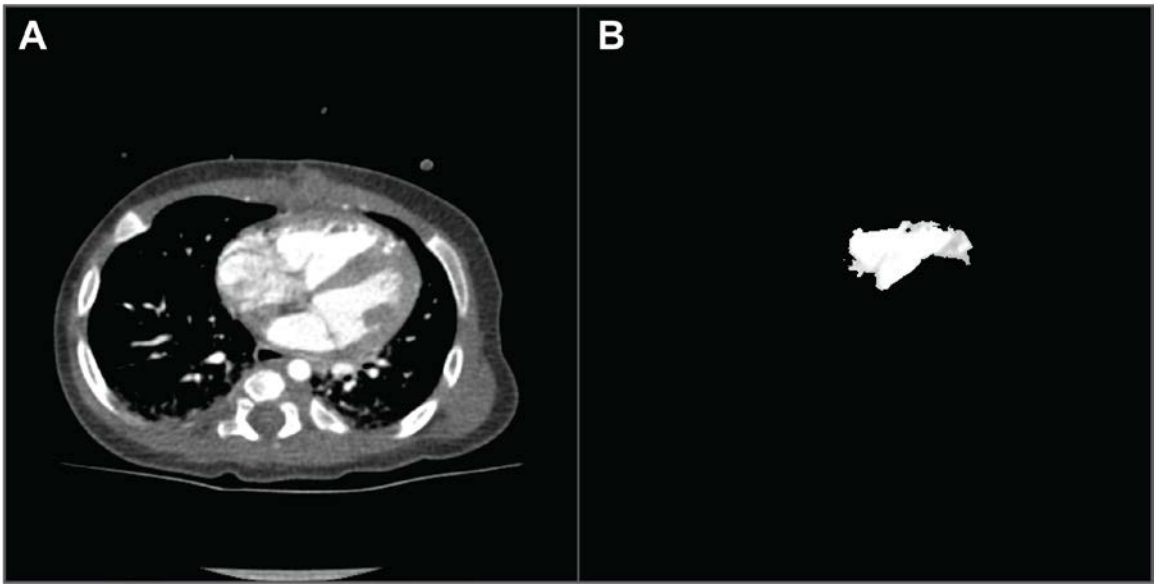

Figure 8A: Contrast-enhanced CT scan. B) Masked subset from CT scan.
The mask is of the right ventricle.

Computational cardiac anatomies were then imported into a 3D engineering software suite, Geomagic (3DSystems, Rock Hill, SC, USA), for additional post-processing. In order to better utilize the human visual system, the cardiac subsets were differentiated via a standardized color scheme as defined in Table 1. Generally, the right heart (including vena cava, right atrium, right ventricle, and pulmonary arteries) were colored with blue hues. The blue coloration signified structures containing oxygen-poor blood in a normal heart. Conversely, the left heart (including pulmonary veins, left atrium, left ventricle, and aorta) were colored with red hues signifying structures containing oxygen-rich blood in a normal heart. The color scheme was maintained even in cases were

the oxygen-nature of the blood was uncertain or reversed (such as cases of transposition of the great arteries). For patient-tracking purposes, each virtual model was labeled with a unique identifier. The computational post-processing method and results are shown in Figure 9.

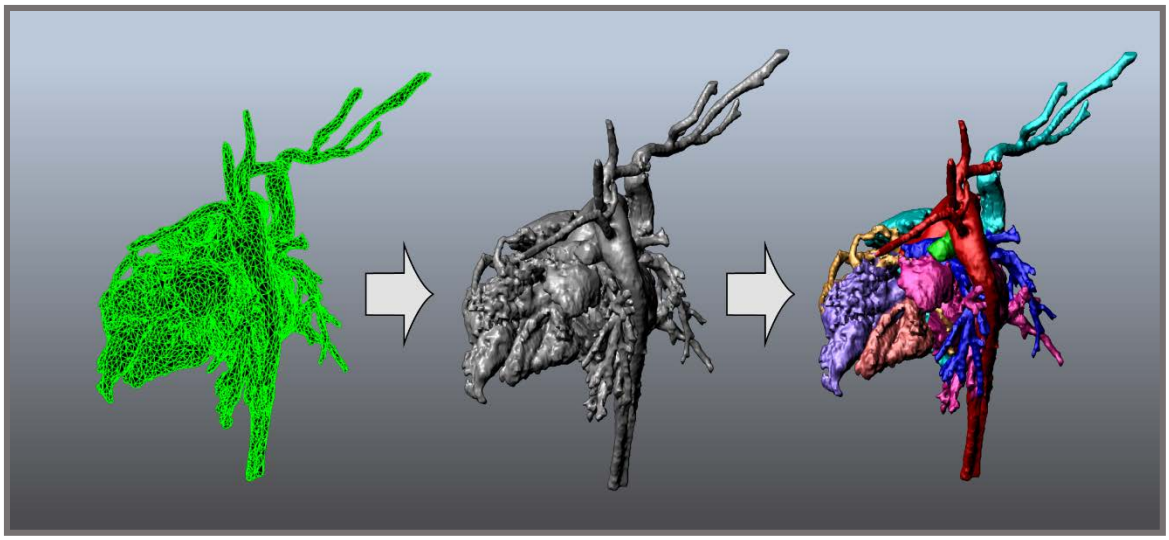

Figure 9: Left: The surface mesh based on a reconstruction is shown. Green outlines highlight the polygonal construction of the virtual model. Middle: a surface shaded model is shown. Morphological differentiation is perceived to be difficult. Right: The final colored surface mesh model. Colors differentiate the components of the heart based on a standardized color scheme in Table 1.

Geomagic also ensured 3D print viability by confirming that the mesh conformed to a water-tight standard[4]. The resulting models were packaged in a Virtual Reality Markup

[4] A surface mesh is comprised of 2D, polygonal (commonly triangular) elements describing the surface of an object. In instances where holes, intersecting polygons, or overlapping polygons exist on the surface, the mesh is not considered water-tight as there is no consistent computational definition for what is interior and exterior to the model. For 3D printing, this topological error results in uncertainty for what areas should be printed or excluded. 3D printing failures or inconsistencies are common in the presence of a non-watertight manifold.

Language (VRML2.0) file. This file format allows for color information to be retained. A final computational rendering is shown in Figure 10.

Table 1: The standardized color scheme was developed in conjunction with a radiologist at St. Joseph's Hospital and Medical Center.

Anatomical Structure(s)	Color	RGB Values	Hex Value
Aorta	Red	255:000:000	FF0000
Left Atrium	Bright Pink	255:030:164	FF1EA4
Left Ventricle	Light Red	255:105:105	FF6969
Pulmonary Arteries	Dark Blue	000:000:225	0000FF
Right Atrium & Vena Cava	Turquoise	000:255:255	00FFFF
Right Ventricle	Lavender	145:112:255	9170FF
Anomalous Structure	Green	000:255:000	00FF00
Coronaries	Light Orange	255:172:064	FFAC40

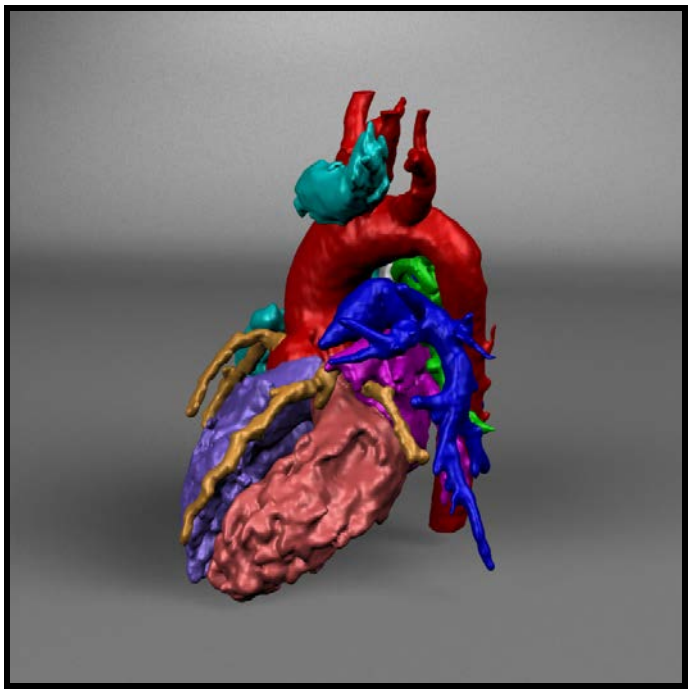

Figure 10: A computational reconstruction of a patient's congenital heart defect. The defect is Tetralogy of Fallot with multiple aorto-pulmonary collateral arteries. The standardized color scheme has been applied.

2.2.3 3D Printing and Post-Processing

Computer numerical control (CNC) cutting is a subtractive manufacturing process in which a physical object, based on a computer model, is created by selective removal of media from a work piece such as wood, metal or plastic. This process lacks the degrees-of-freedom needed for printing complex cardiovascular geometries. Accordingly, an in-house process was used to construct patient-specific PHDMs, using additive manufacturing – also known as 3D printing – technologies. This manufacturing process generates a physical object, based on computer model, through the deposition of media.

For the developed process, the color-coded computational models were 3D printed with a gypsum-based powder media in a zPrinter 650 (3D Systems, Rock Hill, SC, USA) 3D printer. This 3D printing technology uses a full cyan-magenta-yellow-key-ink (CMYK-ink), cyanoacrylate infiltration system. The printer deposits a 0.1 mm thick, flat layer of gypsum powder on a build platform. Print heads jet a cyanoacrylate binding agent and colorant onto the gypsum layer. The build platform drops 0.1 mm and the entire process is repeated continuously until the PHDMs have been fully printed. A schematic of the specific 3D print technology used can be seen in Figure 11.

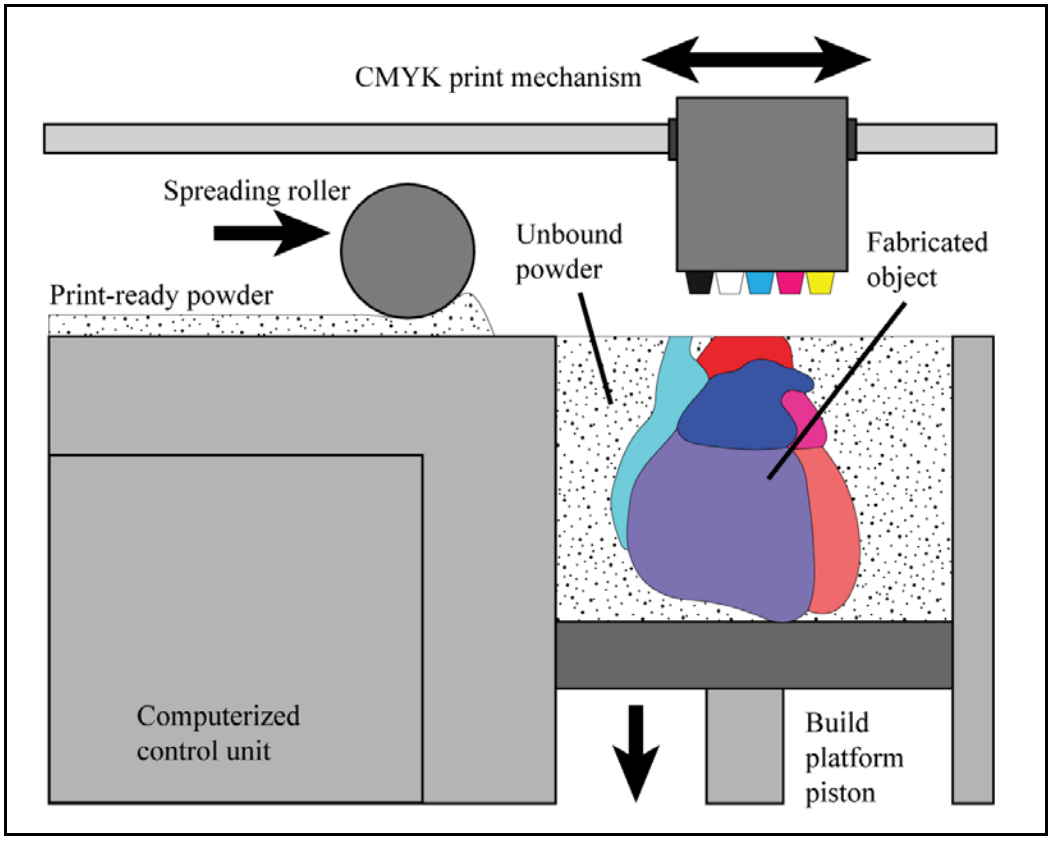

Figure 11: Schematic of the inkjet 3D printing process. A roller spreads a layer of powder on the build platform. A CMYK ink-cyanoacrylate print cartridge binds the single layer of powder together through inkjet deposition. The build platform lowers and the process is continuously repeated until the 3D print is complete.

Following removal from the 3D printer, the PHDMs were coated with three layers of clear enamel. Aerosolized coatings prevented surface inconsistencies while promoting even enamel distribution. Application of the first layer was enhanced with 20 mmHg vacuum pressure via a vacuum chamber. The vacuum-enhanced coating promoted enamel infiltration into the porous model media, thereby increasing durability and improving surface aesthetics. A final PHDM used for surgical planning is shown in Figure 12.

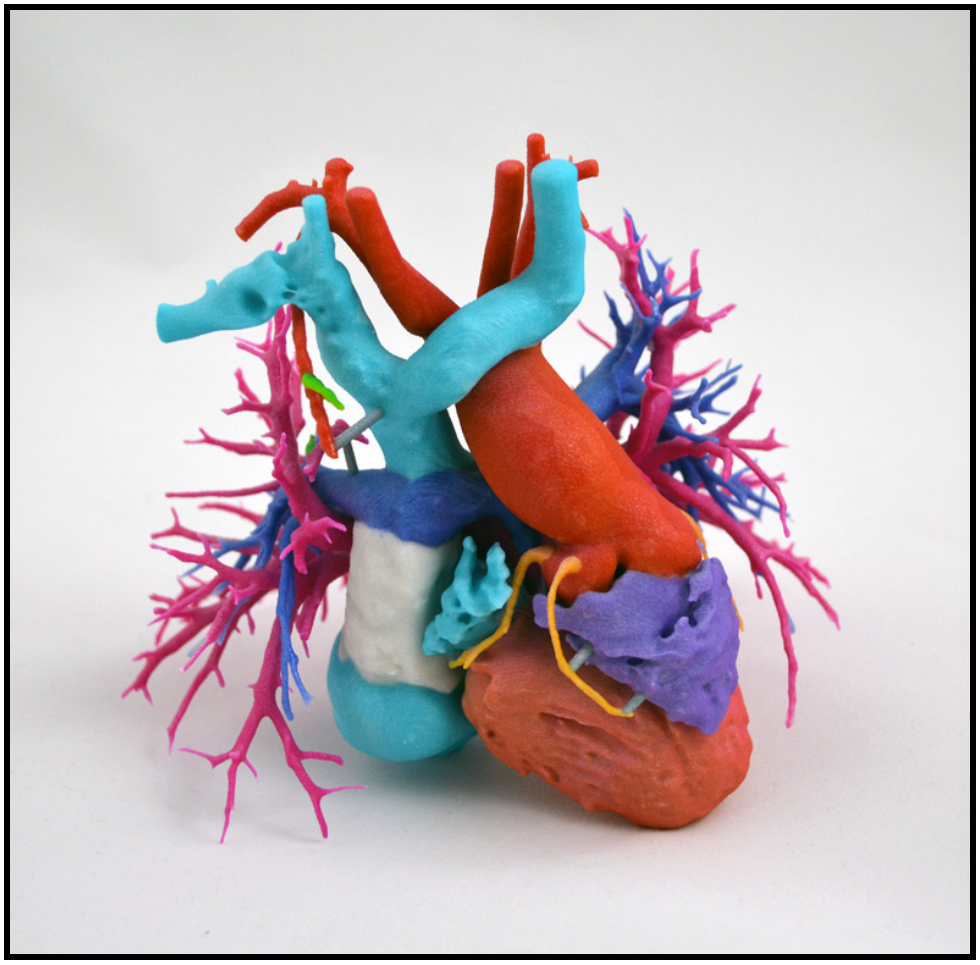

Figure 12: A fully-developed PHDM prior to use in a surgical consultation.

2.2.4 Design Modification

The design of any medical device undergoes an iterative process utilizing user feedback in subsequent design modifications. The PHDMs are no exception to this engineering design process. In fact, over the 5 years of surgical integration, the PHDMs have had many design modifications to address encountered challenges to use. Table 2 is an abridged list of requirements and design modifications.

Table 2: Design modifications for the PHDMs to address clinical needs.

	Engineering requirements	**Design modifications**
A	Production Time: A PHDM must be able to be completed within an emergent timeframe	• Integrated workflow into clinical environment to get immediate feedback on computational modeling • Moved structure differentiation from 2D segmentation to 3D modeling • Utilized on-site clinical image software system to decrease segmentation time
B	Durability: The PHDM to withstand the hostile user (i.e., the clumsy cardiologist)	• Added support structures to unsupported vessels, such as coronary arteries • Coated models in layers of clear enamel
C	Product Aesthetic: The PHDM must function as an educational tool (as validated by education studies), but also be appealing to families (not be rejected by the patient-family)	• Established strict RGB values for PHDMs for consistency • Coated models in layers of clear enamel
D	Longevity: The PHDMs must be tracked for future patient anatomy analysis or education studies	• Developed numbering scheme for case tracking • Printed labels on models

2.2.5 Model Validation

Each final PHDM used for surgical planning went through an iterative design process where a radiologist or cardiologist qualitatively assessed color-coding and anatomical accuracy at each modeling stage. When errors were encountered, the models were adjusted accordingly and rechecked. Each model was also evaluated by at least one other medical professional at the end of the process. Additionally, the virtual and estimated physical volumes for the initial 20 models were compared quantitatively with a t-test to verify PHDM accuracy. The virtual volumes were obtained directly from Mimics and the estimate physical volumes were obtained from 3DPrint (3D Systems, Rock Hill, SC, USA), the software that communicates directly with the 3D printer.

2.2.6 Technology Acceptance Model

Following a surgery, the cardiothoracic surgeon completed a TAM-questionnaire. The questionnaire was developed considering the constraints of an active, patient-care environment. Too many questions would impede clinical care. Four questions, seen in Table 3, were established using a generalized TAM model [25], [26].

Table 3: The TAM survey and available responses. The survey was placed directly into the post-surgical report for every cardiothoracic surgery.

1. Was a 3D printed model used for the preparation of or during surgery/intervention? a. Yes (during planning only) b. Yes (during surgery only) c. Yes (during planning and surgery) d. No
2. In your opinion, did use of the 3D printed model enhance your ability to execute a surgical repair? a. Yes b. No
3. If no model was used, did you note any additional morphological defects or unexpected variations unseen in the standard planning process? a. [Free text response]
4. Please provide any additional information describing the impact of the 3D printed model during the planning or execution of this patient's surgery? a. [Free text response]

For every CHD patient that underwent cardiothoracic surgery, the associated surgeon would complete the questionnaire following surgery. A qualitative and limited quantitative analysis was performed on the anonymized results from the study.

2.2.7 Post-surgical Analysis

Due to the literature-based correlation of surgical length of time to morbidity and mortality, the effects of PHDM-based planning were analyzed via a one-way analysis of variance (ANOVA). Response variables included 1) *operating room length of time* (minutes),

defined as the time differential from when the patient is wheeled into the operating room to the time he or she is wheeled out and 2) c*ase length of time* (minutes), the duration of the surgery. Direct morbidity and mortality was analyzed via contingency tables (with Fisher's exact test). Response variables included 1) *30 day readmission* (yes/no), the binary response whether the patient had to be readmitted to the hospital within 30 days of hospital discharge, and 2) *30 day mortality* (yes/no), the binary response whether the patient died post-surgery within 30 days of hospital discharge.

2.3 Surgical Planning Case Studies

Two case studies are presented here to illustrate anecdotal utility of PHMDs for 1) interventional planning and 2) patient-family education.

2.3.1 Multiple Aorto-Pulmonary Collateral Arteries Case Study

Tetralogy of Fallot (TOF), pulmonary atresia (PA), and major aorto-pulmonary collateral arteries (MAPCAs) need complex interventions, and pre-natal diagnosis allows for appropriate peri-partum planning. A patient was diagnosed *in utero* as presenting with TOF/PA/MAPCAs. Cardiac CT scanning with a minimal radiation protocol at 1 day of age confirmed this dual pulmonary blood supply from pulmonary arteries and MAPCAs. The true pulmonary arteries were hypoplastic and confluent and appeared distributed to all major lung segments.

3D CT reconstruction and 3D printing were performed to illustrate the absolute, anatomic location of the MAPCAs and their relative location in relation to pulmonary arteries. The PHDM was utilized in the surgical planning consultation two days prior to surgery. On day 7, the patient was transferred to the destination surgical institution. The reconstruction and PHDM (available in the operative suite) were used to guide successful placement of a large central aorto-pulmonary shunt. In addition, the PHDM was used as a map for subsequent coil embolization of 2 of 3 known aortopulmonary collaterals. The third was found to be atretic. The PHDM-enhanced planning helped focus catheter-based intervention and is perceived to be the reason for reduced fluoroscopy (radiation) time and contrast exposure. The central shunt remains in place to promote growth of confluent native pulmonary arteries. The patient is awaiting complete repair.

Based on the clinicians experience with the PHDM, 3D printing of CT datasets may provide significant advantages in pre-procedural planning in many additional cases. This method can allow for reduction in fluoroscopy time, resulting in lower radiation exposure, and may allow reductions in general anesthesia exposure and cardiopulmonary bypass time (where present), possibly resulting in lower complication rates.

The PHDM was also used as a didactic tool to help educate the patient's parents and about their son's cardiac anatomy and associated malformations. The patient's mother can be seen holding the PHDM in Figure 13. The educational experience was embraced by the patient's family. Surprisingly, the PHDM was utilized as a coping mechanism by the family. The mother and father received tattoos of the PHDM. Inclusion of this rapidly developing technology within cardiovascular centers needs further study, but has the

potential to revolutionize diagnosis, patient-family education, and patient and patient-family coping mechanisms.

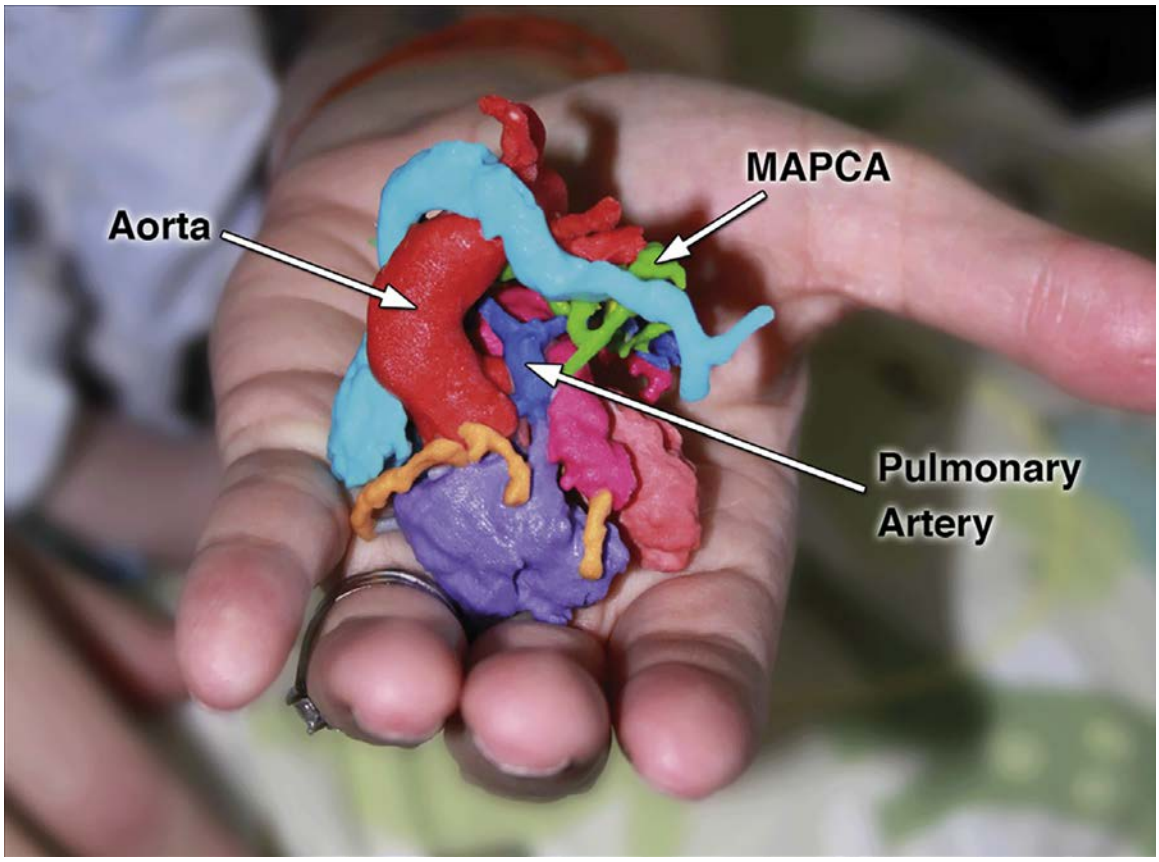

Figure 13: A PHDM in the hand of a patient's mother. The patient has Tetralogy of Fallot, pulmonary atresia, and major aorto-pulmonary collateral arteries.

2.3.2 Hypoplastic Left Heart Syndrome Case Study

Patient-family education is an important component of the clinical care process that is often overlooked. A 1 month old male presented with a CHD lesion, single ventricle, at birth. Diagnosis of hypoplastic left heart syndrome was confirmed via ultrasound. A contrast-

enhanced CT scan was performed as part of the clinical care process and as a means for surgical planning. The patient's family was non-english speaking, and the institution's interpreter did not cover the specific language spoken by the family. A non-medical interpreter was brought in to explain to the parents the diagnosis and surgical plan for the patient. As common to many institutions, a 2D schematic drawing was created to illustrate the anatomical malformation. The clinical staff and interpreter observed that the family appeared to fail to understand the diagnosis and surgical plan. A PHDM was created of the patient's anatomy and provided to the clinical staff. The interpreter and the clinical staff used the PHDM for patient-family education. The family embraced the PHDM as a means of patient-family education and asked to keep the model following surgical repair. An early surgical palliation was completed successfully.

The case study illustrates a role for the PHDM outside the confines of the surgical conference room and the surgical suite. The patient-family should not be overlooked as a part of the clinical care process. In fact, better education of the patient-families has been linked to reduced readmissions and perceived improvement in clinical outcomes [35], [36]. The role of PHDMs in patient-family education warrants further study.

2.4 Results of Surgical Planning Study with PHDMs

2.4.1 Model Validation

A gross volumetric comparison of computational model from reconstruction to material estimate, by the 3D printer interface, was made for the initial 20 hearts. There was no

statistical difference in measured mean between surface mesh model and output of the 3D printing software when adjusting for bleed compensation[5]. An experimental volume measurement via displacement was not performed due to porosity of the PHDM media.

All models were qualitatively validated by a medical professional (cardiothoracic surgeon, cardiologist, or radiologist) prior to 3D printing. All models were approved for anatomical accuracy from the available medical images.

2.4.2 Surgical Results

Between September 1, 2012 and December 31, 2014, 928 primary-case cardiothoracic surgeries took place at a collaborating pediatric hospital. Of these cases, 79 cases received PHDMs for surgical planning. Thirty-three cases were identified as being planned with a PHDM fitting the restrictive inclusion criteria (Section 2.2.1) for subsequent ANOVA analysis. Fitting the same inclusion criteria, 113 cases are identified as being planned through traditional (non-PHDM) methods. The effects of PHDM-based planning on the operating room length of time and case length of time were analyzed via a one-way ANOVA.

First, the effect of the PHDM-based planning on the entire block of restricted criteria was analyzed as seen in Tables 4 and 5.

[5] The 3D printing technology jets a binding agent onto a powder media. Bleed compensation is the hardware's attempt to control error of the binding agent bleeding beyond its initial contact point. In the model validation, bleed compensation was the default printing mode.

Table 4: ANOVA table illustrating the effect of PHDM-based planning on operating room length of time and case length of time. Green cells illustrate the lower, preferred mean time for surgeries planned with a PHDM.

Operating room length of time (PHDM vs Traditional Planning): all included patients

Source	D.F.	Adj. S.S.	Adj. M.S.	F-Value	P-Value
PHDM	1	866	865.6	0.07	0.798
Error	144	1894507	13156.3		
Total	145	1895372			

Planning	N	Mean (minutes)	StDev	95 CI
Traditional	113	333.5	114.5	(312.2, 354.9)
PHDM	33	327.7	115.5	(288.3, 367.2)

Case length of time (PHDM vs Traditional Planning): all included patients

Source	D.F.	Adj. S.S.	Adj. M.S.	F-Value	P-Value
PHDM	1	1916	1916	0.18	0.674
Error	144	1557292	10815		
Total	145	1559208			

Planning	N	Mean (minutes)	StDev	95 CI
Traditional	113	229.33	101.81	(209.99, 248.66)
PHDM	33	220.7	111.3	(184.9, 256.4)

Table 5: Contingency tables illustrating the effect of PHDM-based planning on 30-day readmission and 30-day mortality. Fisher's exact test was used to determine probability for the rejection of the stated null hypothesis.

30-day Readmission (PHDM vs Traditional Planning): all included patients

Count Total%	No 30-day Readm.	30-day Readm.	Total	Fisher's Exact Test
No PHDM	31 22.30%	78 56.12%	109 78.42%	Null Hypothesis: • Probability of readmission is greater for surgeries planned with a PHDM • P-value = 0.1609
PHDM	12 8.63%	18 12.95%	30 21.58%	
Total	43 30.94%	96 69.06%	139 100.0%	

30-day Mortality (PHDM vs Traditional Planning): all included patients

Count Total%	No 30-day Mort.	30-day Mort.	Total	Fisher's Exact Test
No PHDM	111 76.03%	2 1.37%	113 77.40%	Null Hypothesis: • Probability of 30 day mortality is greater for surgeries planned with a PHDM • P-value = 0.5978
PHDM	33 22.60%	0 0.00%	33 22.60%	
Total	144 96.63%	2 1.37%	146 100.0%	

While ANOVA and Fisher's exact test failed to illustrate PHDM effect with a p-value less than 0.05, every response variable trended toward more favorable outcomes for PHDMs. As there are many different types of surgeries and associated complexities, surgeries were further blocked in order to estimate PHDM effect for specific diagnoses.

For example, double outlet right ventricle (DORV) presenting with the transposition of the great arteries (TGA) variation cases and well as truncus arteriosus cases were analyzed independent of other cases with regards surgical time response variables. The ANOVA tables for this analysis are in Table 6 and 7.

Table 6: ANOVA tables for the effect of PHDM in planning for DORV-TGA cases. Response variable include operating room length of time and case length of time.

Operating room length of time (PHDM vs Traditional Planning): DORV-TGA

Source	**D.F.**	**Adj. S.S.**	**Adj. M.S.**	**F-Value**	**P-Value**
PHDM	1	28998	28998	2.16	0.179
Error	8	107185	13398		
Total	9	136184			

Planning	**N**	**Mean (minutes)**	**StDev**	**95 CI**
Traditional	8	466.1	121.1	(371.8, 560.5)
PHDM	2	331.5	67.2	(142.8, 520.2)

Case length of time (PHDM vs Traditional Planning): DORV-TGA

Source	D.F.	Adj. S.S.	Adj. M.S.	F-Value	P-Value
PHDM	1	26368	26368	1.88	0.207
Error	8	111962	13995		
Total	9	138330			

Planning	N	Mean (minutes)	StDev	95 CI
Traditional	8	359.4	118.4	(262.9, 455.8)
PHDM	2	231.0	117.4	(38.1, 423.9)

Table 7: ANOVA tables for the effect of PHDM in planning for truncus cases. Response variable include operating room length of time and case length of time.

Operating room length of time (PHDM vs Traditional Planning): Truncus

Source	D.F.	Adj. S.S.	Adj. M.S.	F-Value	P-Value
PHDM	1	18371	18371	2.25	0.185
Error	6	49087	8181		
Total	7	67458			

Planning	N	Mean (minutes)	StDev	95 CI
Traditional	6	452.7	99.0	(362.3, 543.0)
PHDM	2	342.00	7.07	(185.50, 498.50)

Case length of time (PHDM vs Traditional Planning): Truncus

Source	D.F.	Adj. S.S.	Adj. M.S.	F-Value	P-Value
PHDM	1	11267	11267	1.47	0.271
Error	6	45959	7660		
Total	7	57226			

Planning	N	Mean (minutes)	StDev	95 CI
Traditional	6	321.7	95.9	(234.2, 409.1)
PHDM	2	235.00	1.41	(83.57, 386.43)

Similar to the ANOVA of the aggregate data, ANOVA of the DORV-TGA subset and truncus arteriosus subset have a p-value above 0.05 (not statistically significant); however,

trends illustrate decreased operating room and case length of time with PHDM-based planning.

The other subsets of primary diagnoses revealed similar ANOVA trends. All of the subsets failed to achieve a p-value less than 0.05; however, all mean times for operating room length of time and case length of time were less when planned with PHDMs in comparison to traditional planning methods. In order to maintain brevity in this section, the remaining ANOVA tables are in Appendix A.

2.4.3 Technology Acceptance Results

The post-operative TAM survey was placed into the clinical care process on October 14, 2014. Through the end of the year, 19 cases received survey responses with 4 cases planned with a PHDM.

Favorable responses outweighed other responses in the TAM questions. The average TAM score was significantly higher in the perceive usefulness domain as evidenced by the responses to TAM question 2 as seen in Table 8. Responses to TAM questions 3 and 4 supported both perceived usefulness and perceived ease-of-use through free text responses.

Table 8: Technology acceptance model survey responses for the utility of PHDMs for surgical planning.

Technology Acceptance Model Survey (19 responses)		
Question:	%	Answer
In your opinion, did use of the 3D printed model enhance your ability to execute a surgical repair? (4 applicable cases)	100%	Yes
	0.00%	No
If no 3D model was used but CT/MR was used, did you note any additional morphological defects or unexpected variations unseen in the planning process? (14 applicable cases)	21.4%	Yes
	78.6%	No

TAM question 1 separates the patient population into the two cohorts: PHDM cohort and traditional planning cohort. For surgeries in which a model was available, surgeons completed the second question "[D]id use of the 3D printed model enhance your ability to execute a surgical repair?" All responses by the surgeons revealed strong support for PHDM as a perceived effective tool. In addition, question 3 asks "If no 3D model was used but CT/MR was used, did you note any additional morphological defects or unexpected variations unseen in the planning process?" Of the available 14 responses, surgeons recognized 3 cases where additional or unexpected anatomical presentation occurred.

Due to the lack of negative survey responses (no variance), the survey fails to yield statistically significant responses (defined here as a p-value less than 0.05). Despite the lack of statistical significance, the available data and anecdotal responses for TAM questions 3 and 4 suggest strong potential for the PHDMs role in enhancing pre- and peri-

operative surgical planning. Discussion of the results and recorded surgeon vignettes from free-text responses follows.

2.5 Discussion and Conclusions for Surgical Planning

2.5.1 Impact of PHDM as a surgical tool

The advent of versatile, readily available, and cost-effective 3D printing technology has made it possible to create uniquely useful PHDMs. The PHDMs represent complex heart anatomy in a true-to-life, physical form that is patient-specific and color-coded with a standardized, optimized map. The developed workflow allows for rapid construction of the congenital models, sometimes same day as the acquisition of medical images. The models were delivered to the weekly pre-surgical planning conference or emergent meetings prior to surgery; some models were utilized perioperative in the surgical suite. Examples of the finalized PHDMs can be seen in Figure 14.

PHDMs are anatomical replicas with a primary intent on educating the surgeon about patient-specific morphology. With regards to the restricted-inclusion criteria cases, PHDM-planned surgeries consistently resulted in reduced operating room and case length of time. The ANOVA tables for the combined case-population and the blocked-case-populations reveal a potential trend. Every table illustrates that mean time for the operating room and case length were less when the case was planned with a PHDM. The reduction of these durations may lead to lower morbidity and mortality, especially through the reduction of duration-associated infections [6]. The potential reduction of morbidity and

mortality achieves the primary goal of this technology: create a better mechanism of surgical planning in order to improve patient outcomes.

Effects associated to reduced operating room length of time and longer stays due to infection and morbidity include patient-related and hospital related costs. Costs related to morbidity post-surgery are offset by the patient/patient-family, insurance companies, and hospitals. In addition, the time allocated for an operation has an associate costs; either a direct cost per time unit or indirect cost per procedure (depending on the hospital's business model) [31]–[33]. By reducing the time an operation takes, the hospital will save both money and resources that would have likely been consumed in a longer operation. PHDMs can reduce surgical and room duration and indirectly save individuals or institutions resources.

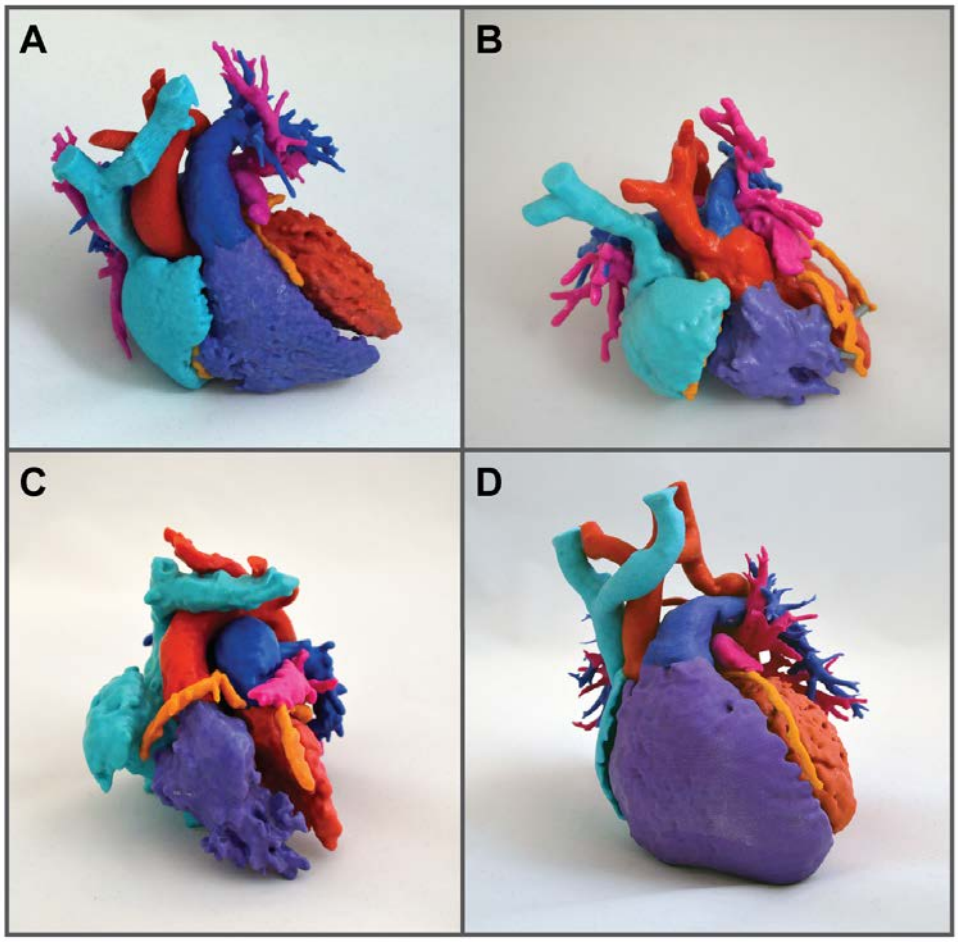

Figure 14: A) PHDM of a normal heart, B) truncus arteriosus, C) TGA, D) coarctation of the aorta.

The results of the TAM surveys further suggest that PHDMs are an accepted new technology and that PHDMs positively benefited the surgical planning process. While the questions were limited in complexity to maintain efficiency of clinical workflow, the overall perception regarding utility (responses to question 2) revealed positive behavioral attitude and, therefore, intention to use PHDMs in standard of care. To better understand the particular behaviors behind the intention to use, responses to qualitative questions 3 and 4 were analyzed. Findings from the responses suggest that PHDMs benefited the

cardiothoracic surgeons in several key areas: 1) improved spatial cognition, 2) improved surgical planning, 3) avoided potential pitfalls, and 4) complimented traditional medical imaging.

There was consensus among the cardiothoracic surgeons that PHDM aided in the spatial understanding of adjacent anatomical structures. For example, a patient was diagnosed with a Tetralogy of Fallot lesion and an aberrant coronary artery. The following response to question 3 illustrates the aided spatial awareness that the PHDM provided:

> "[W]e needed to understand the relationship between the pulmonary arteries and the anomalous coronary arteies [sic], and needed to plan the reconstruction of the RVOT[6]. [T]he 3D model helped understand these [relationships.]"

The four-fold morphological defect of Tetralogy of Fallot includes a severely stenosed pulmonary artery. The planned intervention for this patient and CHD presentation was a surgical palliation including the placement of a shunt between the aorta and pulmonary artery. The shunt attempts to normalize pulmonary blood flow and pressures by reducing the impact of the pulmonary obstruction inherent to Tetralogy of Fallot. For this particular patient, the placement of a shunt was complicated by aberrant coronary arteries which were lying in the intended path of the shunt. The accurate PHDM afforded the surgeons the ability to plan the surgery with an absolute-scale representation. The representation

[6] Right ventricular outflow tract

facilitated the planning of the path for the shunt in order to avoid coronary impingement and obstruction.

The positive response in the previous anecdote was not an aberration in attitude of responses. In fact, the PHDM assisted in the viewing of structures difficult to see in the current standard-of-care process. The following response to question 3 illustrates the benefit of augmenting the current planning process with a PHDM:

> "[The PHDM] helped delineate all anatomic relationships and specifically the pulmonary veins which were difficult to see on echo. The model was also useful to determine where we would place the Glenn/how to perform the surgery."

This response illustrates utility beyond simple spatial awareness, but also as a tool that goes beyond other imaging modalities. The PHDM model helped to visualize vessels that were difficult to see in an ultrasound (echocardiogram) due to the patient's size and low pulmonary blood flow. The planning capacity of the PHDM was also illustrated. The Glenn procedure involves the redirection of venous blood (from the superior vena cava) directly into the pulmonary arteries so that upper limb and head blood can bypass the pulmonary obstruction and proceed directly to the lungs for reoxygenation. The procedure entails the severing of the superior vena cava from the right atrium and the reinsertion of the vessel into the pulmonary artery distal to the obstruction. Understanding the spatial relationship between the superior vena cava and the pulmonary artery is essential for the Glenn procedure.

The PHDMs measured effects on planning (the ANOVA tables) and surgeon intention (the anecdotal vignettes) illustrate the role the PHDM had in establishing the surgeons' spatial understanding of the patient's anatomy by presenting an accurate, absolute-scale reference for the specific patient. In addition, the use of PHDM potentially reduce surgical and operating room length of time for complex surgeries. Morbidity and mortality are suggested to be linked to these time metric [6], a reduction of these times due to effective planning may possible with PHDMs. While the ANOVA tables and associated TAM vignettes demonstrate the efficacy of the PHDM, the process and final model have limitations.

2.5.2 Study Limitations

There are several limitations to the current surgical planning study. While this study is not a clinical trial, the outcomes analysis and deployment of the TAM study share several attributes of a clinical trial: patient inclusion/exclusion criteria, imaging protocol, and surgeons. Accordingly, the analysis of PHDM based surgical planning shared many of the clinical trial limitations, specifically the biases that are well recorded in literature [34].

First, the method of analysis compared time metrics between surgeries planned with PHDM and traditionally-planned surgeries. Surgeries were further blocked into primary diagnoses for subsequent analysis. Secondary or tertiary diagnoses that would complicate surgeries were not included in the analysis nor were patient qualifiers such as additional congenital defects, syndromes, or chromosomal abnormalities. Furthermore, the surgical procedure was not a blocking factor for the analysis. The number of and combination of

procedures would make trends difficult to observe through traditional ANOVA testing. Without a much greater patient population and stricter inclusion criteria, these additional factors would confound the ANOVA analysis.

As for the TAM study, the two cardiothoracic surgeons that utilized the PHDMs were not principal investigators in the study; however, the surgeons were aware that the intent of the study was to gauge PHDM efficacy for surgical planning. In clinical trials where intent is known by the participants, a detection bias may be present [34]. A detection bias can occur when the recording of an outcome is subconsciously affected by the participants' preconceptions. Post-surgical responses are an observation of the surgical planning process after the completion of a surgery. Observations made in this manner may also yield the detection bias as the surgeon may subconsciously be looking for additional benefits of the PHDM or disassociating adverse surgical events from the PHDM. Evidence of this bias may be present in the 100% positive response rate to the PHDMs perceived efficacy. Without a larger sample size and stricter inclusion protocols, the potential for detection bias is difficult to control. A multi-site study with pre-, peri-, and post-surgical assessments could further limit the detection bias while also revealing more of the habits-of-mind behind surgeon interaction with a PHDM.

PHDMs were already established at the collaborating institution for complex CHD cases. Establishing a randomized trial may be seen as unethical as the institution already perceived the PHDMs to be effective and part of standard-of-care. For example, cases in which morphology was perceived to be complex were more likely to receive a PHDM planning, while geometrically simple and low-risk cases were less likely to receive a

PHDM for planning. A randomized trial would take the decision away from the surgeons who already have the ability to request a model.

Furthermore, the availability of data for PHDM effectiveness on “simple” cases is perceived to be low. The subsequent surveying could have been affected by the reporting bias. Reporting bias occurs when interesting or significant events are more likely to be recorded. For this study, it is unknown whether a reporting bias positively or negatively affected the outcomes. Complex CHD repair entail higher risks than simple CHD procedures. PHDMs were used in more complex situations in which the model could be seen as a factor for a poor outcome, although clinicians never reported this negative observation. To minimize the reporting bias, a randomized, multi-center study where PHDMs are not the standard-of-care would be ideal. The rigid protocol with a randomized control cohort would yield results with less perceived biases.

2.5.3 PHDM Limitations

The PHDMs have several shortcomings including the current technological capabilities and associated ethical implications. In the current iteration, the PHDMs represent only the blood volume internal to cardiac structures and the bounding lumen; no valves or other complex tissues are represented. This is a limitation largely associated with the medical image modality.

The models included in the study were derived from contrast-enhanced CT scan. In CT scans, intensity values seen on an image is derived from the degree of radio-opacity for the particular tissue. Intensity values of most thoracic soft tissues are very similar to the

values representing myocardium as seen in Figure 15; thus differentiation and segmentation of myocardium from surrounding tissues is difficult and time consuming. To compensate for this limitation, segmentation and reconstruction from MRI datasets is performed. Unfortunately, MRI-based reconstruction has its own limitations, particularly, the spatial resolution (the amount of voxels defining a space) is considerably smaller when compared to CT scans. PHDMs constructed from MRI data have the appearance of being smoothed as a consequence of reduced spatial fidelity as seen in Figure 16.

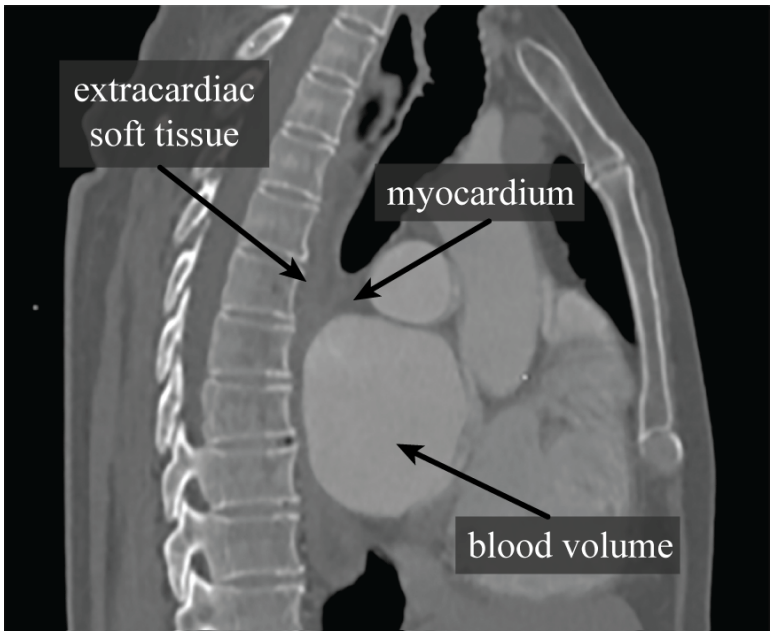

Figure 15: Contrast-enhanced CT scan. Blood volumes have a higher intensity value than surrounding soft tissue. The soft tissue muscle of the heart (myocardium) is indistinguishable from the extracardiac soft tissue.

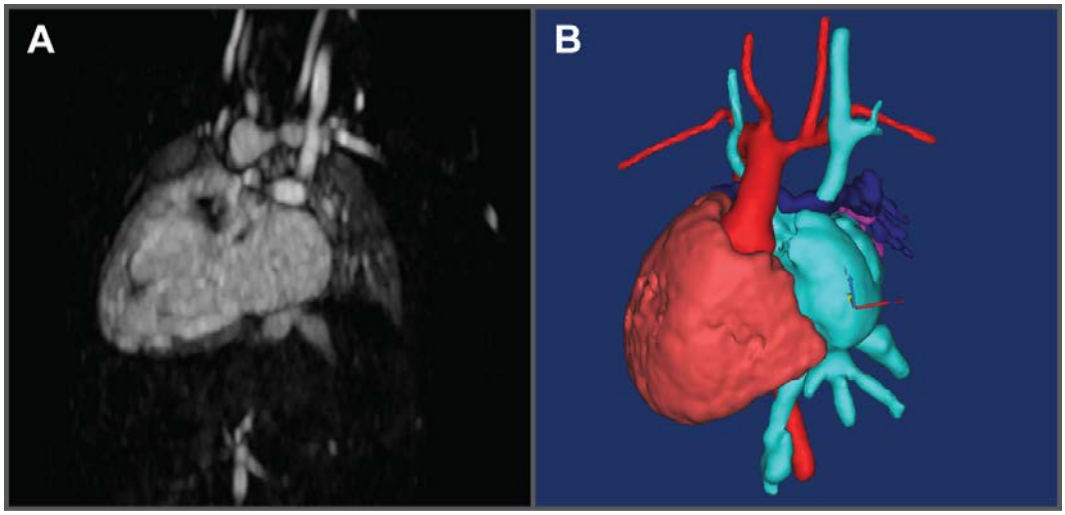

Figure 16: The reduced spatial resolution of an MRI image results in a blurry picture. The reconstruction from this acquisition results in a "smooth" geometric representation.

Current technological constraints of CT and MRI image modalities restrict reconstruction of small, complex structures, such as valves and small vessels. Valves and small vessels typically fall within the sub-voxel space; that is a single voxel will represent valve tissue as well as surrounding blood volume. The average intensity of this voxel appears closer to the intensity of the sounding voxels. These voxels would likely be included in the segmented masks for the structures surrounding it rather than its own mask. Until CT- or MRI-protocols, image processing techniques, and reconstruction technologies enable finer voxel resolution, PHDMs will lack these sub-voxel structures.

Lastly, the patient's safety must be taken into account when constructing a PHDM. PHDMs printed at a collaborating institution, both within and beyond the confines of the TAM study, were largely based on contrast-enhanced CT scans. While CT technology was used for increased spatial fidelity for diagnosis (when compared to the available MRI technology), CT scans do have the added risk of radiation exposure. The TAM study

presented here did not further expose patients to ionizing radiation as all medical images were part of the standard-of-care process. MRI, with non-ionizing radiation, is an appealing alternative for diagnosis especially as its spatial fidelity is improving due to advances in image processing technologies.

2.5.4 Concluding Remarks on PHDMs

Despite these study biases and modeling limitations, the surgical PHDM study demonstrates trends for reduced operating room and case length of time. The added benefit may be attributed to better surgeon preparedness. This preparedness may yield better patient outcomes with lower chances for morbidity and mortality. The utility of planning with a PHDM is supported by the TAM study which demonstration that PHDMs for surgical planning may increase surgeon familiarity of patient-specific morphology and help surgeon plan for a complex CHD repair. A multi-center clinical trial could show the measured effect of the PHDM on critical surgical factors such as 30 day outcome, case length of time, or cardiopulmonary bypass time. Illustrating reductions in morbidity and mortality in patients with CHDs would aid in the acceptance, by the greater medical community, regarding the efficacy of PHDM as a surgical planning tool. Acceptance of the technology is already high at the collaborating hospital where over 200 hearts have been printed for clinical planning. In fact, additional, non-cardiac departments are investigating utility of 3D printing for their respective cases.

2.6 CHD Education

2.6.1 Introduction

Beyond the pre- and peri-operative surgical enhancement, PHDMs have a potential in enhancing medical education. Currently, heart models play an active role in educating medical professionals in many roles and at many levels (e.g., pre-medical students, medical students, residents, fellows, nurses, etc.). The most basic heart models are 2D diagrams, as found in the pages of canonical medical education texts such as *Gray's Anatomy* and *Netter's Atlas of Human Anatomy* [37], [38]. These 2D drawings can only show a single view of the cardiovascular anatomy which may not capture all structures necessary for complete education. Additional windows or unnatural perspectives can provide additional anatomic landmarks; however, the 2D limitation still exists.

Anatomical dissection is a prominent feature in many medical educational settings. Learners investigate the human body through the removal of tissue and exposure of anatomical landmarks. This educational method utilizes the human visual system and allows a 3D appreciation of structures. However, cadaver specimens have limitations. Given an assumption that cadavers represent an analogous, normal distribution sample of the living population, it can be assumed that less than 2% of the cadavers will present with CHD lesions, and even fewer would present with untreated CHD lesions [4]. This specimen-population creates a limitation to learning experiences for specific congenital defects. For instance, 7% of the living CHD population (0.13% of the general population) are estimated to have Tetralogy of Fallot [1]. This would imply that, at most, only 0.13%

of cadavers would present with Tetralogy of Fallot. In this example, very few learners would likely interact with a Tetralogy of Fallot cadaver heart, and even fewer learners would interact with a Tetralogy of Fallot cadaver heart prior to any surgical intervention. While this limitation may be mitigated through long term preservation of specimens, the availability of specific defects is still limited in an educational setting. Another cadaveric limitation includes the shape and presentation of the deceased's cardiovascular anatomy when compared to a similar, living anatomical specimen. A living patient's heart would be filled with blood as well as be impacted by surrounding tissues. A cadaveric heart would not have these features and may, therefore, appear deflated or altered from its natural, *in situ* shape and presentation. To overcome these population and morphological limitations inherent to cadaveric specimens, manufactured models can capture the shape of a living heart without any concern for an available cadaver population.

Manufactured models can reproduce specific anatomical malformations for targeted learning experiences. More recently, 3D virtual heart models have emerged, offering a number of benefits [39]–[41]. Specifically, the 3D nature and interactivity of the models benefit spatially advanced and convergent learners, respectively, who are common to medical student populations. Those benefits are also offered by physical heart models, like the 2500 Heart (GPI Anatomicals, Lake Bluff, IL, USA) and Classic Heart (American 3B Scientific, Tucker, GA, USA), which provide additional benefits to kinesthetic learners because such models can be manipulated by hand. In fact, studies have shown that integrating physical heart models into traditional didactic programs helps to access both hemispheres of the brain and improves retention [42]. Learning studies specific to CHDs have also demonstrated the benefits of using physical heart models [43].

Conventional manufactured models have limitations associated to geometric complexity as well as patient specificity. Many of the idealized cardiovascular models are produced through a casting process, such as the Classic Heart. While this manufacturing technique reduces costs associated with production of numerous models, the mold must be idealized to facilitate release of the final cast. This idealization results in the removal of undercuts or small unsupported vessels. The geometric simplification results in the loss of fidelity and may impact the educational efficacy of the model should too many structures be simplified or removed.

In addition, manufacturing processes are optimized for a run of multiple casts. Individualized models, such as from specific defects or unusual case studies, are unlikely to be seen as cost effective. To further complicate the fabrication of unique heart models, there over 90 different CHD categories and over 3000 possible defect combinations [1], [44]. As a result, representative CHD models for medical education are scarcely available. Tooling for idealized or patient-specific cardiovascular models can commonly range from $25,000-$60,000. 3D printing technologies may be leveraged to overcome both of these geometric-related issues. In contrast, the proposed PHDMs can be built to-scale directly from any CHD patient's image data and are fully color-coded with a standardized, educationally-optimized map.

Toward this aim, a study was developed to examine the learning impact and technology acceptance of PHDMs for education. Two cohorts were established: nurses using PHDMs and nurses using traditional textbook illustrations. The two cohorts received the same delivery of content knowledge. A study utilizing pre- and post-assessments examined the utility of PHDMs as an educational tool against the textbook status quo.

2.6.2 Methods: Education Study

A learner population comprised of nurses from various clinical institutions and departments was identified as study participants. Participants were randomized and separated into two cohorts: PHDM cohort and traditional (2D drawing) cohort.

The content knowledge of the study was aimed at the “normal” heart and five major CHD classifications: Tetralogy of Fallot, transposition of the great arteries, truncus arteriosus, coarctation of the aorta, and hypoplastic left heart syndrome. These CHD categories were identified by cardiologists and cardiothoracic surgeons at a collaborating institution as the areas of greatest perceived impact in CHD education.

The education study was designed to be modular and deployable. Toward this aim, video modules with associated visual aids were developed for each cohort. Content of the videos was established by a collaborating cardiologist and nurse educator. Two sets of videos were developed for each heart category. The content knowledge, delivered through a narrated script, was kept consistent between the two video sets. However, the videos differed with regards to visuals. One set of videos showed photos of PHDMs, while the other set featured traditional drawings of CHDs. Screen captures from the videos can be seen in Figure 17.

Non-video, visual aids were also developed for each cohort. The PHDM-cohort received 3D prints (PHDMs) of the normal and five related CHDs. The PHDMs were scaled for durability, but were otherwise unaltered from patient-specific data. The 2D drawing cohort received print outs of drawings used in the videos. The drawings were patterned after the canonical textbook illustrations created by the National Center on Birth

Defects and Developmental Disabilities (NCBDDD) [45]. Alterations were made to make the drawings more analogous to the patient-derived PHDMs. For example, the illustration of the hypoplastic left heart syndrome was modified from the NCBDDD drawings to enlarge the patent ductus arteriosus to better match the patient-derived PHDM. Color schemes used in the illustrations matched the standardized color scheme for the PHDM. Since myocardium was present on the illustrations and not the PHDM, the myocardium was given a color pattern. Final drawings were verified by a cardiothoracic surgeon and nurse educator for anatomical accuracy.

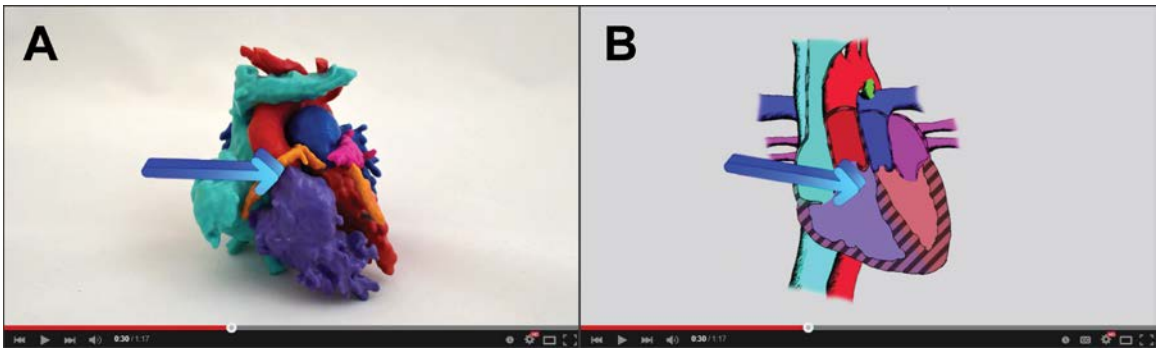

Figure 17: Still images from the video modules. A) PHDM of transposition of the great arteries. B) Anatomical drawing of transposition of the great arteries.

An attempt was made to be modality-agnostic with regards to the cohort-restricted videos and visual aids. A pen-and-paper assessment, without any illustrations or photos, was created. The questions in the assessment were developed toward eliciting responses related to CHD understanding and spatial relationship of anatomical structures. The test was used as a pre-assessment to gauge nurse familiarity with CHDs. Following the pre-assessment, a nurse would sit in front of a laptop or tablet computer and play the videos

related to his or her cohort while interacting with the cohort-appropriate visual aids. Following the videos, nurses completed the post-assessment with the same content as the pre-assessment. An additional section was added to the post-assessment. This additional section probed technology acceptance of the PHDMs. A schematic diagram of the study seen in Figure 18.

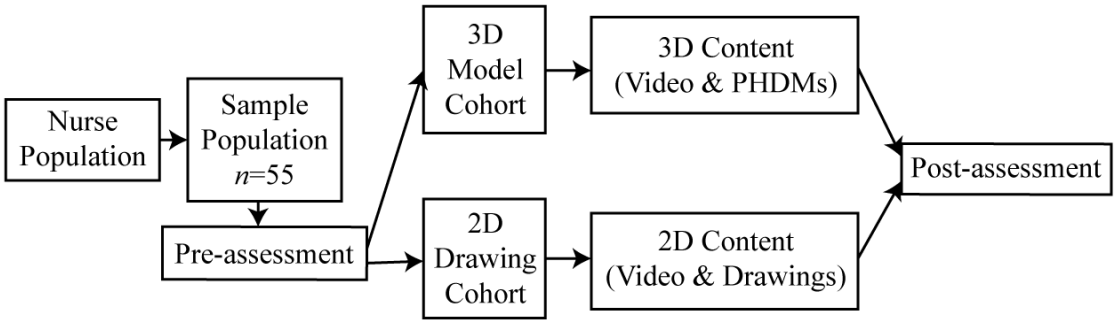

Figure 18: A schematic diagram of the nurse education study. The two educational cohorts split for content knowledge delivery, but the schematic path converges where the cohorts participate in the same pre- and post-assessment.

The nurse educational study was performed at one medical center. Fifty-five nurses (n=55) participated in the study, where no monetary compensation for participation was provided. Department/specialization was recorded as a potential factor affecting acquisition of cardiac-focused content knowledge. Two regression models were developed to examine three response variables: 1) post-assessment mean grade (y_1), 2) grade improvement from pre-assessment to post-assessment (y_2), and 3) the mean corrected grade change (y_3). The last response variable is determined through the correction of a wrong pre-assessment response to a correct post-assessment response.

The main factors and corresponding, coded levels for the regression model were:

Factor A: Modality

2D Drawings (0)

PHDMs (1)

Factor B: Department/Specialization

Non-cardiac Specializations (0)

Cardiac Specializations (1) [7]

The general regression model that was applied to three response variables:

$$y_{1,2,3} = \beta_0 + \beta_A x_A + \beta_B x_B + \beta_{AB} x_A x_B + \epsilon, \quad (1)$$

where y_i represents the response variables. x_i represents a factor level value (0, 1), different experimental factors are indicated by subscripts (i.e., A and B), the interaction between factors are indicated by complex subscripts (i.e., AB). β estimates the effect created by factors (where β_0 is the grand mean for the learning experiment), and experimental error (or person-to-person variation) is indicated by ϵ.

[7] Cardiac specializations included nurses working in the cardiovascular intensive care unit (CVICU).

2.6.3 Methods – Technology Acceptance Model

A 22 question, expanded-TAM survey was included on the post-assessment following the content knowledge test. Questions probed awareness/presence-of-mind, perceived usefulness, perceived ease-of-use, enjoyment, generalized attitude, and intention to use. The 5-point Likert scale was used for responses to all questions, and a t-test was used to determine potential statistical significance of mean responses.

2.6.4 Results of Educational Study with PHDMs

To establish significance of factors (modality of educational aid and specialization of nurses), a full ANOVA table of factors and interactions was developed for the mean of post-assessment scores. The post-assessment mean score ANOVA table is seen in Table 9.

Table 9: ANOVA table for the effect of modality and nurse specialization on post-assessment score mean. An asterisk denotes statistical significance with a p-value less than 0.05.

Source	**D.F.**	**Adj. S.S.**	**Adj. M.S.**	**F-Value**	**P-Value**
Regression	3	1394.97	464.991	3.34	0.026
x_A	1	647.42	547.421	4.65	0.036*
x_B	1	260.14	260.143	1.87	0.178
$x_A x_B$	1	5.26	5.263	0.04	0.847
Error	51	7096.52	139.147		
Total	54	8491.50			

Based on the ANOVA table and using a p-value less than 0.05 for significance, only the modality of the educational aid is statistically significant on the mean of the post-assessment score. Since modality is the only significant factor, a two-sample t-test was performed to determine the mean of each group, 2D drawings and PHDMs. The two-sampled t-test is seen in Table 10.

Table 10: Two-sample t-test for the difference of mean test scores between 2D drawings nurse cohort and PHDMs nurse cohort. An asterisk denotes statistical significance with a p-value less than 0.05.

Media	**n**	**Mean**	**Std. Dev.**
2D Drawings	31	86.9	14.8
PHDMs	24	94.9	6.82
Difference ($\mu_{PHDM} - \mu_{2D}$)		+8.07	
T-Test of Difference	p-value 0.010*		

The two-sample t-test illustrates significance of the post-assessment means between the 2D drawing cohort and the PHDM cohort.

Writing the regression equation with the effects and mean results in the following:

$$y_1 = 83.67 + 5.82x_A + 9.18x_B + 1.32x_Ax_B + \epsilon; \quad (2)$$

however, as modality is the only statistically significant factor, the regression model can be truncated to the single factor. The revised equation follows:

$$y_1 = 86.87 + 8.07x_B + \epsilon. \quad (3)$$

Grade improvement was determined through difference between post-assessment score and pre-assessment score. To establish significance of experimental factors for grade improvement, an ANOVA analysis was performed. The grade improvement ANOVA table is seen in Table 11.

Table 11: ANOVA table for the effect of modality and nurse specialization on grade improvement from pre- to post-assessment. Significance was determined via a p-value less than 0.05.

Source	**D.F.**	**Adj. S.S.**	**Adj. M.S.**	**F-Value**	**P-Value**
Regression	3	44.794	14.9313	4.61	0.006
x_A	1	8.813	8.813	2.72	0.105
x_B	1	11.478	11.4775	3.54	0.066
x_Ax_B	1	0.019	0.0192	0.01	0.939
Error	51	165.315	3.2415		
Total	54	210.109			

Based on the ANOVA table and using a p-value less than 0.05 for significance, no factor is statistically significant. However, both modality and nurse specialization illustrate trends towards educational effect. Both, PHDM and non-cardiac specialty nurses trend toward showing stronger improvement.

Accuracy of correction was also analyzed with an ANOVA table as seen in Table 12.

Table 12: ANOVA table for the effect of media and nurse specialization on mean corrected grade change. Significance was determined via a p-value less than 0.05.

Source	**D.F.**	**Adj. S.S.**	**Adj. M.S.**	**F-Value**	**P-Value**
Regression	3	2056.8	685.597	4.03	0.012
x_A	1	411.5	411.5	2.42	0.126
x_B	1	519.3	519.255	3.06	0.086
$x_A x_B$	1	2.5	2.457	0.01	0.905
Error	51	8665.7	169.915		
Total	54	10722.5			

Based on the ANOVA table and using a p-value less than 0.05 for significance, no factor is statistically significant on the accuracy of correction. Both, PHDM and non-cardiac specialty nurses trend toward mean corrected grade change.

2.6.5 Results from Technology Acceptance Study

The responses of the 55 nurse participants were generally favorable responses. The average TAM score for cardiac specialized nurses was higher in the usefulness domain; however, non-specialized nurses showed a higher attitudinal (positive) response to the PHDMs.

Table 13 (following page): Technology acceptance model survey including mean responses and standard deviations for the PHDM cohort. The percent difference between PHDM TAM response and traditional TAM response are recorded. Mean difference percent is highlighted in green when found to be statistically significant according to a two-sample t-test and a p-value less than 0.05; otherwise, the value is highlighted in yellow.

Technology Acceptance Questions	**Score Mean ± Std. Dev.**	**Mean Difference**
Awareness/Presence		
The drawing/model helps me understand the defect.	4.33 ± 0.70	+23.24%
The drawing/model helps me understand the spatial relationship of cardiovascular structures.	4.38 ± 0.77	+31.67%
The patient derived drawings/models helps me appreciate anatomical variations.	4.17 ± 0.70	+24.20%
Perceived Usefulness		
The drawing/model improved my understanding with regards to spatial relationship of anatomy.	4.08 ± 0.72	+21.71%
The drawing/model in conjunction with the video improved my understanding with regards to spatial relationship of anatomy.	4.08 ± 0.65	+24.10%
The drawing/model improved my understanding with regards to congenital heart defects.	4.25 ± 0.85	+21.99%
The drawing/model in conjunction with the video improved my understanding with regards to congenital heart defects.	4.21 ± 0.83	+20.79%
The educational module gave me a greater confidence in explaining congenital heart defects to patient-families.	3.88 ± 0.85	+15.50%
What I have learned in the educational module will impact my patient care.	3.54 ± 0.88	+05.57%
The educational module was an effective use of my time.	4.00 ± 0.72	+21.57%

Technology Acceptance Questions	Score Mean ± Std. Dev.	Mean Difference
Perceived Ease-of-Use		
The drawing/model was easy to understand.	3.50 ± 0.66	-01.36%
This video was clear.	4.13 ± 1.02	+14.17%
The module did not take an unnecessary amount of time to complete.	4.04 ± 0.99	+01.04%
The module was effective with some instruction.	4.04 ± 0.86	+09.90%
The module would be effective without any instruction.	2.75 ± 0.69	+00.29%
Enjoyment		
I enjoyed this module as an educational tool.	4.21 ± 0.88	+19.69%
I enjoyed this module regardless of the potential educational value.	4.00 ± 0.93	+14.81%
Attitude		
The module will improve my clinical care.	3.75 ± 0.90	+06.65%
I have a positive attitude about this module.	4.17 ± 0.82	+11.35%
Intention-to-Use		
The module encourages me to learn more about congenital heart disease.	4.21 ± 0.78	+07.82%
I wish modules like this were created for other common anatomical variations.	4.38 ± 0.77	+20.02%
I would recommend this module for other clinical care professionals.	4.21 ± 0.98	+19.69%

2.6.6 Discussion and Conclusions

Many physical and illustrative models exist of the normal human heart [37], [44]. As such, it was expected that the nurses would have a similar educational background and similar fundamental understanding of the human heart. Responses to questions[8] 1 and 2 of the content knowledge portion of the assessments that probed understanding of normal anatomy were equal between the cohorts at 100%. This suggests that the assumption of foundational knowledge is correct. The focus of the assessments, therefore, was on the

[8] Please see Appendix B for a full copy of the nurse learning assessment.

development of knowledge of CHD with an emphasis of spatial understanding. Attempts were made to make all delivered content knowledge homogenous between the two cohorts. For example, video content and color information were kept consistent between the two cohorts.

Overall, the PHDM cohort achieved a higher mean score (p-value=0.036) and improved score (not statistically significant) in the education study. From the post-assessment ANOVA table (Table 9) and the two-sample t-test (Equation 1), the effect of media (2D Drawings or PHDMs) is significant on the grade means. In addition, the mean grades are statistically greater from the PHDM cohort than the 2D drawing cohort. The PHDM cohort was able to consistently achieve grades that were 8% higher than the opposing cohort. The PHDM, on a surface level, appear to be a significantly better educational tool than textbook illustrations. Analysis of specific answers suggests reasons for the learning differences between the cohorts.

Physical, 3D models are able to more accurately represent complex 3D structures such as CHD. Questions 5 and 9 focused on spatial relationships between cardiovascular structures in the presence of CHD. In transposition of the great arteries, the pulmonary artery and the aorta are switched at the morphological origin. In conventional anatomical positioning, the aorta becomes the most anterior great vessel. Both mean score and mean differential trended higher in the PHDM cohort than the 2D cohort. These results illustrate the 2D drawings are less effective at communicating spatial relationships.

The collective results make it clear that the proposed use of PHDM offer unique benefits. Similar trends were observed in an additional CHD-related education study [22] and in another study involving nursing students (i.e., the color-coded physical heart model

variant was most effective in both studies); however, the sample size in this earlier study was too small to establish statistical significance.

Additional findings, while not statistically significant, illustrate learning trends. The improvement from pre- to post-assessment (mean differential grade) for the PHDM cohort was greater than 7% for non-cardiac specialties (p-value=0.126). Similarly, non-cardiac specialties, learning with the PHDMs, were more likely to change a wrong answer to a correct answer (p-value=0.105). These data points suggest that nurses in cardiac specialties were set in their content knowledge, whether correct or incorrect in the responses. This data also suggests that the PHDMs may be a more effective tool for non-cardiac specialized nurses, nurses earlier in training (prior to career differentiation), or pre-graduate nurses.

This evidence for educational impact may help the development of future educational programs that best target learning habits of specific demographics. This can be achieved through the optimization of the regression model presented in Equation 1. That model can be used to optimize the learning outcomes of specific demographics of medical curricula (i.e., maximize the response variables, Y, in Equation 3) by adjusting the key categorical level values (i.e., those for factors A and B). Through implementing the coded values, post-assessment mean scores are greatest with A=PHDM and B=cardiac specialized nurses. However, while not statistically significant, improvement of grades, implying development of content knowledge, is best achieved though A=PHDM and B=non-cardiac specialized nurses as the educational cohort.

While the value added by the PHDMs' physical form is relatively straight forward, the proposed color-coding standard adds value in more subtle ways. First, the standard is

consistent across all models in the PHDM library, and accordingly facilitates the identification of common structures among different models. Second, the standard allows vessels carrying oxygenated blood to be easily distinguished from those carrying deoxygenated blood in non-shunted anatomy, thereby communicating physiology in parallel with anatomy. Third, abnormal vessels are also made easily identifiable by leveraging characteristics of the human visual system; abnormalities are highlighted in green against the largely blue and red pallet of the rest of the heart. The proposed color-coding, thus, allows an observer to glean information quickly from a specific model, which facilitates improved recognition and/or understanding of heart anatomy. In fact, a related study demonstrated significant educational benefits when the color-coding standard was applied to computational models of CHDs instead of a monochrome or random color scheme [46]. As the current education study showed, the color-coding can also be applied in parallel with physical modeling to further enhance learning. Besides strict content knowledge development analysis, it is critical to examine the technology acceptance of this novel tool for education. For this study, the TAM was developed in the post-assessment through 22 questions; the mean responses to these questions are in Table 13. In the domain of perceived usefulness, two questions probed the participant's perception of the PHDM as an effective tool. Mean responses to both questions were statistically greater (two-sampled t-test) than the mean responses to the 2D drawings. Besides the added spatial characteristics, participants perceived the PHDMs to better convey content knowledge of CHD.

For direct perceived ease-of-use, no response means for PHDMs were statistically greater than 2D drawings; however, qualitative characteristics can be observed. The video,

the mechanism for content knowledge in this study, was perceived to be effective and an efficient use of time. Low differences between the cohorts is likely due to the group having the same content delivered, only the visual aid differentiated the two cohorts.

Indirect (or extended) ease-of-use domains illustrated a mixture of statistically significant and non-significant responses. Of the significant responses, the PHDM cohort perceived the study to be enjoyable as an education tool. This feature is significant to technology acceptance according to the expanded TAM models [47]. In the intention-to-use domain, participants stated their desire for the educational experience and 3D models to be translated to other anatomies and anatomical variations. Further illustrating the positive outlook for the educational experience was the participants' high grade of likelihood to recommend the educational experience with PHDMs to other clinical professionals.

The TAM attempts to understand the adoption of a new technology and incorporates both perceived usefulness and perceived ease of use [25]. Additional domains have been expanded by subsequent research to additional behavioral outlooks such as enjoyment, attitude, and intention to use [47]. The PHDMs excelled as a tool likely to be adopted into use according to participant responses.

2.6.7 Limitations

The PHDMs and associated study both have limitations. First, the PHDMs are developed through a multi-disciplinary research initiative. This complex development process utilizes advanced imaging software and the latest in 3D printing technologies. Both software and

hardware needed to construct the PHDMs are expensive to purchase and maintain. The PHDMs are estimated to cost around $75 in materials. These advanced educational materials cost considerably greater than color textbook illustrations or mass-produced, idealized heart models.

To address these concerns, a mixed manufacturing approach may significantly reduce the creation an operating costs for educational material development. 3D printing can be utilized to develop mold for many casting processes. Casting instead of 3D printing for every model will significantly drive down costs of manufacturing.

The study also has limitations. While some aspects of the educational study achieved statistical significance (observed here as a p-value<0.05), not all aspects of the study achieved this threshold. For example, 3 of the 52 participants were male. Understanding learning habits between sexes may enhance the PHDM educational efficacy. For instance, one sex may benefit by 3D anatomical representations over the other sex. The study performed was unable to make this distinction.

In addition, the study was performed with two participant groups. Groups were separated into different rooms to watch the video series. While a proctor was present in the room to prevent nurses from communicating, an ideal environment would be a single participant isolated in one room for the duration of the study. Despite these limitations, the trends observed in assessments provide a promising future for PHDMs in clinical education.

Lastly, the study focused on the content knowledge differences between the two groups of learners. The study did not focus on the habits of mind with regards to how the learners interacted with PHDMs. A protocol analysis educational study could address these

learning behaviors. In-depth interviews before, during, and after the learning modules may help to describe the role the PHDMs have in the learning process. By better understanding the educational mechanisms behind the PHDMs, the models can be refined to better meet the needs of the greater medical education community.

2.7 Concluding Remarks

This study investigated the effects of PHDMs in an educational environment by engaging with nurse participants in an educational experience. Experimental results showed that nursing cohorts that learned with PHDMs performed better on modality-agnostic tests than cohorts that learned with 2D drawings. Furthermore, PHDMs achieved higher ratings in perceived usefulness and perceived ease-of-use than 2D drawings in a TAM survey. These results are promising for the adoption of PHDMs in the nurse education environment. Additional studies will be needed to determine if the results of this study can be extrapolated to other medical educational environments or even non-medical educational environments.

CHAPTER 3

VIRTUAL IMPLANTATION OF MCS DEVICES

3.1 Introduction

The SynCardia 70cc TAH, an MCS device, is comprised of two separate, fabricated ventricles and features adjustable ventricular orientation. Each ventricular device is comprised of a multi-layer urethane shell with the internal volume separated by an elastomer diaphragm. One side of the device's partition is confluent with an extracorporeal pneumatic driver via conduits. The opposite side of the partition is confluent with the patient's blood and cardiovascular circuit. The pneumatic driver engages with the partition via a dynamic pressure gradient. During systole, the driver increases pneumatic pressure by deforming the diaphragm and decreasing available volume for the blood. A one way valve connected to the inflow closes, forcing blood through the outflow tract and into the body. During diastole, the pneumatic driver ceases, and pressure in the blood volume overcomes the pressure in the air partition. The outflow valve closes and the inflow valve opens forcing blood to enter the ventricular device. This process enables the device to partially fill at a fixed percentage to simulate a heart stroke. The entire process is illustrated in Figure 19 [20].

In some adolescent and small adult patients with advanced, biventricular heart failure awaiting transplant, the TAH has been utilized as an assist device [48]. The TAH was chosen for these higher risk patients as the device has demonstrated a reduced incidence of stroke and transient ischemic attacks [20], [48]. Unfortunately, the

deployment of the TAH in pediatrics and undersized adults is limited. Of the 1,061 patients placed on the TAH, only 21 (2%) were under the age of 18 years of age[9]. The limitation is largely due to the adult-oriented size of the device and its poor capabilities of gross fit in a smaller thoracic chest. Device performance or patient viability may be adversely affected by thoracic impingement or other fit complications.

For proper fit and function, the recommended minimum body surface area (BSA) is 1.7 m^2 and the anteroposterior (AP) distance between the sternum and spine at the level of T10 is 10 cm [48]. These criteria represent a significant barrier for TAH in the pediatric and small adult population. In addition, there are few certified pediatric centers with the experience of implanting a TAH in children. The needs for device modification to accommodate complex congenital anatomies for children, small adults, or adults with structural anomalies constricting available thoracic space remain challenges to deploying the TAH in pediatrics in this current era [21].

[9] The number of patients placed on the 70cc TAH was accurate as of December 13, 2013 when provided by SynCardia Systems Inc.

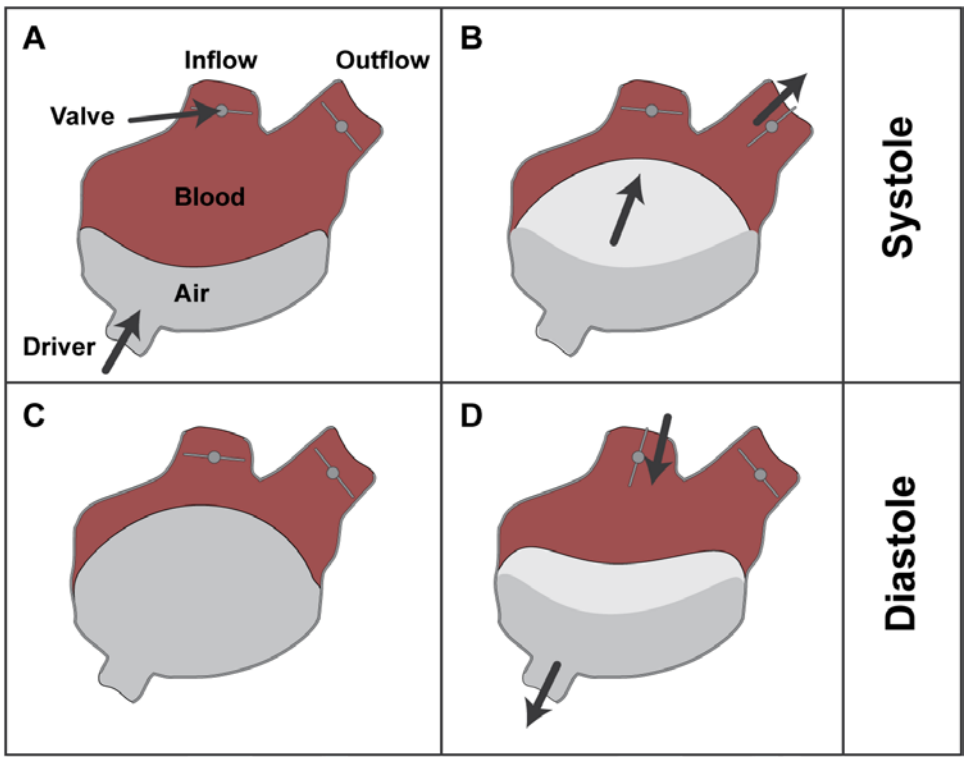

Figure 19: The cardiac cycle of the TAH operates by transporting pressurized air in and out of the pneumatic chambers of the left and right ventricles in synchronization through the attached percutaneous drivelines connected to the external pneumatic driver. A and B illustrate the systole analogue heart stroke. C and D illustrate the diastole analogue heart stroke.

The eligibility criteria has been established through analysis of cadaveric surgeries and anatomical metrics of the normal adult population[10]. That is, the criteria is intended to be representative of a majority of the normalized population, disregarding anatomical anomalies and outliers such as patients with congenital diseases or skeletal deformities. For smaller patients and patients with abnormal thoracic dimensions, the population-based metric may be ineffective in describing the potential fit of a device. The current criteria with its lack of specificity will have three possible outcomes with regards to true patient

[10] The description regarding establishment of eligibility criteria was provided by SynCardia Systems.

eligibility. The first outcome (1) is that the current criteria is sufficient in describing a patient's eligibility, where adequate or inadequate dimensions (true positives and true negatives) are identified and treated accordingly. The second outcome (2) is a false positive where the criteria suggests good fit of the device, but poor fit would occur in the operating room. This may be caused by unusual thoracic conditions such as pectus excavatum creating further barriers to fit. The last outcome (3) is a false negative where failure to meet criteria results in patients rejection; however, a device would have actually fit without significant complications. For example, a patient with DCM, where cardiac anatomy is enlarged to near-adult size, may allow placement of an adult-sized device, is an example of a false negative.

The potential for false positives and false negatives is tied to the relatively patient-agnostic eligibility criteria. By leveraging the latest in image processing and 3D visualization, the sensitivity (probability of a true positive) and specificity (probability of a true negative) can be increased. Image processing and 3D visualization enables patient specific data to be compared to manufacturing specifications for a more detailed analysis regarding fit. In addition, the novel methods – described as "virtual surgery" – enable further integration of the clinician's experience into the fit analysis. Thus, a mechanism for surgical planning is enhanced with prediction and mitigation of complications. Virtual surgery, as its name implies, allows a clinician to approach fit analysis in the same manner as approaching the surgery itself. With regards to TAH virtual surgery, the clinician virtually resects ventricles, places device, optimizes device orientation, closes the virtual sternum, and looks gross device fit. The methods, evaluations on virtual sensitivity and

specificity, and clinical implications of the virtual surgery, performed on 29 patients, are discussed.

3.2 Methods

Cardiothoracic surgery teams at participating institutions identified 29 patients in advanced heart failure. Each institution recognized the 70cc TAH as a potential candidate for palliation and bridge-to-transplantation. While established eligibility criteria suggested 10 cm at T10 (measured sternum-to-spine) and 1.7 m^2 for BSA, 11 patients (37.9% of possible candidates) failed to meet at least one of those criteria. BSA values are not recorded at every institution, and several institutions failed to provide metrics (height and weight) to calculate BSA. T10 measurements were calculated for all patients; 10 patients (34.5% of possible candidates) failed to meet the T10 criteria. The novel virtual implantation procedure was implemented on all 29 patients including the under-sized patients.

3.2.1 Image Acquisition and Reconstruction

Per standard-of-care at the participating institutions, the patients received a CT scan. Unlike all image acquisitions for PHDMs, CT scans from the various institutions were less likely to have a contrast agent; only 62.1% of the participating cases (18 patients) had a contrast-enhanced CT.

Imaging protocols were not homogenized over the participating institutions as the imaging was part of standard-of-care. Spatial resolution of the CT datasets varied from

patient-to-patient and institution-to-institution. Slice thickness (resolution in z-direction) commonly ranged from 0.325mm to 0.9mm; pixel spacing (resolution in x- and y-direction) ranged from 0.325mm to 0.625mm. The resulting images were packaged into DICOM files. Per HIPAA standards, data were anonymized prior to transmission to the data coordinating institution.

The DICOM files were imported into Mimics Innovation Suite. While the software facilitated image segmentation, skeletal structures and airways were segmented for every patient dataset. For datasets acquired with contrast-enhancement, cardiac anatomy subsets were segmented: left atrium (including pulmonary veins), right atrium (including vena cava), left ventricle, right ventricle, pulmonary arteries, aorta, and coronary arteries. The segmented masks were reconstructed into 3D surface mesh models. Computational cardiac anatomies were differentiated via the previously defined (Table 1) standardized color scheme as seen in Figure 20A.

For non-contrast CT datasets, cardiovascular anatomy could not be segmented from surrounding soft tissue. The lack of segmentation for reconstruction would make subsequent processes difficult. To overcome the lack of anatomical information. Target discs were created and placed in the approximate position of the 4 native heart valves as seen in Figure 20B.

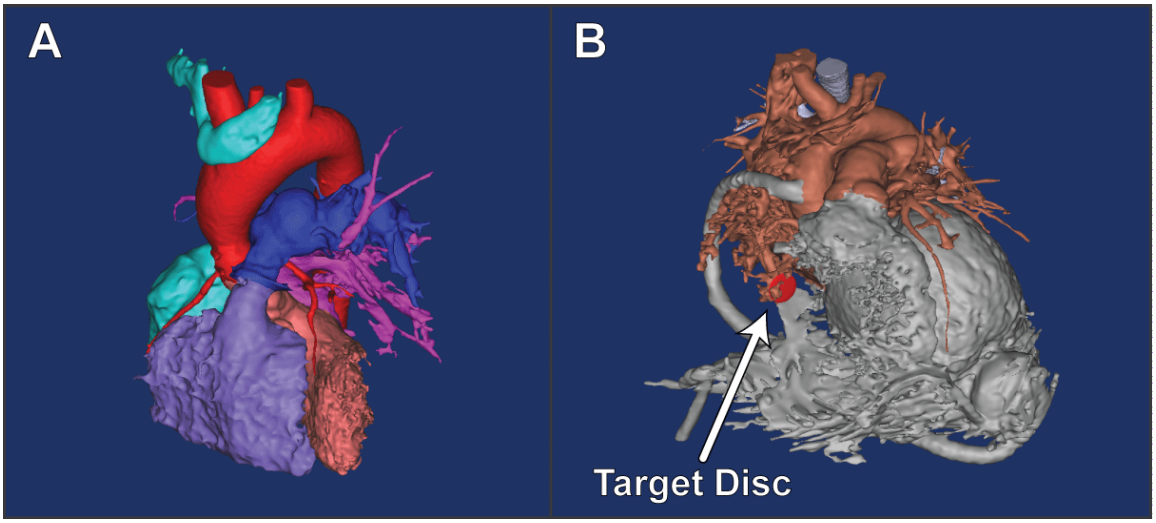

Figure 20: A) Reconstruction of heart failure anatomy from a contrast-enhanced CT dataset. B) The reconstruction from a CT with insufficient contrast. A target disk was used to approximate location of the tricuspid valve.

3.2.2 Surface Mesh Generation of MCS Devices

A 70cc TAH device was laser scanned in order to obtain a surface mesh model. The laser scan utilized passive sensor and image-based modeling technology leveraging photogrammetry. A 2D grid was projected onto the surface of the TAH device while cameras recorded the 3D distortion of the projected grid. Image processing techniques permitted the development of a surface mesh from shape information grid curvature [49].

The data was imported into Geomagic where a surface mesh was generated from the point cloud data. Geometric holes or data aberrations were removed. Device volume and surface area was compared to experimental values provided by SynCardia Systems. The laser scan data was exported as a stereolithography file (.stl), a format that contains surface mesh information.

3.2.3 Virtual Implantation

Anatomical reconstructions were imported back into Mimics and re-registered to the axial, sagittal, and coronal medical images. The process proceeded as a virtual analogue of the actual TAH surgery. The computational models of the ventricles were excised and the computational 70cc TAH models were imported and implanted. The inflow of the right device was placed adjacent to the right atrium and the tricuspid valve, while the outflow was placed next to the pulmonary trunk and pulmonary valve. The inflow of the left device was placed adjacent to the left atrium and mitral valve, while the outflow was placed next to the aortic root and aortic valve. The two device lobes, while constraining the inflow and outflow locations, were moved closer together and posterior to the sternum, where possible. A cardiothoracic surgeon guided the placement and optimization of the TAH and verified the realistic implantation (given the available data); a virtual implantation can be seen in Figure 21A. An outline of the device was projected on the 2D CT slices in order to correlate virtual model location to patient anatomy as seen in Figure 21B.

The surgeon examined the virtual implantation, using both quantitative and qualitative metrics, to determine fit. Quantitative metrics include measured TAH overlap on the thoracic skeleton, great vessels, airways, and diaphragm. Overlap between virtual TAH device and anatomy observed in images would imply displacement or impingement of patient anatomy. The cardiothoracic surgeon gave his observations on the virtual fit and the potential implications on an actual surgery.

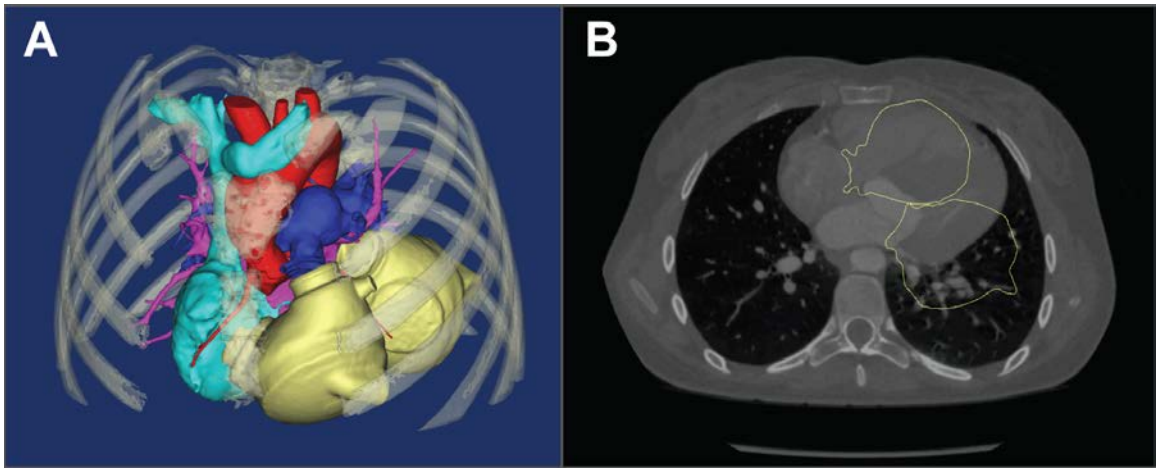

Figure 21: A) Virtual implantation of the 70cc TAH. B) Contour overlays illustrating the relationship be of the virtual implanted TAH and the current cardiovascular anatomy.

The results of the virtual procedure were sent to originating institutions in the form of videos illustrating implantation and a text summary by the collaborating surgeon. No attempt was made to supersede the existing eligibility criteria; the virtual implantation information only supplemented the current fit scheme.

3.2.4 Hybrid Technology Acceptance Study

Due to the uncontrolled protocols of the 20 participating clinical institutions, a clinical trial with homogenized inclusion/exclusion, imaging protocols, and outcome metrics was not feasible. A technology acceptance study was established in its place to determine feasibility and potential adoption for a clinical trial.

The following information was requested from the participating institutions:

1. What did your institution record as the T10 measurement?
2. What did your institution record as the BSA?
3. What is the patient's age and sex?
4. What was/were the main cardiovascular defect(s)?
5. Did you find the virtual implantation helpful in assessing MCS device fit or potential complications?
6. Was the 70cc TAH implanted?
7. If "No" to #6, were potential fit complications the main concern?
8. If "Yes" to #6, were there any fit-related complications?
9. Would you choose to exercise virtual fit analyses prior to future MCS surgeries if the option were available to your institution?
10. Do you have any feedback that will make this technology more useful to you or your institution in the future?

3.3 Virtual Implantation Case Studies

Two case studies illustrate the virtual implantation through 1) a retrospective implantation to investigate post-surgical complications and 2) a prospective implantation of a modified device design.

3.3.1 MCS Implantation Case Study – Retrospective

A case study succinctly illustrates the current eligibility criteria deficits and the early development of the virtual implantation technique. A 14-year-old male presented with 3-week history of cough, shortness of breath, upper respiratory tract symptoms, and fever. An echocardiogram revealed biventricular dysfunction with an ejection fraction of 15-17%; an ejection fraction less than 40% is considered reduced [10]. Multiple clots were present in the left ventricle and left ventricular outflow tract. The patient was diagnosed as having dilated cardiomyopathy, severe biventricular dysfunction, and ventricular arrhythmias. Advanced heart failure medical optimization was initiated with intravenous inotropic support.

The patient acutely decompensated and was placed on extracorporeal life support (ECLS) as a means for short-term medical optimization. He was accepted for heart transplantation and placed on the Status 1-A waiting list (the most urgent classification for the waiting list). After 8 days of ECLS support without a donor becoming available, the decision was made to transition to an MCS device.

The medical team chose to deploy a 70cc TAH as a bridge-to-transplantation. The patient failed to meet the recommended fit criteria for the TAH: BSA greater than 1.7 m^2 and an anterior-posterior (AP) distance of the thoracic cavity measured at T10 to be greater than 10 cm. The patient's BSA was 1.5 m^2 with AP distance at T10 was 9.8 cm. A preoperative chest CT scan assisted in the final determination to proceed with TAH-implantation.

A median sternotomy was performed to open the chest. The width of the pericardium and distance from the anterior of the spine to the posterior table of the sternum were measured and the dimensions confirmed image findings. Despite the undersized thoracic space, the clinicians believed there to be adequate space for the TAH. The decision was made to continue the TAH implantation. The ventricles and all native heart valves were excised, and the TAH was implanted without incident. A transesophageal echocardiogram confirmed successful implantation of the TAH and showed no impingement of the left and right atrium.

The sternum was closed on postoperative day 1. During closure, the left pericardium was opened and the TAH was shifted to the left pleural space to reduce pulmonary vein impingement, as evidenced on echocardiography. A study by LePrince *et al.* suggests this technique to be useful in small patients with a BSA between 1.5 and 1.6 m^2 [48]. Echocardiogram at the time of chest closure revealed unobstructed systemic and pulmonary venous return.

The patient had no major hemodynamic events such as bleeding or stroke. Postoperative care was complicated by an opacification of the left lung, seen on the chest x-ray (CXR) on post-operative day 1. Clinicians feared that the device was impinging on structures unobserved in the echocardiogram. Contrast-enhanced CT was acquired of the thoracic cavity and confirmed the respiratory findings of the CXR. To analyze possible obstruction of pulmonary vasculature and bronchi, 3D reconstruction was performed. Image processing via segmentation rendered the 2D slice data into 3D computational models. Cardiovascular, respiratory and skeletal (including costal cartilage) structures

were segmented from the CT, using Mimics. These segmented masks were reconstructed into 3D surface mesh models and imported into 3D modeling software.

Since the TAH device is manufactured with a radio-transparent urethane, the exterior surface of the device does not show up on CT images. Only the internal air and blood volume of the device can be detected. To obtain a clear spatial relationship of the device to surrounding tissues, a geometric representation of the device's surface was needed. The computational model of the laser-scanned TAH was imported into the 3D modeling software alongside the patient's anatomical reconstruction. The surface mesh of the TAH was aligned to its segmented lumen from the CT reconstruction. The combination of patient data and scanned data provided an inclusive and accurate view of the TAH's impact on the surrounding anatomy. The virtual 3D model demonstrated no compression of the pulmonary veins by the device. The 3D reconstruction confirmed that the size and location of the TAH were not constricting factors for the cardiovascular or respiratory structures. The decision was made to not re-open the patient's chest.

The left lung was found to be atelectatic (filled with fluid) and improved with aggressive recruitment maneuvers. A bronchoscopy revealed some mucus plugs found in the left bronchial tree that were suctioned. The patient was extubated successfully on postoperative day 6. Following extubation, the patient was able to quickly advance in his diet and ambulate throughout the hospital. The patient was supported with the TAH for 11 days prior to successful heart transplantation.

This case study confirms that the TAH can be successfully deployed in selected pediatric patients who have a smaller BSA than 1.7 m^2. This patient's postoperative course was complicated by left lung atelectasis. A chest CT with 3D reconstruction was crucial in

visualizing the pulmonary arteries and veins and bronchial structures to rule out compression from the device. The success of utilizing CT with segmentation and 3D modeling, as seen in this case study, demonstrates the potential for patient-specific device fit analysis. A study by Dowling, *et al.* acknowledged CT with 3D reconstruction as a powerful tool in predicting appropriate fit of any potential candidate who was considered for implantation of the AbioCor Implantable Replacement Heart System [51]. SynCardia has recently manufactured a new 50 cc TAH that has received a Humanitarian Device Designation for pediatric bridge-to-transplantation by the FDA. As development and testing of this new technology progresses, its future deployment and utilization will broaden pediatric application of TAH. In fact, the following case study builds on the work discussed here. A virtual implantation comparison between a 70cc and 50cc TAH was developed in an emergent scenario.

3.3.2 MCS Implantation Case Study – 70cc vs 50cc

A 53-year-old female in advanced heart failure was initiated with intravenous inotropic support for medical optimization. The decision was made to transition to a 70cc TAH as a bridge-to-transplantation. The patient failed to meet the recommended fit criteria for the TAH; the patient's AP distance at T10 was 9 cm. Following the implantation, surgeons were unsuccessful in closing the sternum. The surgeons left the chest open hoping that trama-induced swelling would reduce over time; this reflects other literature delayed closure for TAH implantation [48]. In following days, the sternum would still not close. Surgeons requested virtual implantation of the 70cc TAH from a pre-operative CT scan.

3D reconstruction was performed. Image processing via segmentation rendered the 3D computational models of the anatomy. Cardiovascular, respiratory and skeletal (including costal cartilage) structures were segmented from the CT. These segmented masks were reconstructed into 3D surface mesh models and imported into 3D modeling software. Virtual implantation of the 70cc TAH revealed high potential for thoracic wall impingement in addition to less-than-ideal orientation of the inflow and outflow cuffs; this orientation complication can result in obstruction of pulmonary vessels further affecting pulmonary blood pressure. At the request of SynCardia Systems, the 50cc TAH was virtually implanted in the same dataset.

In addition to the methods presented in the section 3.2.2, a surface mesh model of the 50cc TAH needed to be constructed. For the 50cc TAH, SynCardia Systems provided a solid (computer-aided design or CAD) mesh model. The CAD drawings had to be parameterized and tessellated to a surface mesh representation. The surface mesh data was exported as a stereolithography file.

Following the optimized placement of the smaller MCS device, thoracic wall impingement was eliminated while complications in orientation were considerably reduced, although not eliminated. The results of the orientation were shared with the clinical institution, and the decision to transfer the patient to the 50cc TAH was made.

Surgeons disconnected the synthetic cuffs of the 70cc TAH, removed the device, and inserted the 50cc TAH. Following standard procedure, the cuffs were reconnected to the smaller TAH. Following the operation, the patient's sternum was successfully closed. Echocardiogram revealed ideal pulmonary blood flow and pressures. Since closure, the patient had no major hemodynamic events such as bleeding or stroke. Not only does this

case study illustrate the potential of virtual implantation to avoid fit-related complications, but it also illustrates the role of choosing the best-fit size for a specific patient.

3.4 Results

3.4.1 Results of the Virtual Implantations

Twenty-nine patients were identified as potential candidates for the 70cc TAH. Ages ranged from 10-67 years with BSA ranging from 1.19 - 2.29 m^2 (from available information). These patients underwent virtual implantation. From the 11 patients that failed at least one of the tradition eligibility criteria, 4 patients (36.4%) were determined to be a possible fit according to the cardiothoracic surgeon utilizing the virtual implantation. These patients represent a potential false negative rate (with regards to the current eligibility criteria) at 13.8%. Furthermore, of the 18 patients that passed T10 eligibility criteria, 3 patients (16.7%) were deemed an “ill-fit” according to the cardiothoracic surgeon. These patients represent a potential false positive rate (with regards to the current eligibility criteria) at 10.3%. A complete list of patients, eligibility criteria, and virtual implantation results are in Table 14.

Table 14: Results from virtual implantation. Failure with regards to traditional eligibility criteria are highlighted in light red. Instances where traditional eligibility criteria does not pass fit, but virtual implantations illustrates potential fit are denoted as a false negative (F.N.). Instances where traditional eligibility criteria passes fit, but virtual implantations illustrates potential complications are denoted as a false positive (F.P.). Instances where institutions withheld information is identified as "not provided" (N.P.). Yes* refers to cases where the 50cc TAH was approved, but the 70cc TAH was rejected.

Pt	Sex	Age (yrs)	Country of Origin	T10 (cm)	BSA (m2)	Passed virtual implant-ation	TAH Device Placed	False Positive/ Negative to T10
1	Male	14	USA	9.0	1.56	Yes	No	F.N.
2	Female	12	USA	9.8	1.42	No	No	
3	Female	14	USA	9.5	1.75	Yes	No	F.N.
4	Male	14	USA	7.5	2.06	Yes	No	F.N.
5	Male	16	USA	10	N.P.	Yes	No	
6	Male	14	USA	13	2.29	Yes	No	
7	Female	16	USA	9.8	1.19	No	No	
8	Male	45	USA	11	N.P.	Yes	No	
9	Female	26	USA	10.09	1.62	No	No	
10	Female	19	USA	10	N.P.	No	No	F.P.
11	Male	17	USA	10.5	N.P.	Yes	No	
12	Male	67	Croatia	12.7	N.P.	Yes	Yes	
13	Female	36	Croatia	8.9	N.P.	No	No	
14	Male	32	Czech Republic	15	1.76	Yes	No	
15	Female	46	UK	9.2	N.P.	Yes	No	F.N.
16	Male	30	UK	15	2.16	Yes	Yes	
17	Male	43	USA	12.5	1.758	Yes	Yes	
18	Male	53	Slovenia	10.5	N.P.	Yes	Yes	
19	Female	34	Slovenia	10.5	N.P.	No	No	F.P.
20	Male	61	USA	11	N.P.	Yes	No	
21	Male	16	USA	9.7	N.P.	No	No	
22	Male	52	Croatia	13.5	N.P.	Yes	No	
23	Male	48	Croatia	15	N.P.	Yes	No	
24	Female	16	USA	10.5	1.66	No	No	F.P.
25	Female	19	France	8.5	N.P.	Yes*	Yes*	
26	Female	53	USA	10.9	N.P.	Yes*	Yes*	
27	Male	10	USA	8.5	N.P.	No	No	
28	Female	37	USA	11	2.1	Yes	No	
29	Female	55	USA	12.5	N.P.	Yes	No	

3.4.2 Results of the Hybrid Technology Acceptance Study

The TAM survey was completed by 31.6% of participating institutions[11]. All respondents indicated that they would prefer using the virtual implantation procedure for MCS device fit analyses in the future. The breakdown of case and TAM is shown in Table 15. Only one institution provided extra feedback on the utility of the virtual implantation. In particular, they commented that there was not a sufficient technological framework for transmitting the medical images. However, the mechanism for medical image transmission was beyond the scope of this virtual implantation technology.

[11] The originating institution was not surveyed to mitigate potential biases.

Table 15: Results from virtual implantation technology acceptance study. Six out of the 19 participating institutions completed surveys; 100% of respondents said they would like to utilize virtual implantation processes in the future to in in MCS device fit prediction. Instances where institutions failed to respond to the survey are identified with "N.P." (not provided).

Pt	Country of Origin	Fails (one of eligibility criteria)	Passed virtual implantation	TAH Device Placed	Would you utilize the process for future MCS cases?
1	*USA*	*Fail*	*Yes*	*No*	
2	*USA*	*Fail*	*No*	*No*	
3	*USA*	*Fail*	*Yes*	*No*	
4	*USA*	*Fail*	*Yes*	*No*	
5	*USA*	*Pass*	*No*	*No*	
6	*USA*	*Pass*	*Yes*	*No*	*Yes*
7	*USA*	*Fail*	*No*	*No*	*Yes*
8	*USA*	*Pass*	*Yes*	*No*	*N.P.*
9	*USA*	*Fail*	*No*	*No*	*Yes*
10	*USA*	*Pass*	*No*	*No*	*N.P*
11	*USA*	*Pass*	*Yes*	*No*	*N.P*
12	*Croatia*	*Pass*	*Yes*	*Yes*	*N.P*
13	*Croatia*	*Fail*	*No*	*No*	*Yes*
14	*Czech Republic*	*Pass*	*Yes*	*No*	*N.P*
15	*UK*	*Fail*	*Yes*	*No*	*N.P*
16	*UK*	*Pass*	*Yes*	*Yes*	*N.P*
17	*USA*	*Pass*	*Yes*	*Yes*	*Yes*
18	*Slovenia*	*Pass*	*Yes*	*Yes*	*N.P*
19	*Slovenia*	*Pass*	*No*	*No*	*N.P*
20	*USA*	*Pass*	*Yes*	*No*	*N.P*
21	*USA*	*Fail*	*No*	*No*	*N.P*
22	*Croatia*	*Pass*	*Yes*	*No*	*N.P*
23	*Croatia*	*Pass*	*Yes*	*No*	*N.P*
24	*USA*	*Pass*	*No*	*No*	
25	*France*	*Fail*	*Yes*	*Yes*	*Yes*
26	*USA*	*Pass*	*Yes**	*Yes**	*N.P*
27	*USA*	*Fail*	*No*	*No*	*N.P*
28	*USA*	*Pass*	*No*	*No*	*N.P*
29	*USA*	*Pass*	*No*	*No*	*N.P*

3.5 Discussion and Conclusion

The SynCardia 70cc TAH and other adult-orientated MCS devices have potential for pediatric and small adult heart failure populations. Case studies show that the TAH can fit in patients beneath the eligibility criteria without complications relating to fit (see Section 3.3) [21]. A prospective fit analysis confirms the anecdotal implications of the undersized patient case studies.

If the false negative results of the study hold true for the larger population, we can present a theoretical vignette as to the unnecessary rejection of patients due to the current, restrictive criteria. A direct linear regression would illustrate that with a 10.3% false negative rate and the number of patients that have received a TAH (n=1,061), approximately 109 patients were theoretically and unnecessarily excluded for consideration of the TAH, since the device has been approved for use. This number would be further inflated when considering all patients that were considered for a device, but did not receive one. While the specific false negative rate is not statistically significant, the potential for additional patient inclusion is promising. Furthermore, with approximately 400 hearts transplanted in pediatrics each year, additional MCS deployments could be life-saving.

As a contra positive vignette, the false positive rate was found to be at 6.9%. Again, if the trends discuss here hold true for a larger population, there is the potential that 73 patients, out of the 1,061 total, suffered fit complications. These complications may have needed follow up surgery, further risking the patient's life, or may have resulted in in increased morbidity or mortality. However, this is speculative as the rates of these

complications are currently not well tracked. The STS is a small subset of American institutions and may not provide a thorough enough image to validate the potential complications related solely to fit.

Immediate fit considerations include the closure of the patient's chest following surgery. In cases where the chest could not be closed, a higher incidence of device malfunction, bleeding, infection, and death were observed [20], [48]. In addition to closure-related complications, issues following anatomical impingement are predicted for undersized chest including respiratory complications and aberrant cardiovascular pressures. The virtual implantation provides a method for viewing the potential fit within the thoracic skeleton. This gross fit is the first step in determining patient viability for the TAH device.

Beyond the rigid definitions of passing or failing the virtual fit, the virtual optimization process opens windows into patient care or complication mitigation. Results and surgeon observations of a virtual implantation for a 43 year old male with complex CHD consisted of a video illustrating fit in addition to text describing fit and potential complications:

> "Based on the reconstruction and virtual implantation, the 70cc TAH appears to fit within the current ventricular mass; however, there is no significant room for movement of the device due to the sternum and costal cartilage. Consideration will have to be made regarding the current placement of pacing leads prior to surgery. … Although the device appears to fit in the area of the ventricular mass, device orientation will likely be

> affected by the strategy utilized to manage the transposed great vessels, either maintaining the existing atrial level reconstruction (Mustard) and directing the outflow to the appropriate great vessel, or by restoring normal atrial configuration and directing outflow grafts to corresponding great vessel. … Consideration of retention of the atrial baffle with persistent superior limb obstruction should be made. If atrial baffle is not retained, the TAH may need to be moved in addition to the construction of unique baffle or arterial switch."

This institution that chose to proceed with 70cc TAH was provided with a wealth of information prior to a surgery. Some of the information, such as the atrial baffle, may require additional surgical devices. Knowing the potential for surgical complications, such as needing additional equipment or novel cut down procedures, may decrease surgical time as well as reduce complications related to surgeon making decisions in real-time in the operating room. A proper, protocol-controlled clinical trial will be needed to validate the assertions made regarding surgical planning.

These case series and limited quantitative analysis illustrates the potential utility, and applied utility, of the virtual implantation of the 70cc TAH. In fact, the same technology was applied to two other MCS devices during the course of this study. This study also illustrates concerning deficits in the current eligibility criteria. The lack of specificity and sensitivity suggests that 24.1% of the study's cohort (6 out of the 29 patients), without virtual implantation, would have received less-than-optimal fit planning by the current, patient-agnostic criteria alone. Lastly, the virtual implantation technique

can help predict fit-related complications or, in the absence of better options, complications that may be mitigated by sufficient surgical planning.

The techniques explored in the virtual implantation of the TAH are not limited to the single MCS device. The same technique and procedure was applied to an undersized patient with the HeartWare (HeartWare International, Framingham, MA, USA) MCS device. In this case, the patient was far below the normal size recommendation and failed to pass virtual fit.

In addition to device fit, similar questions exist in heart transplantation regarding donor heart selection criteria. For instance, a cardiothoracic surgeon listing a pediatric patient on the heart transplantation donor list must specify the range of hearts the institution is willing to accept. The metrics for size of the donor heart are specified by the donor's height and weight. It is perceived by collaborating cardiothoracic surgeons, that this current selection criteria is insufficient in patient-specific care. The surgeons must establish the largest acceptable donor population for the recipient while avoiding a heart that is too large or too small to function properly. In fact, the virtual heart transplantation procedure was carried out on a single patient so far due the perceived success of the virtual implantation of the TAH. In addition, other anatomical transplantations are being pursued for the virtual surgery.

3.5.1 Implications of Technology Acceptance Study

Besides the efficacy of the virtual implantation, it is critical to examine the perceived utility and ease-of-use of the novel tool. Without technology acceptance from

medical professions, the tool, no matter how capable, will not be adopted into use. For this study, the TAM was developed as a follow-up survey to the implantation results. In the domain of perceived usefulness, two questions (#5 and #8) probed the participants' perception of the virtual implantation as an effective tool. All participants to the survey responded in the positive. The virtual implantation technology was "helpful in assessing MCS device fit or potential complications." Where the collaborating surgeon suggest ill-fit of the device, survey participants also responded in the affirmative that fit-related complications were a shared concern. The open response question (#10) solicited feedback for future iterations of the virtual implantation tool; only one participant responded directly related to the technology:

> "Yes, we would do the virtual analysis in the future. The virtual implantation allows our surgeon to better prepare for the implantation and have a more educated and guided "idea" on how he will be placing the device. Moreover, it gives us some additional certainty that the device will actually fit."

The virtual implantation process appears to provide a useful tool to the clinical care team at recipient institutions.

Due to the limited extra-curricular time for surgeons and surgeon support staff, the TAM survey was limited in order to promote compliance. Only one question addressed perceived ease-of-use (#9). All survey participants agreed that they would choose to exercise virtual fit analyses prior to MCS surgeries if the option was available. These

answers illustrate that the participants felt that the virtual tool was useful and non-invasive to the current planning process and would use it again in the future. The TAM survey as well as continued use by outside institutions suggests intention to use by cardiothoracic surgeons.

3.5.2 Limitations

The virtual implantation technique here is largely qualitative in determining fit. Where some structures can be seen as binary metrics for fit, such as virtual overlapping of the sternum and the device, the soft tissue impingement must be considered by the surgeon. He or she will ultimately make the decision for implantation. Future iterations of this technology may deploy finite element modeling in conjunction with evidence-based medicine to more accurately predict potential device fit failure. For instance, the device implantation would displace the surrounding tissue causing surrounding structures to deform and possibly narrow. A narrowing of a great vessel to a certain eccentricity may become the new metric for TAH (or MCS) fit. This finite element analysis of device fit has its own limitations. Specifically, there is not yet established foundation for the mechanical properties of tissue based on medical images and anatomical structures. While these overlaps are measured, there is no evidence-based literature that supports acceptable amounts of anatomical impingement. Even if the correlation of mechanical structures to specific anatomical structures could be determined, current generation computational architectures and resources would not likely facilitate virtual implantation in an emergent

timeframe. Future computing capabilities and advanced simulation software may make this finite-element-based virtual implantation process a possibility.

3.5.3 Concluding Remarks on Virtual Implantation

To date, 29 virtual implantations[12], spanning 10 states in the United States and 5 additional countries, have been performed with this technology. The virtual implantation process allows for a more precise selection of a medical device for a specific patient. The virtual implantation process may be capable of expanding the effective inclusion criteria, thus opening a MCS device to a wider potential patient population. At the same time, virtual implantation may help to reject patients who would otherwise result in fit-related and surgical complications. Despite its current limitations of the virtual implantation process, its utility as a clinical decision has been rapidly gaining acceptance, as illustrated by the TAM study; accordingly, the process has been translated to three additional MCS devices.

[12] This complete accounting of TAH virtual implantations includes the procedures discussed in the hybrid TAM study as well as cases preceding the establishment of the hybrid TAM protocols.

CHAPTER 4

ANCILLARY WORK – SURGICAL SIMULATION

4.1 Ventriculostomy Surgical Simulator

4.1.1 Introduction

Medical students and surgical residents develop medical and surgical knowledge through various media including lectures, textbooks, publications, and other content delivery mechanisms [52]. These learning mechanisms are vital to educational success; however, textbook knowledge does not necessarily translate to acquisition and mastery of procedural skills. Development of surgical skills toward mastery requires direct intervention on a patient, specialized educational environments (e.g., a cadaver lab) for and/or a patient simulator [52], [53].

The purpose of a simulator is to develop procedural knowledge. Procedural knowledge involves two main functions as defined by Kahol et al., which are cognitive and psychomotor functions [54]. An effective medical simulation enhances the learning of both behavioral functions [55], [56]. Simulacra, the physical, non-curricular components of simulators, replicate anatomies consistent with learned content knowledge, while the simulator's curricula target the learner's development of procedural skills. Learners are often compelled to reconcile content knowledge with procedural knowledge [57]. Through the use of a simulator, learners progress toward mastery of surgical skills outside of the risk-inherent environment of an operating room [57]–[59]. The learner is free to focus on

the development of cognitive and psychomotor skills without the risk of catastrophic consequences. Simulation in this context is a method of cognitive training that has been thoroughly validated [58], [60]–[63].

Educators can leverage the strengths of medical simulators to effectively teach complex and high-risk surgical procedures, such as placement of an external ventricular drain (EVD). This procedure is used to monitor intracranial pressure (e.g., in trauma patients or patients presenting with a Glasgow coma scale of 3-8 or less [64]) or to treat symptoms of hydrocephalus (such as patients with decreased cerebrospinal fluid (CSF) absorption due to subarachnoid hemorrhage or ventriculitis or patients with CSF pathway obstruction due to tumors, cerebral hemorrhages, etc.)[65]. CSF release is recommended in patients with SAH grade II or higher according to American Heart Association/American Stroke Association [66]. These sources of increased ventricular pressure, and the subsequent need for that pressure to be alleviated, presents a need for surgeon mastery of the ventriculostomy procedure. In fact, placement of an EVD constitutes one of the first bedside procedures learned in residency training and one of the most common procedures performed in the neurosurgical field [67], [68]. To improve neurosurgery education capabilities, the authors developed a ventriculostomy simulator leveraging the latest in rapid prototyping technologies in conjunction with traditional casting techniques (both elastomer and hydrogel). Virtual or mixed simulators for ventriculostomies have been developed previously [67], [70]; however, the prior computer-based simulators had high associated costs in terms of both equipment and facilitators. We describe the development of a cost-effective physical simulator for ventriculostomy placement. The goal of the proposed simulacrum is to facilitate medical simulation by

teaching three cognitive tasks: 1) develop an understanding of the geometry associated to the cranium and its landmarks in relation to the frontal horn of the lateral ventricles, 2) develop an awareness of the common ventriculostomy field of view, and 3) gain familiarity with the instruments and the methods used in deploying a ventricular cannula. The simulacrum features the integration of patient-derived cranium, brain, and lateral ventricular spaces. A simplified gravity-driven pump generates a constant ventricular pressure based on facilitator demands. The material choices for each component provide appropriate turgor and recoil to adequately simulate the surgical experience according to a limited qualitative study. The educational study also serves to establish potential efficacy of the model according to a technology acceptance model (TAM)[25]. The model is an attempt to quantify perceived usefulness and perceived ease-of-use of a new technology. Without the perception of efficacy, the simulator would fail to be adopted into standard educational practice. The techniques for developing the model, the educational study, and the associate advantages and disadvantages are discussed.

4.1.2 Methods – Computational Modeling

The initial computational model for the simulacrum was derived from two datasets. Head MRI data were acquired with 1.5mm slice thickness and 0.488mm pixel spacing in images of 512x512 pixels. Skull CT data were acquired with 0.625mm slice thickness and 0.488mm pixel spacing in images of 512x512 pixels. The resulting images were packaged into two Digital Imaging and Communication in Medicine (DICOM) files and imported into Mimics (Materialise, Lueven, Belgium), a medical image processing software suite.

The software facilitated image segmentation, the process of separating regions of an image into discrete subsets. Three subsets resulted from segmentation: brain, skull, and lateral ventricles. These masks were reconstructed into three-dimensional (3D) surface mesh models. Skull and cerebral models were then imported into an engineering software suite, Geomagic (3DSystems, Rock Hill, SC, USA).

The inferior third of the skull was removed to reduce simulator costs, and the posterior aspect of the skull was removed to create an opening for the installation and removal of the brain model. Two windows were cut from the superior aspect of the skull to allow the interchanging of disposable bone plates for burr-hole placements, allowing multiple attempts during simulation. The brain model was truncated at the same position as the skull model. Undercuts created by deep sulci were removed to prevent issues with molding and casting. The lateral ventricles were also truncated, and a back plate was added to the ventricular system to facilitate molding and casting. The computational models of the brain with ventricles and truncated skull are shown in Figure 22.

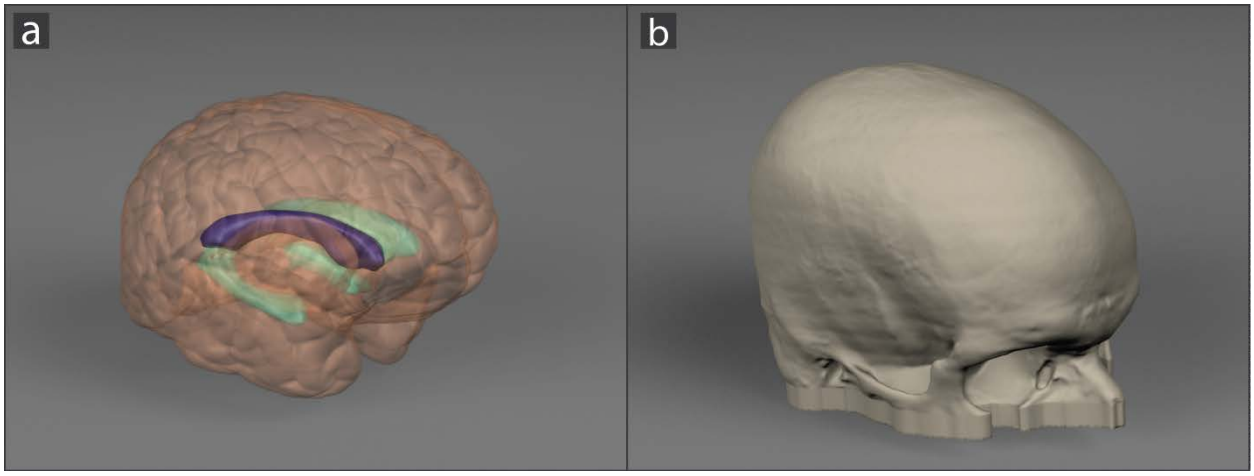

Figure 22: a) Rendering of the brain following MRI reconstruction. The lateral ventricles are highlighted in light blue. The anterior horn of the lateral ventricle rendered in dark blue is used in the final physical model. b) The skull has been truncated to increase durability of the model in addition to cost savings.

4.1.3 Methods – Physical Modeling

The adjusted skull model was printed using a zPrinter 650 (3Dsystems, Rock Hill, South Carolina, USA) with 0.1 mm layer thickness. This additive manufacturing process prints a cyanoacrylate binding agent onto a gypsum-powder medium, creating a final material similar to bonded plaster. Tactile qualities of the composite material are similar to those of actual bone, especially when handled with surgical instruments (e.g., a manual twist drill). Additional bone windows as described in the preceding section were also printed as shown in Figure 2a. A Stratasys Dimension 1200es (Eden Prairie, Minnesota, USA) was used to print the final brain and ventricle models in an acrylonitrile butadiene styrene (ABS) plastic medium with a layer thickness of 0.254mm. This additive process heats a plastic spindle and extrudes it onto a platform, depositing material as a single layer. The process is

repeated layer-by-layer until the model is complete. Support material is removed in a heated, caustic (sodium hydroxide) bath. For the brain and ventricle prints, the plastic surface underwent selective chemical dissolution with a 90:10 by volume solution of xylene and acetone, respectively. The models were submerged in a secondary bath of isopropyl alcohol (91% by volume) to preserve optimal surface quality. Optimal quality is defined as removal of all visible striations inherent to additive manufacturing processes.

A silicone spray release agent (Ease Release 20, Smooth-On, Easton, Pennsylvania, USA) was used to coat the plastic brain model. The plastic brain component was then placed inside a mold box and covered with a temperature resistant casting silicone (MoldMax 60, Smooth-On, Easton, Pennsylvania, USA). This process was repeated with the ventricles. Once cured, plastic components were removed from the silicone molds. A silicone cast was then created in the ventricular mold to generate the two elastomeric ventricular cores as seen in Figure 23b.

A mixture of gelatin and agar gel powder (90:10 by weight) was added to distilled water (at 75°C) to achieve the desired gel concentration (1.2% by weight). The solution was stirred until homogenous and allowed to cool to room temperature. The gel was then placed in a 65°C water bath for an hour and returned to room temperature before another round of heating ensured hydration of the hydrogel powder.

The brain mold and ventricle casts were coated with common cooking oil as a release agent. The heated gelatin/agar solution was poured into the brain silicone mold. The ventricle cores were inserted into molten medium, and the gel was cooled to room temperature. The brain was extracted from the mold prior to ventricular core removal. The

brain model, shown in Figure 23d was placed into the skull model to complete the proposed ventricular simulacrum as shown in in Figure 23a.

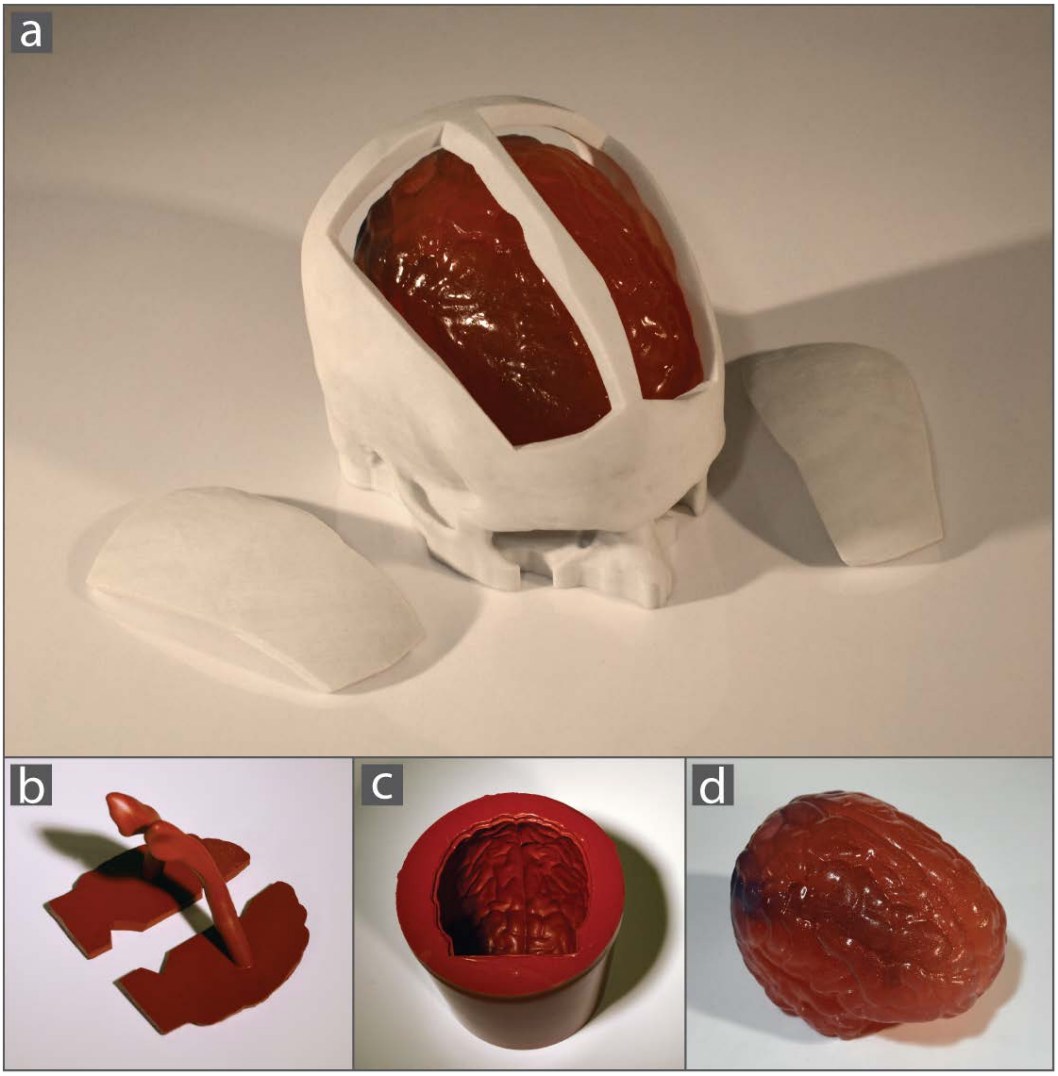

Figure 23: a) Assembled simulator including printed skull and casted brain. The smaller pieces flanking the simulator are replaceable plates providing undamaged sites to each learner for the burr hole drilling component of a ventriculostomy. b) Silicone core-castA simple gravity-driven pump was created to build pressure within the ventricular system. A water reservoir delivered CSF analogue (water) to the ventricles at a constant pressure as determined by the simulator facilitator. A syringe in the drive line allowed simulator facilitators to manually increase ventricular pressure or create unsteady conditions as necessary for a given curriculum. An illustration of the simulator set-up is shown in Figure 24.

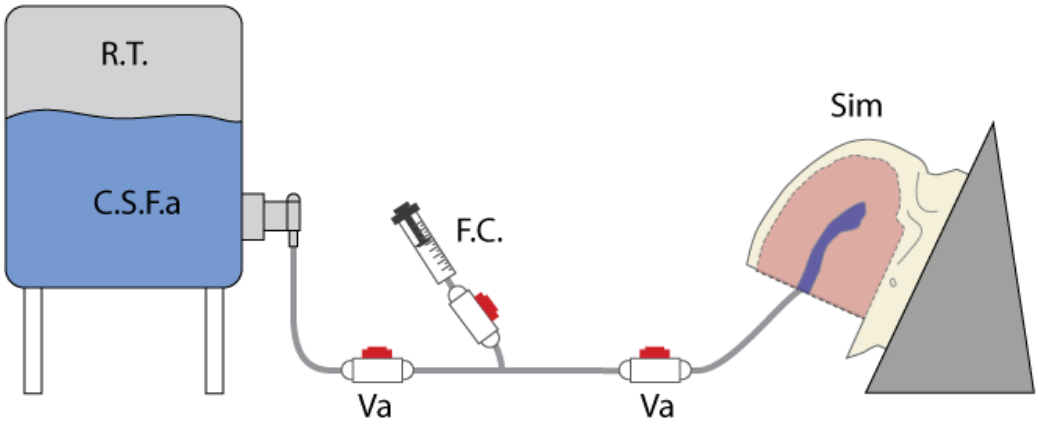

Figure 24: Schematic drawing of the entire simulacrum. The cranium is rendered transparent to show placement of the brain and ventricles. R.T. is reservoir tank, C.S.F.a is cerebrospinal fluid analogue, F.C. is flow control syringe, Va is valve, and Sim is simulacrum.

4.1.4 Methods – Educational and Technology Acceptance Study

The assembled model was trialed by a group of medical students and residents (n=10) to qualitatively determine the simulator's efficacy and establish the foundation for a future multi-cohort educational study. A 4th year post-graduate neurosurgery resident served as the facilitator for this study. A short curriculum based on standard practices used to complete a ventriculostomy was presented to the students. The ventriculostomy procedure started with drilling of a burr hole at Kocher's point, approximately 10 cm posterior to the glabella, a landmark included on the simulator, and 2.5 cm lateral to the midline. Manual twist drill was used to create the burr hole, and the blunt end of the tunneling trocar was used to clear away any bone-analogue chips from the burr hole. A standard ventricular catheter was advanced into the burr hole and brain at an appropriate angle using anatomical

landmarks as guides. The ventricular catheter was advanced approximately 6.5-7cm to the edge of the bone. Placement success was determined by the presence of CSF analog fluid flowing from the ventricular catheter after stylet removal. An observer recorded the number of passes through the brain needed to obtain CSF flow.

Prior to surgical simulation and curricula deployment, students completed a pre-assessment questionnaire evaluating student familiarity with the ventriculostomy procedure. Following simulation, students completed a post-assessment survey with the same questions as the pre-assessment questionnaire. The latter survey included an additional 20 questions based on an expanded TAM model by Davis *et. al*. and Dabholkar and Bagozzi[25], [26]. Domains in this modified TAM include awareness/presence, perceived usefulness, perceived ease-of-use, enjoyment, attitude, and intention-to-use. The standard five-point Likert-scale was used to qualify responses (1 being strongly negative in response, 5 being strongly positive in response).

4.1.5 Results

The simulator was used by 10 individuals with varying degrees of expert level. Medical students (n=4) and residents (n=6) from 0-5 post-graduate years (PGY) utilized the simulator. Five out of the six residents completed the simulation on the first attempt; all medical students and one 2-PGY resident needed multiple attempts to place the catheter into the ventricle. A comprehensive breakdown of all questions and responses related to the technology acceptance component of the survey is included in Table 16. All responses

gauged the perceived educational efficacy (as defined by the domains in the TAM) with means greater than "neutral" (3 on the deployed Likert-scale).

Table 16 (next page): TAM post-assessment responses. TAM post-assessment rating coded on a Likert scale: 1, strongly disagree; 2, disagree; 3, neutral; 4, agree; 5, strongly agree. Means 4.0 and higher are color-coded as green, otherwise coded as yellow. Standard deviations 1.0 and lower are color-coded as green, otherwise coded as yellow. No statistical significance was determined.

Technology Acceptance Questions (n=10)	**Score**		
	mean	**±**	**std. dev.**
Awareness/Presence			
The tactile response of the bone helps me understand how far to drill.	3.7	±	1.0
The tactile response of the brain media helps me understand if the catheter is in the ventricle	3.8	±	0.9
The cranial field of view helps me practice for a realistic intervention.	4.0	±	0.8
The patient derived model helps me appreciate anatomical landmarks.	3.9	±	0.8
Perceived Usefulness			
The simulator improved my performance of a ventriculostomy.	4.1	±	0.7
The simulator improved my understanding of the relationship of the ventricles to the cranium.	4.0	±	0.8
The simulator has increased my confidence in performing a ventriculostomy in a patient.	4.0	±	0.8
What I have learned in the simulator will impacted patient care.	4.0	±	0.8
The simulator was an effective use of my time.	4.2	±	0.8
Perceived Ease-of-Use			
The simulator was not cumbersome or difficult to interact with	4.1	±	0.9
This low cost simulator was well-designed.	4.3	±	0.7
The simulation did not take an unnecessary amount of time to complete.	4.4	±	0.9
The simulator was effective with some instruction.	4.7	±	0.5
The simulator would be effective without any instruction.	3.7	±	0.9
Enjoyment			
I enjoyed this simulator as an educational tool.	4.3	±	0.8
I enjoyed this simulator regardless of the potential educational value.	4.1	±	1.1

Technology Acceptance Questions (n=10)	Score		
	mean	±	std. dev.
Attitude			
The simulator will improve my surgical skills if given time to practice.	4.3	±	1.0
I have a positive attitude about this simulator.	4.6	±	0.6
Intention-to-Use			
The simulator encourages me to practice this medical intervention.	4.1	±	1.0
I wish simulators like this were created for other common procedures.	4.4	±	0.7
I would recommend this simulator for other learners.	4.4	±	0.7

4.1.6 Discussion

There are three basic approaches to medical simulation development: 1) cadaveric tissue models (human or animal), 2) computer-based or virtual reality systems, and 3) synthetic physical models. Each of these approaches has been employed in neurosurgical simulation, and each has its own advantages and disadvantages. For example, cadaveric dissection is well-accepted and introduces students and residents to surgical education early in clinical training [52], [71]. The cost of cadavers and the necessary facilities to preserve, accommodate, and maintain the specimens, however, is increasingly cost-prohibitive [72]. In addition, cadaveric models can lack the anatomical accuracy reflected in living patients. For example, a cadaver will not be able to illustrate the real-time scenario of increased ventricular pressure. One method to circumvent these limiting factors of cost, availability, and ability to simulate real-time pathology is to construct medical simulators. We believe the proposed model has great potential to provide a low cost and effective method of training residents in the following skills: 1) understanding of cranial geometry and its

landmarks in relation to the frontal horn of the lateral ventricles, 2) recognition of the appropriate entry point for ventriculostomy catheter placement, and 3) acquisition of familiarity with the instruments (e.g., manual twist drill, catheters, trocar, etc.) and the methods used in deploying a ventricular catheter. However, inherent to any simulator (physical or virtual) are simplifications of anatomy and physiology.

The proposed simulacrum utilizes advanced rapid prototyping technologies and casting techniques to produce an effective surgical simulator. The simulacrum includes structures that simulate a realistic surgical field. The brain, lateral ventricular system, and skull are all of accurate anatomical scale, given that they are derived from patient data. Ventricular anatomy can be easily manipulated to represent abnormal anatomy if desired (e.g., displacement by a hemorrhage or tumor), since the mold pieces are separated in the casting process (brain parenchyma from ventricles); this compartmentalization in design imparts modular capability to the simulator. Ventricular geometries can be extracted from different patient datasets, reconstructed as 3D geometries, and then printed in a format compatible with the casting methods. A facilitator could have multiple malformed ventricular geometries, simulating a progression of disease or differences among diseased morphologies.

Rapid prototyping has been broadly applied in the medical community [24], [73]. Early applications in generating cerebroventricular simulacra include Bova *et al.* where the modeling of the cranium employed additive manufacturing technology, but the ventricular systems was represented using a computer-generated haptic-feedback system [74]. These early models, while achieving a high level of anatomical complexity, were costly given they are “mixed-simulators” that contain elements of physical modeling as well as virtual,

haptic systems. The systems developed by Bova *et al.* included an electromagnetic tracking system. Our model achieves anatomical accuracy through 3D printing while maintaining low costs with readily available materials. Once initial molds have been created, final brain casts are produced using common and accessible materials. As of the publication date, material costs were approximately $4 per brain model.

Regardless of cost, a simulator can only be considered effective if it facilitates development of cognitive and psychomotor skills. The proposed simulacrum demonstrated utility in conveying the location of the ventricle with respect to anatomical landmarks on the cranium, as evidenced by the pilot educational study. For example, following the insertion of the catheter, the learner is charged with locating the ventricle. 80% of the neurosurgery residents completed a successful ventriculostomy on the first attempt, while all medical students needed multiple attempts to succeed in catheter placement. This result suggests that increased surgical experience (it is assumed a resident has more years of experience than a medical student) results in a stronger performance on the simulator. Conversely, this result suggests that there is a gap to be filled in training medical students to effectively locate ventricles early on in their careers.

Following the simulation study, analysis of the TAM responses revealed positive trends in the perceived efficacy of the simulator. All TAM responses had a mean greater than 3, suggesting that the model is better than the status quo in ventriculostomy education. All questions coded as *perceived usefulness*, *attitude*, and *intent-to-use* had means equal to or greater than 4.0 (positive) with standard deviations at or below 1.0. The positive trends in the TAM responses are evidence of the simulacrum's efficacy.

There are several limitations to the current simulator model. First, the material properties of the brain analogue are not philologically accurate. The human brain is not a homogenous medium with anisotropic material properties. The medium that we have developed are similar to other hydrogel models [63], [76]–[78] that use a homogenous mixture to achieve a constant tactile response. This moderate sacrifice in realism was made to reduce material costs.

Secondly, the simulacrum simulates neither dura nor arachnoid mater. These meningeal layers encapsulate the sub-arachnoid space, which may also exhibit increased CSF pressure in the presence of trauma or disease. Current 3D printing processes make this component of the simulacrum both challenging and impractical to model. Nevertheless, the authors are investigating other casting methods to develop a cost-effective process for simulating arachnoid dissection in future iterations of the simulacrum. Multi-material 3D printing may be another method of simulating the complex stratification and presentation of multiple tissues. Specifically, Digital Material printing (Stratasys, Rehovot, Israel) utilizes a series of photopolymers with a spectrum of Shore hardnesses and other material properties. Future computational modeling schemes may leverage volumetric modeling as opposed to surface mesh modeling to facilitate this multi-material printing. Current mechanisms for multi-material printing require discrete regions describing material properties. A volumetric modeling approach, where voxels can be assigned material properties, may result in a print with a gradient of material properties. For simulacra where cost considerations are less critical, this 3D printing modality may enable the construction of a higher fidelity simulacra.

Another limitation is geometric idealization (to facilitate cost-effective casting process). When reconstructing the brain matter, the inner surfaces of sulci were removed. The final representation includes gyri and impressions of the sulci for the purposes of surface landmarks. While virtual, haptic systems may be able to capture this form of undercut geometry, collaborating neurosurgeons considered these components less important than the cost-effective nature of the simulacrum. The current model only contains the superior lateral horns of the ventricles. Recent advances in elastomeric printing may make these geometric sacrifices unnecessary; however, it will be up to institutions to balance cost with geometric and tactile accuracy.

A limitation to the TAM used to validate the potential efficacy of the simulacra relates to the study size. Only 10 individuals trialed the simulator and provided feedback. The intent of the study was to provide early qualitative support for the simulator, which was favorable. To better gauge the efficacy of the simulator, a multi-cohort, randomized trial should be performed.

4.1.7 Conclusion

EVD placement is one of the most common (yet challenging), life-saving procedures performed by a neurosurgeon, and also one of the first learned in residency training. Since cadaveric models do not reflect “live” or “real-time” anatomical functions of the ventricular system, simulators are a promising route for medical students and interns to learn this high-risk procedure. Haptic-based systems, while effective, have high associated costs. We have developed a low-cost simulacrum to train medical students and

neurosurgical residents in ventriculostomy placement. While 3D printing techniques have enabled anatomical representation, such as the PHDMs, 3D printing can also address more complex educational systems. Advanced 3D printing and casting techniques enabled the creation of a cost-effective simulator with advantageous realism in comparison to state-of-the-art virtual and/or mixed alternatives. An initial qualitative study suggests that the simulacrum may be valuable for neurosurgical education. Future models will aim to enhance anatomical and physiological accuracy by adding the complete ventricular system, as well as additional cranial and brain tissues (e.g., scalp and meninges).

CHAPTER 5

FUTURE BLUEPRINT

5.1 Future Development of PHDMs

The PHDM methods and results in this dissertation illustrate a window into an active translational research initiative. The research has been integrated into clinical and continues to impact patient care and education at collaborating institutions. Despite the high acceptance of this technology at collaborating institutions, PHDMs are not standard-of-care at all major institutions. The greater challenge in any novel biomedical application development, not just PHDM development, is to achieve technological adoption by the greater community.

Towards this aim of technological acceptance, the PHDMs will be used in a multi-center clinical trial. The immediate goal will be to elucidate the impact of the PHDMs on measurable surgical outcomes. This effort will require a prospective study design that rigorously blocks out confounding factors, leaving the analysis to focus on the direct, measurable impact by PHDMs. The results and discussion in Sections 2.4 and 2.5 have already informed the inclusion and exclusion criteria of the proposed clinical trial in order to address these potentially confounding factors. For example, additional exclusion criteria is expected to remove outliers from simple surgeries. Removal of outliers is expected to homogenize response variance, yielding stronger statistical correlation to real-world effects.

The potential impact of the clinical trial should not be understated. Positive results of a clinical trial will be used to leverage the American Medical Association to develop Current Procedural Terminology (CPT) codes for the 3D printing technology. Following the development of CPT codes, hospitals would have a mechanism of billing PHDMs to insurance companies. The potential for reducing morbidity and mortality in conjunction with the potential cost-savings may drive additional hospitals to make 3D printing a standard-of-care. Therefore, this critical clinical trial will be the first major step towards technological adoption by the greater medical community.

5.2 Future Development of Virtual Implantation

The original technology acceptance model described by Davis suggests that perceived usefulness and perceived ease-of-use are critical to the adoption and use of a new technology. The results of the virtual implantation process suggests strong support for usefulness of the technology. This is further supported by the de facto use of the technology by SynCardia Systems for borderline and complex cases. The perceived ease-of-use was also positive according to clinical collaborators; however, the workflow for the technology may be perceived as inefficient due to the number of people needed for the virtual surgery.

The virtual implantation process in its current iteration requires an individual with advanced computational modeling skills. These skills may be common for a biomedical engineer; however, they are uncommon for a medical professional. The expedient fix we have developed is to have a two-person team addressing virtual implantation needs. The skilled engineer reconstructs the anatomy and manipulates the orientation of the device

guided by feedback from the clinician. Miscommunications when talking about translation and rotation in a virtual, 3D environment were common in our experience. The ideal route would be a clinician directly engaging with an easy-to-use technology, removing the need for an engineer intermediary.

To meet this clinical need, an interdisciplinary team is developing a virtual reality (VR) experience. The VR experience includes a headset that a clinician would engage with to view the virtual environment and reconstructed anatomy in stereoscopic vision. Infra-red hand-tracking devices would track the clinicians' hand movements. The clinician would engage with both tools in order to translate and rotate a virtual replica of the medical device into the patient's reconstructed anatomy. The result of this technology would enable the clinician to directly interface with the virtual implantation technology, enhancing the workflow process and augmenting the technological ease-of-use. With regards to the technology acceptance model, the enhanced ease-of-use will ultimately lead to greater adoption of this life-saving virtual surgery technology.

REFERENCES

[1] V. L. Vetter, *Pediatric Cardiology: The Requisites in Pediatrics*. Philadelphia, PA: Mosby, 2006.

[2] M. H. Crawford, J. P. DiMarco, and W. J. Paulus, *Cardiology*, 3 edition. Philadelphia: Mosby, 2009.

[3] S. L. Sadowski, "Congenital Cardiac Disease in the Newborn Infant: Past, Present, and Future," *Crit. Care Nurs. Clin. North Am.*, vol. 21, no. 1, pp. 37–48, Mar. 2009.

[4] C. Mavroudis, C. Backer, and R. F. Idriss, *Pediatric Cardiac Surgery*, 4 edition. Hoboken, NJ: Wiley-Blackwell, 2012.

[5] "STS Fall 2014 Harvest," Duke Clinical Research Institute.

[6] A. C. Gelijns, A. J. Moskowitz, M. A. Acker, M. Argenziano, N. L. Geller, J. D. Puskas, L. P. Perrault, P. K. Smith, I. L. Kron, R. E. Michler, M. A. Miller, T. J. Gardner, D. D. Ascheim, G. Ailawadi, P. Lackner, L. A. Goldsmith, S. Robichaud, R. A. Miller, E. A. Rose, T. B. Ferguson Jr., K. A. Horvath, E. G. Moquete, M. K. Parides, E. Bagiella, P. T. O'Gara, and E. H. Blackstone, "Management Practices and Major Infections After Cardiac Surgery," *J. Am. Coll. Cardiol.*, vol. 64, no. 4, pp. 372–381, Jul. 2014.

[7] R. M. Lang, L. P. Badano, W. Tsang, D. H. Adams, E. Agricola, T. Buck, F. F. Faletra, A. Franke, J. Hung, L. P. de Isla, O. Kamp, J. D. Kasprzak, P. Lancellotti, T. H. Marwick, M. L. McCulloch, M. J. Monaghan, P. Nihoyannopoulos, N. G. Pandian, P. A. Pellikka, M. Pepi, D. A. Roberson, S. K. Shernan, G. S. Shirali, L. Sugeng, F. J. T. Cate, M. A. Vannan, J. L. Zamorano, and W. A. Zoghbi, "EAE/ASE Recommendations for Image Acquisition and Display Using Three-Dimensional Echocardiography," *Eur. Heart J. - Cardiovasc. Imaging*, vol. 13, no. 1, pp. 1–46, Jan. 2012.

[8] J.-L. Coatrieux, C. Toumoulin, C. Hamon, and L. Luo, "Future trends in 3D medical imaging," *IEEE Eng. Med. Biol. Mag.*, vol. 9, no. 4, pp. 33–39, Dec. 1990.

[9] M. Bailey, "Interacting with direct volume rendering," *IEEE Comput. Graph. Appl.*, vol. 21, no. 1, pp. 10–12, Jan. 2001.

[10] C. W. Yancy, M. Jessup, B. Bozkurt, J. Butler, D. E. Casey, M. H. Drazner, G. C. Fonarow, S. A. Geraci, T. Horwich, J. L. Januzzi, M. R. Johnson, E. K. Kasper, W. C. Levy, F. A. Masoudi, P. E. McBride, J. J. V. McMurray, J. E. Mitchell, P. N. Peterson, B. Riegel, F. Sam, L. W. Stevenson, W. H. W. Tang, E. J. Tsai, and B. L. Wilkoff, "2013 ACCF/AHA Guideline for the Management of Heart Failure A Report of the

American College of Cardiology Foundation/American Heart Association Task Force on Practice Guidelines," *Circulation*, vol. 128, no. 16, pp. e240–e327, Oct. 2013.

[11] L. A. Allen, L. W. Stevenson, K. L. Grady, N. E. Goldstein, D. D. Matlock, R. M. Arnold, N. R. Cook, G. M. Felker, G. S. Francis, P. J. Hauptman, E. P. Havranek, H. M. Krumholz, D. Mancini, B. Riegel, and J. A. Spertus, "Decision Making in Advanced Heart Failure," *Circulation*, p. CIR.0b013e31824f2173, Mar. 2012.

[12] G. W. Dec and V. Fuster, "Idiopathic Dilated Cardiomyopathy," *N. Engl. J. Med.*, vol. 331, no. 23, pp. 1564–1575, Dec. 1994.

[13] A. I. Dipchand, L. B. Edwards, A. Y. Kucheryavaya, C. Benden, F. Dobbels, B. J. Levvey, L. H. Lund, B. Meiser, R. D. Yusen, and J. Stehlik, "The Registry of the International Society for Heart and Lung Transplantation: Seventeenth Official Pediatric Heart Transplantation Report—2014; Focus Theme: Retransplantation," *J. Heart Lung Transplant.*, vol. 33, no. 10, pp. 985–995, Oct. 2014.

[14] M. M. Givertz, "Ventricular Assist Devices Important Information for Patients and Families," *Circulation*, vol. 124, no. 12, pp. e305–e311, Sep. 2011.

[15] E. Alboliras, *Atlas of Neonatal Cardiology*. Hoboken, NJ: John Wiley & Sons, 2014.

[16] C. S. D. Almond, R. R. M. Thiagarajan, G. E. Piercey, K. Gauvreau, E. D. Blume, H. J. Bastardi, F. Fynn-Thompson, and T. P. Singh, "Waiting List Mortality Among Children Listed for Heart Transplantation in the United States," *Circulation*, vol. 119, no. 5, pp. 717–727, Feb. 2009.

[17] J. C. Fang and J. Stehlik, "Moving Beyond 'Bridges'∗," *JACC Heart Fail.*, vol. 1, no. 5, pp. 379–381, Oct. 2013.

[18] A. Fuchs and H. Netz, "Ventricular assist devices in pediatrics," *Images Paediatr. Cardiol.*, vol. 3, no. 4, pp. 24–54, 2001.

[19] M. Colvin-Adams, J. M. Smith, B. M. Heubner, M. A. Skeans, L. B. Edwards, C. Waller, J. J. Snyder, A. K. Israni, and B. L. Kasiske, "OPTN/SRTR 2011 Annual Data Report: Heart," *Am. J. Transplant.*, vol. 13, pp. 119–148, Jan. 2013.

[20] J. G. Copeland, R. G. Smith, F. A. Arabia, P. E. Nolan, G. K. Sethi, P. H. Tsau, D. McClellan, and M. J. Slepian, "Cardiac Replacement with a Total Artificial Heart as a Bridge to Transplantation," *N. Engl. J. Med.*, vol. 351, no. 9, pp. 859–867, Aug. 2004.

[21] S. S. Park, D. B. Sanders, B. P. Smith, J. Ryan, J. Plasencia, M. B. Osborn, C. M. Wellnitz, R. N. Southard, C. N. Pierce, F. A. Arabia, J. Lane, D. Frakes, D. A. Velez, S. G. Pophal, and J. J. Nigro, "Total artificial heart in the pediatric patient with biventricular heart failure," *Perfusion*, vol. 29, no. 1, pp. 82–88, Jan. 2014.

[22] F. Ejaz, J. Ryan, M. Henriksen, L. Stomski, M. Feith, M. Osborn, S. Pophal, R. Richardson, and D. Frakes, “Color-coded patient-specific physical models of congenital heart disease,” *Rapid Prototyp. J.*, vol. 20, no. 4, pp. 336–343, Jun. 2014.

[23] B. N. Roszelle, L. F. Gonzalez, M. H. Babiker, J. Ryan, F. C. Albuquerque, and D. H. Frakes, “Flow diverter effect on cerebral aneurysm hemodynamics: an in vitro comparison of telescoping stents and the Pipeline,” *Neuroradiology*, vol. 55, no. 6, pp. 751–758, Jun. 2013.

[24] G. Wurm, M. Lehner, B. Tomancok, R. Kleiser, and K. Nussbaumer, “Cerebrovascular Biomodeling for Aneurysm Surgery Simulation-Based Training by Means of Rapid Prototyping Technologies,” *Surg. Innov.*, vol. 18, no. 3, pp. 294–306, Sep. 2011.

[25] F. D. Davis, R. P. Bagozzi, and P. R. Warshaw, “User Acceptance of Computer Technology: A Comparison of Two Theoretical Models,” *Manag. Sci.*, vol. 35, no. 8, pp. 982–1003, Aug. 1989.

[26] P. A. Dabholkar and R. P. Bagozzi, “An attitudinal model of technology-based self-service: Moderating effects of consumer traits and situational factors,” *J. Acad. Mark. Sci.*, vol. 30, no. 3, pp. 184–201, Jun. 2002.

[27] V. Venkatesh, “Determinants of perceived ease of use: Integrating control, intrinsic motivation, and emotion into the technology acceptance model,” *Inf. Syst. Res.*, vol. 11, no. 4, pp. 342–365, Dec. 2000.

[28] J. L. Moreno Cegarra, J. G. Cegarra Navarro, and J. R. Córdoba Pachón, “Applying the technology acceptance model to a Spanish City Hall,” *Int. J. Inf. Manag.*, vol. 34, no. 4, pp. 437–445, Aug. 2014.

[29] W. R. King and J. He, “A meta-analysis of the technology acceptance model,” *Inf. Manage.*, vol. 43, no. 6, pp. 740–755, Sep. 2006.

[30] A. K. Yarbrough and T. B. Smith, “Technology Acceptance among Physicians A New Take on TAM,” *Med. Care Res. Rev.*, vol. 64, no. 6, pp. 650–672, Dec. 2007.

[31] B. Cardoen, E. Demeulemeester, and J. Beliën, “Operating room planning and scheduling: A literature review,” *Eur. J. Oper. Res.*, vol. 201, no. 3, pp. 921–932, Mar. 2010.

[32] F. Dexter and A. Macario, “Changing allocations of operating room length of time from a system based on historical utilization to one where the aim is to schedule as many surgical cases as possible,” *Anesth. Analg.*, vol. 94, no. 5, pp. 1272–1279, table of contents, May 2002.

[33] R. J. M. M. Does, T. M. B. Vermaat, J. P. S. Verver, S. Bisgaard, and J. Van Den Heuvel, "Reducing Start Time Delays in Operating Rooms," *J. Qual. Technol.*, vol. 41, no. 1, pp. 95–109, Jan. 2009.

[34] N. Pandis, "Sources of bias in clinical trials," *Am. J. Orthod. Dentofacial Orthop.*, vol. 140, no. 4, pp. 595–596, Oct. 2011.

[35] D. Peter, P. Robinson, M. Jordan, S. Lawrence, K. Casey, and D. Salas-Lopez, "Reducing Readmissions Using Teach-Back: Enhancing Patient and Family Education," *JONA J. Nurs. Adm.*, vol. 45, no. 1, pp. 35–42, Jan. 2015.

[36] U. F. Trummer, U. O. Mueller, P. Nowak, T. Stidl, and J. M. Pelikan, "Does physician–patient communication that aims at empowering patients improve clinical outcome?: A case study," *Patient Educ. Couns.*, vol. 61, no. 2, pp. 299–306, May 2006.

[37] H. Gray, T. P. Pick, and R. Howden, *Gray's Anatomy: The Unabridged Running Press Edition Of The American Classic*, Unabridged edition. Philadelphia: Running Press, 1974.

[38] F. H. Netter, *Atlas of Human Anatomy*. Elsevier Health Sciences, 2014.

[39] T. Huk, "Who benefits from learning with 3D models? the case of spatial ability," *J. Comput. Assist. Learn.*, vol. 22, no. 6, pp. 392–404, 2006.

[40] J. Contessa, K. A. Ciardiello, and S. Perlman, "Surgery Resident Learning Styles and Academic Achievement," *Curr. Surg.*, vol. 62, no. 3, pp. 344–347, May 2005.

[41] J. M. V. Mammen, D. R. Fischer, A. Anderson, L. E. James, M. S. Nussbaum, R. H. Bower, and T. A. Pritts, "Learning Styles Vary Among General Surgery Residents: Analysis of 12 Years of Data," *J. Surg. Educ.*, vol. 64, no. 6, pp. 386–389, Nov. 2007.

[42] S. DeYoung, *Teaching strategies for nurse educators*, 2nd ed. Upper Saddle River, N.J: Prentice Hall, 2009.

[43] M. D. Aldridge, "Using Models to Teach Congenital Heart Defects: A Hands-on Approach," *Dimens. Crit. Care Nurs.*, vol. 28, no. 3, pp. 116–122, May 2009.

[44] C. E. Mullins and D. C. Mayer, *The Mullins and Mayer Atlas of Congenital Heart Disease*. Charlottesville, VA, USA: Scientific Software Solutions.

[45] (first), "Congenital Heart Defects," *Centers for Disease Control and Prevention*, 18-Jul-2014. [Online]. Available: http://www.cdc.gov/ncbddd/heartdefects/specificdefects.html. [Accessed: 28-Nov-2014].

[46] T. Ralhan, R. Richardson, K. Diab, and E. Alboliras, "Effectiveness of standardized color-coding of anatomical structures in 3D reconstructions of congenital heart

diseases using CCTA," presented at the St. Joseph's Hospital and Medical Center. Academic Excellence Day, Phoenix, AZ, 2010.

[47] F. D. Davis, "Perceived Usefulness, Perceived Ease of Use, and User Acceptance of Information Technology," *MIS Q*, vol. 13, no. 3, pp. 319–340, Sep. 1989.

[48] P. Leprince, N. Bonnet, S. Varnous, A. Rama, P. Léger, A. Ouattara, M. Landi, J. Szefner, I. Gandjbakhch, and A. Pavie, "Patients with a body surface area less than 1.7 m2 have a good outcome with the CardioWest Total Artificial Heart," *J. Heart Lung Transplant. Off. Publ. Int. Soc. Heart Transplant.*, vol. 24, no. 10, pp. 1501–1505, Oct. 2005.

[49] F. Remondino and S. El-Hakim, "Image-based 3D Modelling: A Review," *Photogramm. Rec.*, vol. 21, no. 115, pp. 269–291, Sep. 2006.

[50] M. Jessup, W. T. Abraham, D. E. Casey, A. M. Feldman, G. S. Francis, T. G. Ganiats, M. A. Konstam, D. M. Mancini, P. S. Rahko, M. A. Silver, L. W. Stevenson, and C. W. Yancy, "2009 Focused Update: ACCF/AHA Guidelines for the Diagnosis and Management of Heart Failure in Adults," *Circulation*, vol. 119, no. 14, pp. 1977–2016, Apr. 2009.

[51] R. D. Dowling, L. A. Gray, S. W. Etoch, H. Laks, D. Marelli, L. Samuels, J. Entwistle, G. Couper, G. J. Vlahakes, and O. H. Frazier, "Initial experience with the AbioCor implantable replacement heart system," *J. Thorac. Cardiovasc. Surg.*, vol. 127, no. 1, pp. 131–141, Jan. 2004.

[52] J. C. McLachlan, J. Bligh, P. Bradley, and J. Searle, "Teaching anatomy without cadavers," *Med. Educ.*, vol. 38, no. 4, pp. 418–424, 2004.

[53] K. R. V. Sickle, E. M. Ritter, and C. D. Smith, "The Pretrained Novice: Using Simulation-Based Training to Improve Learning in the Operating Room," *Surg. Innov.*, vol. 13, no. 3, pp. 198–204, Sep. 2006.

[54] K. Kahol, M. Vankipuram, and M. L. Smith, "Cognitive simulators for medical education and training," *J. Biomed. Inform.*, vol. 42, no. 4, pp. 593–604, Aug. 2009.

[55] K. Khan, T. Pattison, and M. Sherwood, "Simulation in medical education," *Med. Teach.*, vol. 33, no. 1, pp. 1–3, Jan. 2011.

[56] J. C. Hall, C. Ellis, and J. Hamdorf, "Surgeons and cognitive processes," *Br. J. Surg.*, vol. 90, no. 1, pp. 10–16, 2003.

[57] M. Ujiki and J. Zhao, "Simulation Training in Surgery," *Dis. Mon.*, vol. 57, no. 12, pp. 789–801, Dec. 2011.

[58] S. B. Issenberg and R. J. Scalese, "Simulation in Health Care Education," *Perspect. Biol. Med.*, vol. 51, no. 1, pp. 31–46, 2008.

[59] R. A. Kockro, A. Stadie, E. Schwandt, R. M. D. Reisch, C. Charalampaki, I. Ng, T. T. Yeo, P. Hwang, L. Serra, and A. M. D. Perneczky, “A collaborative virtual reality environment for neurosurgical planning and training,” *Neurosurg. Novemb. 2007*, vol. 61, no. 5, pp. 379–391, 2007.

[60] Issenberg S, McGaghie WC, Hart IR, and et al, “Simulation technology for health care professional skills training and assessment,” *JAMA*, vol. 282, no. 9, pp. 861–866, Sep. 1999.

[61] D. L. Dawson, J. Meyer, E. S. Lee, and W. C. Pevec, “Training with simulation improves residents’ endovascular procedure skills,” *J. Vasc. Surg.*, vol. 45, no. 1, pp. 149–154, Jan. 2007.

[62] T. P. Grantcharov, V. B. Kristiansen, J. Bendix, L. Bardram, J. Rosenberg, and P. Funch-Jensen, “Randomized clinical trial of virtual reality simulation for laparoscopic skills training,” *Br. J. Surg.*, vol. 91, no. 2, pp. 146–150, 2004.

[63] R. A. Chaer, B. G. DeRubertis, S. C. Lin, H. L. Bush, J. K. Karwowski, D. Birk, N. J. Morrissey, P. L. Faries, J. F. McKinsey, and K. C. Kent, “Simulation Improves Resident Performance in Catheter-Based Intervention,” *Ann. Surg.*, vol. 244, no. 3, pp. 343–352, Sep. 2006.

[64] Brain Trauma Foundation, American Association of Neurological Surgeons, and Congress of Neurological Surgeons, “Guidelines for the Management of Severe Traumatic Brain Injury, 3rd edition,” *J. Neurotrauma*, vol. 24 Suppl 1, pp. S1–106, 2007.

[65] Brain Trauma Foundation, American Association of Neurological Surgeons, and Congress of Neurological Surgeons, “Guidelines for the Management of Severe Traumatic Brain Injury, 3rd edition,” *J. Neurotrauma*, vol. 24 Suppl 1, pp. S1–106, 2007.

[66] E. S. Connolly Jr, A. A. Rabinstein, J. R. Carhuapoma, C. P. Derdeyn, J. Dion, R. T. Higashida, B. L. Hoh, C. J. Kirkness, A. M. Naidech, C. S. Ogilvy, A. B. Patel, B. G. Thompson, P. Vespa, American Heart Association Stroke Council, Council on Cardiovascular Radiology and Intervention, Council on Cardiovascular Nursing, Council on Cardiovascular Surgery and Anesthesia, and Council on Clinical Cardiology, “Guidelines for the management of aneurysmal subarachnoid hemorrhage: a guideline for healthcare professionals from the American Heart Association/american Stroke Association,” *Stroke J. Cereb. Circ.*, vol. 43, no. 6, pp. 1711–1737, Jun. 2012.

[67] G. M. J. Lemole, P. P. Banerjee, C. Luciano, S. Neckrysh, and F. T. Charbel, “Virtual reality in neurosurgical education: part-task ventriculostomy simulation with dynamic visual and haptic feedback.,” *Neurosurgery*, vol. 61, no. 1, pp. 142–149, Jul. 2007.

[68] T. Rehman, A. Rehman, A. Rehman, H. H. Bashir, R. Ali, S. A. Bhimani, and S. Khan, “A US-based survey on ventriculostomy practices,” *Clin. Neurol. Neurosurg.*, vol. 114, no. 6, pp. 651–654, Jul. 2012.

[69] L. Lai and M. K. Morgan, “The impact of changing intracranial aneurysm practice on the education of cerebrovascular neurosurgeons,” *J. Clin. Neurosci.*, vol. 19, no. 1, pp. 81–84, Jan. 2012.

[70] R. Yudkowsky, C. Luciano, P. Banerjee, A. Schwartz, A. Alaraj, G. M. J. Lemole, F. Charbel, K. Smith, S. Rizzi, R. Byrne, B. Bendok, and D. Frim, “Practice on an Augmented Reality/Haptic Simulator and Library of Virtual Brains Improves Residents’ Ability to Perform a Ventriculostomy. [Miscellaneous Article],” *J. Soc. Simul. Healthc. Febr. 2013*, vol. 8, no. 1, pp. 25–31, 2013.

[71] I. Netterstrøm and L. Kayser, “Learning to be a doctor while learning anatomy!,” *Anat. Sci. Educ.*, vol. 1, no. 4, pp. 154–158, 2008.

[72] A. Winkelmann, “Anatomical dissection as a teaching method in medical school: a review of the evidence,” *Med. Educ.*, vol. 41, no. 1, pp. 15–22, 2007.

[73] T. Mashiko, K. Otani, R. Kawano, T. Konno, N. Kaneko, Y. Ito, and E. Watanabe, “Development of 3-dimensional Hollow Elastic-model for Cerebral Aneurysm Clipping Simulation Enabling Rapid and Low-cost Prototyping,” *World Neurosurg.*

[74] F. J. Bova, D. A. Rajon, W. A. Friedman, G. J. Murad, D. J. Hoh, R. P. Jacob, S. Lampotang, D. E. B. Lizdas, G. Lombard, and J. R. Lister, “Mixed-Reality Simulation for Neurosurgical Procedures.,” *Neurosurg. Oct. 2013*, 2013.

[75] P. S. D’Urso, R. G. Thompson, R. L. Atkinson, M. J. Weidmann, M. J. Redmond, B. I. Hall, S. J. Jeavons, M. D. Benson, and W. J. S. Earwaker, “Cerebrovascular biomodelling: a technical note,” *Surg. Neurol.*, vol. 52, no. 5, pp. 490–500, Nov. 1999.

[76] M. A. Bauman, G. T. Gillies, R. Raghavan, M. L. Brady, and C. Pedain, “Physical characterization of neurocatheter performance in a brain phantom gelatin with nanoscale porosity: steady-state and oscillatory flows,” *Nanotechnology*, vol. 15, no. 1, p. 92, Jan. 2004.

[77] S. S. Basati, T. J. Harris, and A. A. Linninger, “Dynamic Brain Phantom for Intracranial Volume Measurements,” *IEEE Trans. Biomed. Eng.*, vol. 58, no. 5, pp. 1450–1455, May 2011.

[78] C. Luyet, V. Hartwich, N. Urwyler, P. M. Schumacher, U. Eichenberger, and A. Vogt, “Evaluation of a novel needle guide for ultrasound-guided phantom vessel cannulation*,” *Anaesthesia*, vol. 66, no. 8, pp. 715–720, 2011.

APPENDIX A

ANOVA TABLES FOR SURGICAL PLANNING RELATED OUTCOMES

Operating room length of time (PHDM vs Traditional Planning): Tetralogy of Fallot with Pulm Atresia or Pulm Absent Valve

Source	D.F.	Adj. S.S.	Adj. M.S.	F-Value	P-Value
PHDM	1	352	352.1	0.03	0.855
Error	14	142514	10179.5		
Total	15	142866			

Planning	N	Mean (minutes)	StDev	95 CI
Traditional	12	365.1	106.4	(302.6, 427.6)
PHDM	4	354.3	77.2	(246.1, 462.4)

Case length of time (PHDM vs Traditional Planning): Tetralogy of Fallot with Pulm Atresia or Pulm Absent Valve

Source	D.F.	Adj. S.S.	Adj. M.S.	F-Value	P-Value
PHDM	1	6.8	6.75	0.00	0.976
Error	14	99161.0	7082.93		
Total	15	99167.8			

Planning	N	Mean (minutes)	StDev	95 CI
Traditional	12	257.0	84.7	(204.9, 309.1)
PHDM	4	255.5	82.2	(165.2, 345.8)

Operating room length of time (PHDM vs Traditional Planning): Pulmonary Atresia with Ventricular Septal Defects and Muliple Aorto Pulmonary collateral arteries (pseudotruncus)

Source	D.F.	Adj. S.S.	Adj. M.S.	F-Value	P-Value
PHDM	1	22614	22614	1.25	0.301
Error	7	127034	18148		
Total	8	149648			

Planning	N	Mean (minutes)	StDev	95 CI
Traditional	2	527.0	99.0	(301.8, 752.2)
PHDM	7	406.4	139.8	(286.0, 526.8)

Case length of time (PHDM vs Traditional Planning): Pulmonary Atresia with Ventricular Septal Defects and Muliple Aorto Pulmonary collateral arteries (pseudotruncus):

Source	D.F.	Adj. S.S.	Adj. M.S.	F-Value	P-Value
PHDM	1	26811	26811	1.53	0.256
Error	7	122477	17497		
Total	8	149289			

Planning	N	Mean (minutes)	StDev	95 CI
Traditional	2	425.0	79.2	(203.8, 646.2)
PHDM	7	293.7	139.2	(175.5, 411.9)

Operating room length of time (PHDM vs Traditional Planning): Vascular ring

Source	D.F.	Adj. S.S.	Adj. M.S.	F-Value	P-Value
PHDM	1	0.12	0.12	0.00	0.944
Error	13	25851.5	1988.58		
Total	14	25851.6			

Planning	N	Mean (minutes)	StDev	95 CI
Traditional	11	179.5	48.6	(150.4, 208.5)
PHDM	4	179.3	27.5	(131.1, 227.4)

Case length of time (PHDM vs Traditional Planning): Vascular ring

Source	D.F.	Adj. S.S.	Adj. M.S.	F-Value	P-Value
PHDM	1	2815	2815	1.93	0.188
Error	13	18973	1459		
Total	14	21788			

Planning	N	Mean (minutes)	StDev	95 CI
Traditional	11	98.7	41.9	(73.8, 123.6)
PHDM	4	67.8	21.9	(26.5, 109.0)

Operating room length of time (PHDM vs Traditional Planning): Single ventricle

Source	D.F.	Adj. S.S.	Adj. M.S.	F-Value	P-Value
PHDM	1	26	25.74	0.00	0.956
Error	86	723959	8418.13		
Total	87	723985			

Planning	N	Mean (minutes)	StDev	95 CI
Traditional	74	322.1	88.7	(300.9, 343.3)
PHDM	14	320.6	107.1	(271.9, 369.4)

Case length of time (PHDM vs Traditional Planning): Single ventricle

Source	D.F.	Adj. S.S.	Adj. M.S.	F-Value	P-Value
PHDM	1	110	110.4	0.02	0.896
Error	86	551501	6412.8		
Total	87	551612			

Planning	N	Mean (minutes)	StDev	95 CI
Traditional	74	217.42	77.97	(198.91, 235.92)
PHDM	14	214.4	91.0	(171.8, 256.9)

APPENDIX B

NURSE EDUCATION ASSESSMENT

The pre- and post-assessment used in Section 2.6 is reproduced here in its original formatting.

CIRCLE YOUR COHORT: 2D 3D

Participation and completion of the assessment will be considered consent in this study.

Pre-Assessment/Questionnaire

Fill in the blanks:

1. A normal heart is made up of _____ chambers. The _____ side of the heart receives blood from the body and sends it to the lungs to be oxygenated. The _____ side receives oxygenated blood from the lungs and sends it out to the body.

2. In normal anatomy, the _____ is the largest artery in the body and stems from the left ventricle.

3. In normal anatomy, the pulmonary artery stems from the _____ and takes deoxygenated blood to the lungs.

4. In a few words, a congenital heart defect could be described as:

_____

_____

Circle the best answer:

5. A ductus arteriosus is:
   a) A connection linking the aorta and pulmonary artery
   b) An opening in the heart while in utero between the atria to bypass the lungs
   c) An extra chamber of the heart
   d) An normal opening in the heart once the baby is born

6. A patient with pulmonary valvular stenosis has a problem with:
   a) Too much pulmonary blood flow
   b) Too little pulmonary blood flow
   c) Too little systemic blood flow

7. Which of the following defects best describes the following: The aorta stems from the right ventricle taking blue blood to the body and the pulmonary artery arises from the left ventricle taking red blood to the lungs.
   a) Transposition of the Great Arteries
   b) Tetralogy of Fallot
   c) Coarctation of the Aorta
   d) Hypoplastic Left Heart Syndrome
   e) Truncus Arteriosus

CIRCLE YOUR COHORT: 2D 3D

8. Which of the following defects best describes the following: Pulmonary valve is obstructed or narrowed making it difficult to get blood to the lungs. The right ventricle is hypertrophied. A hole exists between the ventricles and the aorta is dedicated to both right and left ventricle. Shunting may exist.
    a) Transposition of the Great Arteries
    b) Tetralogy of Fallot
    c) Coarctation of the Aorta
    d) Hypoplastic Left Heart Syndrome
    e) Truncus Arteriosus

9. Which of the following defects best describes the following: A restriction of the aorta increases blood flow to the head and upper body but decreases flow to the lower body.
    a) Transposition of the Great Arteries
    b) Tetralogy of Fallot
    c) Coarctation of the Aorta
    d) Hypoplastic Left Heart Syndrome
    e) Truncus Arteriosus

10. Which of the following defects best describes the following: The left ventricle does not develop properly, secondary to limited or no flow through mitral or aortic valve is present. The right ventricle is the major pumping chamber. Shunting is always required.
    a) Transposition of the Great Arteries
    b) Tetralogy of Fallot
    c) Coarctation of the Aorta
    d) Hypoplastic Left Heart Syndrome
    e) Truncus Arteriosus

11. Which of the following defects best describes the following: the pulmonary artery and aorta fail to divide into two separate vessels, resulting in high amounts of pulmonary blood flow.
    a) Transposition of the Great Arteries
    b) Tetralogy of Fallot
    c) Coarctation of the Aorta
    d) Hypoplastic Left Heart Syndrome
    e) Truncus Arteriosus

11. In transposition of the great arteries, which great vessel's origin is most anterior?

CIRCLE YOUR COHORT: 2D 3D

Anonymous ID

Post-Assessment/Questionnaire

Fill in the blanks:

1. A normal heart is made up of _____ chambers. The _____ side of the heart receives blood from the body and sends it to the lungs to be oxygenated. The _____ side receives oxygenated blood from the lungs and sends it out to the body.

2. In normal anatomy, the _____ is the largest artery in the body and stems from the left ventricle.

3. In normal anatomy, the pulmonary artery stems from the _____ and takes deoxygenated blood to the lungs.

4. In a few words, a congenital heart defect could be described as:

_____

_____

Circle the best answer:

5. A ductus arteriosus is:
   a) A connection linking the aorta and pulmonary artery
   b) An opening in the heart while in utero between the atria to bypass the lungs
   c) An extra chamber of the heart
   d) An normal opening in the heart once the baby is born

6. A patient with pulmonary valvular stenosis has a problem with:
   a) Too much pulmonary blood flow
   b) Too little pulmonary blood flow
   c) Too little systemic blood flow

7. Which of the following defects best describes the following: The aorta stems from the right ventricle taking blue blood to the body and the pulmonary artery arises from the left ventricle taking red blood to the lungs.
   a) Transposition of the Great Arteries
   b) Tetralogy of Fallot
   c) Coarctation of the Aorta
   d) Hypoplastic Left Heart Syndrome
   e) Truncus Arteriosus

CIRCLE YOUR COHORT: 2D 3D

8. Which of the following defects best describes the following: Pulmonary valve is obstructed or narrowed making it difficult to get blood to the lungs. The right ventricle is hypertrophied. A hole exists between the ventricles and the aorta is dedicated to both right and left ventricle. Shunting may exist.
    a) Transposition of the Great Arteries
    b) Tetralogy of Fallot
    c) Coarctation of the Aorta
    d) Hypoplastic Left Heart Syndrome
    e) Truncus Arteriosus

9. Which of the following defects best describes the following: A restriction of the aorta increases blood flow to the head and upper body but decreases flow to the lower body.
    f) Transposition of the Great Arteries
    a) Tetralogy of Fallot
    b) Coarctation of the Aorta
    c) Hypoplastic Left Heart Syndrome
    d) Truncus Arteriosus

10. Which of the following defects best describes the following: The left ventricle does not develop properly, secondary to limited or no flow through mitral or aortic valve is present. The right ventricle is the major pumping chamber. Shunting is always required.
    f) Transposition of the Great Arteries
    g) Tetralogy of Fallot
    a) Coarctation of the Aorta
    b) Hypoplastic Left Heart Syndrome
    c) Truncus Arteriosus

11. Which of the following defects best describes the following: the pulmonary artery and aorta fail to divide into two separate vessels, resulting in high amounts of pulmonary blood flow.
    a) Transposition of the Great Arteries
    b) Tetralogy of Fallot
    c) Coarctation of the Aorta
    d) Hypoplastic Left Heart Syndrome
    e) Truncus Arteriosus

11. In transposition of the great arteries, which great vessel's origin is most anterior?

CIRCLE YOUR COHORT: 2D 3D

Technology Acceptance Survey

Please rank the following statements:

1 : greatly disagree 2 : disagree 3 : neutral 4 : agree 5 : greatly agree

Awareness & Presence:	---	-	0	+	+++
The drawing/model helps me understand the defect.	1	2	3	4	5
The drawing/model helps me understand the spatial relationship of cardiovascular structures.	1	2	3	4	5
The patient derived drawings/models helps me appreciate anatomical variations.	1	2	3	4	5
Perceived Usefulness:					
The drawing/model improved my understanding with regards to spatial relationship of anatomy.	1	2	3	4	5
The drawing/model in conjunction with the video improved my understanding with regards to spatial relationship of anatomy.	1	2	3	4	5
The drawing/model improved my understanding with regards to congenital heart defects.	1	2	3	4	5
The drawing/model in conjunction with the video improved my understanding with regards to congenital heart defects.	1	2	3	4	5
The educational module gave me a greater confidence in explaining congenital heart defects to patient-families.	1	2	3	4	5
What I have learned in the educational module will impact my patient care.	1	2	3	4	5
The educational module was an effective use of my time.	1	2	3	4	5
Perceived Ease-Of-Use:					
The drawing/model was easy to understand.	1	2	3	4	5
This video was clear.	1	2	3	4	5
The module did not take an unnecessary amount of time to complete.	1	2	3	4	5
The module was effective with some instruction.	1	2	3	4	5
The module would be effective without any instruction.	1	2	3	4	5

CIRCLE YOUR COHORT: 2D 3D

Playfulness:

I enjoyed this module as an educational tool.	**1**	**2**	**3**	**4**	**5**
I enjoyed this module regardless of the potential educational value.	**1**	**2**	**3**	**4**	**5**

Attitude:

The module will improve my clinical care.	**1**	**2**	**3**	**4**	**5**
I have a positive attitude about this module.	**1**	**2**	**3**	**4**	**5**

Intention to Use:

The module encourages me to learn more about congenital heart disease.	**1**	**2**	**3**	**4**	**5**
I wish modules like this were created for other common anatomical variations.	**1**	**2**	**3**	**4**	**5**
I would recommend this module for other clinical care professionals.	**1**	**2**	**3**	**4**	**5**